



NTNU – Trondheim
Norwegian University of
Science and Technology

Heat Recovery in Combination with Different Heat Pump Solutions for Energy Supply

Atle Solberg

Master of Energy Use and Energy Planning

Submission date: June 2015

Supervisor: Hans Martin Mathisen, EPT

Co-supervisor: Maria Justo Alonso, SINTEF

Norwegian University of Science and Technology
Department of Energy and Process Engineering

EPT-M-2015-85

MASTER THESIS

for

Student Atle Solberg

Spring 2015

Heat recovery in combination with different heat pump solutions for energy supply*Varmegjenvinning i kombinasjon med ulike varmepumpeløsninger for energiforsyning***Background and objective**

In new, highly insulated buildings a ventilation system is necessary. The Norwegian building codes (TEK10) demands exchange of at least half the volume of air in the building every hour. This also applies for passive houses. Heating the supply air requires a high share of the building's total energy use, and therefore passive house standard requires heat recovery with an efficiency of at least 80 %. This normally requires use of mechanical balanced ventilation.

The goal of the master thesis is to compare the total energy efficiency of different heat recovery and heat pump solutions. The relevant heat pumps are CO₂ supercritical heat pumps using an accumulation tank for production of domestic hot water and space heating. The study should be on energy use for space heating and domestic hot water in residential buildings.

The thesis will be a continuation of the candidate's project work.

The following tasks are to be considered:

1. Consider the need for further literature survey
2. Decide which cases to include in the study
3. Establish simulation models for the different solutions
4. Perform simulations on the case building with different occupants' behaviour
5. Compare simulation results with regard to energy use and performance

-- " --

Within 14 days of receiving the written text on the master thesis, the candidate shall submit a research plan for his project to the department.

When the thesis is evaluated, emphasis is put on processing of the results, and that they are presented in tabular and/or graphic form in a clear manner, and that they are analyzed carefully.

The thesis should be formulated as a research report with summary both in English and Norwegian, conclusion, literature references, table of contents etc. During the preparation of the text, the candidate should make an effort to produce a well-structured and easily readable report. In order to ease the evaluation of the thesis, it is important that the cross-references are correct. In the making of the report, strong emphasis should be placed on both a thorough discussion of the results and an orderly presentation.

The candidate is requested to initiate and keep close contact with his/her academic supervisor(s) throughout the working period. The candidate must follow the rules and regulations of NTNU as well as passive directions given by the Department of Energy and Process Engineering.

Risk assessment of the candidate's work shall be carried out according to the department's procedures. The risk assessment must be documented and included as part of the final report. Events related to the candidate's work adversely affecting the health, safety or security, must be documented and included as part of the final report. If the documentation on risk assessment represents a large number of pages, the full version is to be submitted electronically to the supervisor and an excerpt is included in the report.

Pursuant to "Regulations concerning the supplementary provisions to the technology study program/Master of Science" at NTNU §20, the Department reserves the permission to utilize all the results and data for teaching and research purposes as well as in future publications.

The final report is to be submitted digitally in DAIM. An executive summary of the thesis including title, student's name, supervisor's name, year, department name, and NTNU's logo and name, shall be submitted to the department as a separate pdf file. Based on an agreement with the supervisor, the final report and other material and documents may be given to the supervisor in digital format.

- Work to be done in lab (Water power lab, Fluids engineering lab, Thermal engineering lab)
 Field work

Department of Energy and Process Engineering, 14. January 2015



Olav Bolland
Department Head



Hans Martin Mathisen
Academic Supervisor

Research Advisor:
Maria Justo Alonso

Abstract

The main purpose of this Master's thesis has been to investigate the performance of different methods of heat recovery from ventilation air. Comparisons have been made with regard to delivered energy for heating of domestic hot water (DHW), space heating and ventilation heating. A single-unit dwelling was used as a basis for the simulations. The house, built in accordance with the Norwegian passive house standard, had a gross internal area of 172.6 m². Seven different combinations of a heat wheel, an exhaust air CO₂ heat pump and an outdoor air CO₂ heat pump was assessed. Direct-acting electricity was used to cover the remaining heat demand in all seven heat recovery models. Three different occupant behaviour models and three different climates (Oslo, Stavanger and Kautokeino) were investigated in order to increase the area of application for the results. The building was simulated in *IDA Indoor Climate and Energy*, while the heat pump performance was post-processed in MATLAB. Several aspects concerning heat recovery, dimensioning, ventilation and heating schedules, heat distribution, etc., have been assessed.

Simulations performed for a family of five with a high consumption of domestic hot water in Oslo showed that the required amount of delivered energy for heating was equal to 115 kWh/m²yr, without any heat recovery. The most used heat recovery method in Norway today, a heat wheel, reduces the energy demand by 34%, down to 76 kWh/m²yr. The most efficient heat recovery model that was found in this report showed a reduction of delivered energy for heating of 68%, down to 36 kWh/m²yr. This heat recovery model consists of a heat wheel and a heat pump utilizing both ventilation exhaust air and outdoor air. The recommended solution for occupants with a high DHW consumption, when economy is taken into account, is based on a heat wheel and an exhaust air CO₂ heat pump. The amount of delivered energy is reduced by 66%, down to 40 kWh/m²yr.

Any further work within this field should look into the choice of refrigerant, improvements on the heat pump model and the impact of different building sizes. A more in-depth investment analysis of the different heat recovery models, including the heat distribution system in the building, should also be assessed.

Sammendrag

Formålet med denne masteroppgaven har vært å undersøke ytelsen til ulike metoder for gjenvinning av ventilasjonsvarme. De ulike løsningene har blitt sammenliknet ut ifra mengden levert energi til bygningen for varmt tappevann, romoppvarming og ventilasjonsvarme. En enebolig på 172.6 m², bygd i henhold til den norske passivhusstandarden, ble brukt som utgangspunkt for simuleringene. Syv ulike kombinasjoner av en roterende varmeveksler og CO₂ luft–vann varmepumpe ble sett nærmere på. Varmepumpen kunne bruk avtrekksluft og/eller uteluft som varmekilde. Direktevirkende elektrisitet er brukt til å dekke den energien som varmepumpen ikke klarer å dekke. Tre ulike bruker-modeller og tre ulike klimaer (Oslo, Stavanger og Kautokeino) ble undersøkt for å øke anvendelsesområdet til resultatene. Bygningen ble simulert i *IDA Indoor Climate and Energy*, mens varmepumpeytelsen ble postprosessert i MATLAB. Flere ulike aspekter som angår varmegjenvinning, dimensjonering, varmedistribusjon, og tidsstyrte ventilasjons- og temperatursettpunkt ble undersøkt.

Simuleringer ble blant annet utført for en familie på fem med et høyt varmtvannsforbruk, boende i Oslo. Den nødvendige leverte energien for varme til bygningen tilsvarte 115 kWh/m²år, dersom bygningen ikke anvendte varmegjenvinning. Den mest brukte løsningen i Norge i dag, en roterende varmeveksler, reduserte energibehovet med 34%, ned til 76 kWh/m²år. Den mest effektive metoden som ble funnet i denne rapporten kunne vise til en reduksjon på 68%, ned til 36 kWh/m²år. Denne løsningen består av en roterende varmeveksler og en varmepumpe som kan utnytte både avtrekksluft og uteluft. Den anbefalte løsningen for beboere med et høyt varmtvannsforbruk, når økonomi er tatt med i betraktningen, er basert på en roterende varmeveksler og et avtrekksvarmepumpe. Behovet for levert energi for å dekke varmebehovet er redusert med 66%, ned til 40 kWh/m²år.

Videre arbeid innen dette temaet bør se på valg av arbeidsmedie, forbedringer på varmepumpemodellen, og ulike bygningsstørrelsers påvirkning på valg av varmegjenvinningsmetode. Dessuten bør det gjennomføres en mer dyptgående investeringsanalyse av de ulike varmegjenvinningsmetodene. En slik analyse bør også se på kostnader for varmedistribusjonssystemet i bygningen.

Preface

This Master's Thesis is the final work of the master's degree in *Energy Use and Energy Planning* at the Norwegian University of Science and Technology in Trondheim, Norway. The thesis is a continuation of the project thesis written during the autumn 2014.

The scope of the Master's Thesis is to assess different combinations of ventilation heat exchangers, and heat pumps for ventilation heat recovery and energy supply to the building. The assignment was proposed by Maria Justo Alonso, research scientist at SINTEF Buildings and Infrastructure in Trondheim. The assignment is connected to the IEA Heat Pump centre Annex 40 – *Heat pump concepts for Nearly Zero-Energy Buildings*. The thesis comprises 30 ECTS credits.

I would like to thank my supervisors, Maria Justo Alonso and professor Hans Martin Mathisen, for valuable support, feedback and advises during my work on this report. I would also like to thank the employees at the Department of Energy and Process Engineering, and the employees at SINTEF Energy Research, who have been available for discussions and counselling. Especially Associate Professor Natasa Nord, together with Senior Engineer Inge Håvard Rekstad, have provided valuable information regarding IDA ICE and CO₂ compressors respectively.

At last, I would like to thank my girlfriend and wife-to-be, Linn Therese, for her love and support during the work on my project and Master's Thesis.

Atle Solberg

Atle Solberg

Trondheim, 11th of June 2015

Table of Contents

Thesis assignment	I
Abstract	III
Sammendrag	V
Preface	VII
1 Introduction	1
2 Theoretical background of heat recovery	3
2.1 Recovery using heat exchangers	4
2.1.1 Regenerative heat exchangers	4
2.1.2 Recuperative heat exchangers	7
2.1.3 Membrane energy exchangers (MEE)	9
2.1.4 Comparison of heat exchangers	9
2.2 Heat recovery using exhaust air heat pumps	12
2.2.1 Thermodynamic basis for CO ₂ heat pumps	13
2.2.2 System configurations	16
2.3 Hybrid heat recovery	19
2.4 Heat pumps for ventilation heat recovery in NS 3031 (2014)	20
3 Literature	23
3.1 Exhaust air heat pump heat recovery	24
3.2 Hybrid heat recovery	27
3.3 Available commercialized products	31
3.3.1 NIBE – heat pump recovery	31
3.3.2 Genvex – hybrid recovery	33
3.3.3 Nilan – hybrid recovery	35
3.3.4 Enervent/Exvent – hybrid recovery	37
3.3.5 Comparison of commercialized products	39
4 Basis for simulations	41
4.1 Building used in simulations	41
4.2 Occupants’ behaviour	43

4.2.1	Standardized occupant behaviour model (NS3031)	43
4.2.2	"Small" occupant behaviour model	44
4.2.3	"Large" occupant behaviour model	45
4.2.4	Comparison of occupant behaviour models	46
4.3	Heat recovery cases	47
4.4	Climates	48
5	Heat recovery simulations in IDA ICE and Matlab	51
5.1	Simulation platform and architecture	51
5.2	Building simulation and heat rec. in IDA ICE	55
5.2.1	Zone division	55
5.2.2	Internal doors	55
5.2.3	Windows, opening of windows and shading	57
5.2.4	IDA ESBO plant	58
5.2.5	Hydronic heating and dimensioning of radiators	61
5.2.6	Ventilation and air handling unit	62
5.2.7	Simulation of heat wheel heat recovery	64
5.3	Heat pump simulations in Matlab	65
5.3.1	Matlab files overview	65
5.3.2	Heat pump model system solution	67
5.3.3	Operating modes	67
5.3.4	Evaporator	68
5.3.5	Compressor	69
5.3.6	Gas cooler	72
5.3.7	Expansion device	74
5.3.8	Mass flow and volume flow	74
5.3.9	Fan energy	75
5.3.10	Solving the system of equations	75
6	Results	79
6.1	Building simulations	79
6.1.1	Heating energy	79
6.1.2	Space heating and ventilation heating power	81
6.1.3	DHW tank temperatures and boiler power	83
6.2	Parameter study	86
6.2.1	Compressor size	86
6.2.2	Evaporator UA value	90

6.2.3	Outdoor air fan volume flow	92
6.2.4	Influence of DHW storage tank volume	94
6.2.5	Influence of night time set-back	96
6.2.6	Reduced ventilation air flow when unoccupied . .	97
6.2.7	Heat wheel efficiency	99
6.3	Sensitivity analysis	100
6.3.1	Isentropic efficiency and compressor heat loss factor	101
6.3.2	Temperature approach value	102
6.3.3	Compressor operating range	103
6.4	General performance	105
6.4.1	Comparison of cases with and without outdoor air	106
6.4.2	Comparison of cases in different climates	108
6.4.3	Composition of heating energy	112
6.4.4	Heat pump for production of DHW only	114
6.4.5	COP duration curves	115
6.5	Economical evaluations	116
7	Discussion	121
7.1	Building model	121
7.2	Heat pump model	123
7.3	Recommended heat recovery case	125
7.4	Validity and area of application for the simulation results	126
8	Conclusion	129
9	Suggestions for further work	131
	Bibliography	133
	Appendix	138
A	Building model	139
A.1	Zone division	139
A.2	Occupants presence schedules	141
A.3	Internal doors	142
A.4	Window blinds control macro	143
A.5	IDA ICE Plant	144

B	Matlab heat pump code	145
B.1	Main script (main.m)	145
B.2	Script containing parameters (parameters.m)	158
B.3	Script containing constants (constants.m)	160
B.4	Function with thermodynamics (thermodynamics.m) . .	161
B.5	Script with preallocations (preallocations.m)	163
B.6	Script clearing parameters (clear_var.m)	165
B.7	Function for isentropic compressor efficiency (eta_is.m)	167
B.8	Function for volumetric compressor efficiency (eta_vol.m)	168

List of Figures

Chapter 2: Theoretical background of heat recovery	3
2.1 Illustration of a rotating wheel heat exchanger	5
2.2 Illustration of the most basic components in a heat pump	13
2.3 T-h diagram showing a general transcritical heat pump cycle	14
2.4 Comparison of average temperature during heat rejection	15
2.5 Transcritical pressure lines for CO ₂	16
2.6 System configuration sketch of air-air/water heat pump	18
2.7 Temp. diff. between discharge air and outdoor air for different efficiencies	19
2.8 Energy flows in an exhaust air heat pump, according to NS 3031 (2014)	21
Chapter 3: Literature	23
3.1 System solution of NIBE F470 (Solsem, 2015a).	33
3.2 System solution of Genvex 185 S/LS (Solsem, 2015a) . .	35
3.3 System solution of Nilan Compact P Nordic	37
3.4 System solution of Exvent Greenair HP	38
Chapter 4: Basis for simulations	41
4.1 Picture of "Karita"	42
Chapter 5: Heat recovery simulations in IDA ICE and Matlab	51
5.1 Architecture of the simulation model	54
5.2 Floor plan of the building "Karita"	56
5.3 Shading objects from nearby buildings illustrated	57
5.4 DHW distribution schedule used in the IDA ICE model	60
5.5 Simplified sketch of system solution simulated in MATLAB	67
5.6 Isentropic and volumetric compressor efficiencies as a function of pressure ratio	71

5.7	Example of how the half-interval search algorithm works	76
Chapter 6: Results		79
6.1	Heating energy budget for "NS3031" occupant behaviour model	80
6.2	Duration curve for space heating and ventilation pre-heating power for Oslo climate	81
6.3	Duration curve for space heating and ventilation heating power for Stavanger climate	82
6.4	Duration curve for space heating and ventilation heating power for Kautokeino climate	82
6.5	Duration curve for temperature at the bottom of DHW tank	84
6.6	Duration curve for DHW boiler power	85
6.7	Optimum compressor volume for "Large" occupant behaviour model (Oslo)	87
6.8	Optimum compressor volume for "Large" occupant behaviour model (Kautokeino)	89
6.9	Delivered energy for heating at different UA values	91
6.10	Delivered energy for heating at different UA values for different climates	92
6.11	Outdoor air fan volume flow influence on delivered energy for heating	93
6.12	Influence of DHW storage tank volume on delivered energy	95
6.13	Influence of reduced air flow rates when unoccupied	99
6.14	Heat wheel efficiency influence on delivered energy	100
6.15	Sensitivity of isentropic efficiency and compressor heat loss	101
6.16	Sensitivity of the temperature approach value	103
6.17	Significance of minimum compressor volume (Oslo, "Large")	104
6.18	Significance of minimum compressor volume (Stavanger, "Small")	105
6.19	Comparison of solutions with and without outdoor air as additional heat source ("Small")	107
6.20	Comparison of solutions with and without outdoor air as additional heat source ("Large")	108

6.21	Comparison of heat recovery cases ("Small")	109
6.22	Comparison of heat recovery cases ("NS3031")	110
6.23	Comparison of heat recovery cases ("Large")	111
6.24	Composition of delivered energy for heating	112
6.25	Composition of delivered energy for heating for different climates	113
6.26	The performance of <i>HWeHP</i> covering DHW only	115
6.27	COP duration curves for "Large" occupant behaviour model	116
6.28	Maximum permissible investment (MPI), Oslo climate	117
6.29	Maximum permissible investment (MPI), Stavanger cli- mate	118

List of Tables

Chapter 2: Theoretical background of heat recovery	3
2.1 Comparison of different heat/energy exchangers	11
2.2 Minimum discharge air temperature from heat exchangers	11
Chapter 3: Literature	23
3.1 Test results for three different commercialized products.	29
3.2 Comparison of the different heat recovery products . . .	40
Chapter 4: Basis for simulations	41
4.1 Thermal properties and energy efficiencies of "Karita" .	42
4.2 Standard figures from NS 3031 (2014) for DHW, lighting and equipment.	44
4.3 Calculation of DHW consumption for "Small" occupant behaviour model	45
4.4 Calculation of DHW consumption for "Large" occupant behaviour model	46
4.5 Comparison of energy posts for the three occupants be- haviour models	46
4.6 Overview of the different heat recovery cases in the report	48
4.7 Climate data used in the simulations	49
Chapter 5: Heat recovery simulations in IDA ICE and Matlab	51
5.1 Deviations from default tank and boiler parameters for DHW system	59
5.2 Deviations from the default tank and boiler parameters for SH and VH system	61
5.3 Deviations from default air handling unit setup in IDA ICE	64
5.4 Description of the different MATLAB files	66
5.5 Optimum CO ₂ gas cooler pressure according to Stene (2014)	73

Chapter 6: Results	79
6.1 Comparison of optimum compressor volume flow at full capacity for Oslo and Kautokeino climate	90
6.2 Influence of night time set-back on delivered energy . . .	96
6.3 Influence of reduced air flow rates when unoccupied . .	98
6.4 All heat recovery solutions compared to no heat recovery	106
6.5 Input parameters for economical calculations	117
6.6 MPI of hydronic heat distribution system	119

Abbreviations

AAHP	Air-air heat pump
AHU	Air handling unit
ASHRAE	American Society of Heating, Refrigerating and Air Conditioning Engineers
AWHP	Air-water heat pump
CFC	Chlorofluorocarbons (group of refrigerants)
COP	Coefficient of performance
CVHD	Compact ventilation and heating device
DHW	Domestic hot water
EAHP	Exhaust air heat pump
GC	Gas cooler
GIA	Gross internal area (BRA in Norwegian). The total floor area within the building envelope, excluding external walls, including area occupied by internal walls, as defined in NS 3940 (2012).
GWP	Global warming potential
HFC	Hydrofluorocarbons (group of refrigerants)
HVAC	Heating, ventilation and air conditioning
IAQ	Indoor air quality
LCA	Life-cycle assessment
LCC	Life-cycle cost
LMTD	Logarithmic mean temperature difference

MPI	Maximum permissible investment
NTNU	Norges teknisk-vitenskapelige universitet (Norwegian University of Science and Technology)
RCHP	Reverse-cycle heat pump. Heat pumps where refrigerant can be reversed using a four-way valve. Can supply heating and cooling.
SFP	Specific fan power [$\text{kW}/(\text{m}^3/\text{s})$]. Power used to move 1 cubic meter of air per second through the ventilation system.
SPF	Seasonal performance factor. Heating output compared to the total power input over the season, including internal heat exchangers, fans and controls.
SGHE	Suction gas heat exchanger, also called internal heat exchanger.
SH	Space heating
SINTEF	Stiftelsen for industriell og teknisk Forskning (The Foundation for Scientific and Industrial Research)
VH	Ventilation heating. (Pre)heating of supply air.
ZEB	Zero Emission Building

Glossary

City water	Water supplied to the building from the waterworks.
Delivered energy	Delivered energy to the building (e.g. electrical energy from the grid).
Discharge air	Ventilation air leaving the building to the surrounding environment.
Exhaust air	Ventilation air removed from zones in the building.
Expansion device	Device used in heat pumps to feed the evaporator with the correct amount of refrigerant. Maintains pressure difference between evaporator and condenser. Usually a valve, but ejectors (commercialized) and expanders (under development) are also possible.
Heating	Heating, unless stated otherwise, is heating of DHW, space heating and ventilation heating.
Hot air heating	Heating of a building through the supply air. Supply air heated to 30°C to 40°C before entering the zone of occupancy.
Net energy demand	Amount of energy needed in within the zones of the building. Efficiency of plant etc. not accounted for.
Outdoor air	Air from the surrounding environment entering the building.
Supply air	Ventilation air supplied to the zone of occupancy.

UA value

U value (overall heat transfer coefficient)
multiplied with heat exchanger area [W/K].

Nomenclature

Latin letters

d	Diameter [m]
s	Specific entropy [kJ/kgK]
v	Specific volume [m ³ /kg]
h	Specific enthalpy [kJ/kg]
Q	Thermal energy [kWh]
\dot{Q}	Thermal energy per time unit [W or kW]
T	Temperature [°C]
\dot{V}	Volume flow [m ³ /s]
W	Compressor energy [kWh]
\dot{W}	Compressor power [W or kW]

Greek letters

η	Efficiency [-]
π	Pressure ratio in heat pump (high pressure divided by low pressure)

Chapter 1

Introduction

In modern, air tight buildings, replacement of the contaminated indoor air with outdoor air is of utmost importance in order to achieve satisfactory indoor air quality. This is normally done using balanced, mechanical ventilation. Replacement of the consumed indoor air with outdoor air leads to a considerable heat loss in cold climates. In developed countries, primary energy used in buildings amounts to about 40% of the total energy consumption (IEA, nd). 50% of the energy consumed in buildings in many developed countries is consumed by the heating, ventilation and air conditioning systems (Calay and Wang, 2013). It is therefore very important to have efficient systems for heat recovery from ventilation air.

The prevalent Norwegian building code states that the heat recovery unit in residential buildings should have a minimum temperature efficiency of 70% during a year, using the energy measures method (Technical Regulations, 2010). In the passive house standard for residential buildings, the minimum temperature efficiency is 80 % during a year (NS 3700, 2013). Even with such high requirements for heat recovery, energy for heating of ventilation air makes out a large part of the total energy budget, together with heating of domestic hot water.

In most new Norwegian buildings, heat recovery is performed using a heat wheel integrated in the air ventilation unit. However, a heat pump could also be used to recover ventilation heat, and at the same time provide heat for space heating and domestic hot water. This report

aims to find the best solution for ventilation heat recovery using a heat wheel and/or a heat pump, for single unit passive house dwellings. Several different combinations are possible. The conclusions are based on simulations carried out on a residential passive house with varying climate and occupant behaviour models.

The results presented in the report are mostly based on delivered energy to the building for heating of domestic hot water, space heating and ventilation heating. The economy of the different heat recovery methods has not been focused on, though some comparisons have been made with regard to the highest permissible investment cost (MPI).

The beginning of the report gives a theoretical introduction to ventilation heat recovery. This includes an overview of the most common heat exchangers, together with information on CO₂ heat pumps and system configurations. The definitions regarding heat recovery using heat pumps are also explained. This chapter is partially based on a project report written during the autumn 2014 (Solberg, 2014).

Thereafter, relevant research literature of heat pump heat recovery and hybrid heat recovery is presented and discussed. The amount of relevant research literature within this field is limited. Existing commercialized products for heat pump heat recovery and hybrid heat recovery are also presented and compared.

The next chapters describe the basis for simulations, the simulation platform and architecture of the simulations. This include defining the different heat recovery cases, occupant behaviour, climates, and so on. The IDA ICE building model is described, together with the developed MATLAB heat pump model.

The simulation results are presented in the next chapter, where they are also discussed, together with appurtenant tables and figures. The result chapter is divided into five sections: The main results from the building simulations are presented. Thereafter, parameters used to design the building and heat pump model are assessed. The sensitivity for some assumed numbers are analysed in the following section. The two last sections look at the general performance of the different heat recovery cases and some economical aspects. A more general discussion is presented in the following chapter. Thereafter comes a conclusion, in addition to suggestions for further work within this field.

Chapter 2

Theoretical background of heat recovery

§13-1 in Technical Regulations (2010) states that all buildings should have satisfactory indoor air quality (IAQ). Satisfactory IAQ is important for the occupants' health and well-being, and is achieved by substituting contaminated air with fresh air. This will, in cold climates such as in Norway, result in an inevitable ventilation air heat loss. Thus, building regulations in countries with a cold climate often demand some sort of heat recovery from ventilation air with a minimum efficiency.

In Norway, using the "Energy measure" method, the requirement is 70% for residential buildings (Technical Regulations, 2010). The yearly minimum temperature efficiency in the residential passive house standard NS 3700 (2013) is 80%.

Ventilation air heat recovery can be achieved using several different methods, though plate heat exchangers and heat wheels are the most common methods in Norway. Heat pumps are extensively used in Sweden for heat recovery from exhaust ventilation systems. However, heat pumps can also be used in balanced ventilation systems, preferably together with a passive heat exchanger. This chapter will look into the theory of the most common heat recovery solutions, with most attention on heat wheels and air-water heat pumps, and also a combination of the two.

2.1 Recovery using heat exchangers

Heat recovery using heat exchangers implies using heat exchangers to directly transfer heat from warm air (exhaust air) to cold air (supply air). This is done with no or a very small consumption of energy. There are several different types of heat exchangers available. They are therefore often divided into two groups distinguished by how they work: Regenerative heat exchangers are cyclic, while recuperative heat exchangers are static. Both types are discussed in the upcoming chapters.

2.1.1 Regenerative heat exchangers

The general working principle of regenerative heat exchangers are alternating exposure of heat accumulating surfaces to warm exhaust air and cold supply air (outdoor air). Thus, the supply and exhaust air ducts must be adjacent. An important property concerning regenerative heat exchangers are their ability to transfer latent heat, in addition to sensible heat. The main advantages are the high efficiency, and no or only limited problems related to frost formation on heat exchanger surfaces. The main disadvantage is an inevitable small transfer of air from exhaust air to supply air, which will contain contaminants. The most common types of regenerative heat exchangers are the rotating wheel and the fixed matrix heat exchanger.

Fixed matrix

The fixed matrix heat exchanger contains two different heat accumulating chambers. Supply air flows through one chamber, while exhaust air flows through the second chamber. The chambers have a large surface in order to improve the heat transfer between the chamber surface and the air flowing through. After a given time, dampers see to that the air flow in the two chambers are switched. Cold supply air is now flowing through the chamber that was heated by the exhaust air, and vice versa. The dampers usually oscillate every minute, controlled by a timer. Transfer of contaminants and odours are a disadvantage with this heat exchanger type, though to a smaller extent than for the rotat-

ing wheel. The heat recovery efficiency can be controlled by changing the settings of the timer controlling the dampers (Novakovic et al., 2007).

Rotating wheel

Rotating wheels go by many names (e.g. thermal wheel, energy wheel, enthalpy wheel, heat wheel, desiccant wheel, dehumidification wheel), where the main working principle is the same. However, differences in material and area of application separates the different subtypes of the rotating wheel. This type of heat exchanger is widely used in newer residential and non-residential buildings in Norway due to its efficiency and its good properties regarding frost formation.

A wheel, covering the entire cross-section of the supply air duct and the exhaust air duct, is rotated by a small electric motor. The wheel consists of many small corrugated ducts allowing the air to pass through. Heat is transferred from the air to the surface of the ducts. As can be seen on figure 2.1, the ducts will alternate between being exposed to hot air (accumulating heat) and cold air (rejecting heat). The efficiency of the rotating wheel may be adjusted by controlling the rotational speed of the wheel.

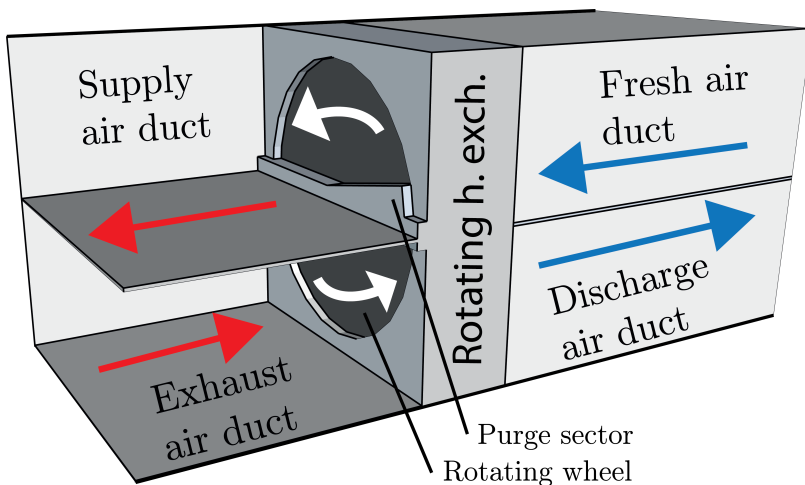


Figure 2.1: Illustration of a rotating wheel heat exchanger

The ducts in the rotating wheel can be made of a hygroscopic material, and the heat exchanger is then called "energy wheel" or "enthalpy wheel". In that case, the energy wheel will be able to transfer sensible *and* latent heat. Rotating wheel ducts made of a non-hygroscopic material can only transfer moisture if moist air condenses on the cold duct surface and is subsequently evaporated on the warm side. This means that humidity can be recovered from the exhaust air, even without a hygroscopic material. This type of heat exchanger is usually called "heat wheel". Heat wheels are the most common solution in modern ventilation units, according to Novakovic et al. (2007). Energy wheels are less used due to higher transfer of odour from exhaust air to supply air, compared to heat wheels, according to Professor Hans Martin Mathisen at NTNU. The odour is transferred with the moisture. However, thermal wheels can be used beneficially in extremely cold climates due to reduced frost formation on the wheel surfaces. The physical dimensions of rotating wheels are rather small, which is a large advantage for use in small compact ventilation units.

The efficiency, depending on air flows compared to size, is usually between 75% and 85%. Petersen et al. (2009) reports that the temperature efficiencies claimed by manufacturers are about the same as in reality, based on measurements on rotating wheels in Norwegian schools.

Heat/energy wheels have only limited or no problems with frost formation. Energy wheels are less troubled than heat wheels. The frosting process is slow, and the indoor moisture production varies during the day (Alonso et al., 2015). Thus, some frosting on surfaces may occur during hours with high moisture production, but this frost will normally defrost at hours with less humidity production. Problems regarding fouling in the heat exchanger are rather small seeing that the flow changes direction in the small wheel ducts several times a minute.

The major drawback is the air leak from exhaust air to supply air. Rotating heat exchangers usually have a purge sector (see figure 2.1) used to minimize the problem. Exhaust air trapped in small ducts when entering the fresh air sector is flushed back to the exhaust air duct, due to the purge sector. An inspection of rotating wheels in Norwegian schools revealed a leakage of 0.2% to 0.4% (Petersen et al., 2009).

2.1.2 Recuperative heat exchangers

Recuperative heat exchangers are static, and transfer heat directly from warm air to cold air. This is usually done by air flows separated by a plate or tube with high thermal conductivity. Heat can also be transferred using a third fluid for transport of energy, which is favourable in cases where the exhaust air duct and the supply air duct are not adjacent.

No air can be carried over from exhaust air to supply air, as long as the heat exchanger is free of defects. This is the main advantage for this type of heat exchangers, seeing that they can be used in highly contaminated zones. However, frost formation in cold climates is a large disadvantage for this heat exchanger type. This problem can be solved by preheating the outdoor air before passing the heat exchanger. The cost is reduced efficiency and thus increased energy consumption.

The most commonly used recuperative heat exchanger is the plate heat exchanger, though the run-around type is also used.

Plate/tube

Plate heat exchangers consist of several layers of corrugated plates, where the corrugated plates increase the surface to volume flow ratio. In the gaps between the plates, supply air and exhaust air are flowing alternately. The flow direction of the two air flows are usually in opposite directions (counter-flow) or at a right angle (cross-flow). The pressure loss in these heat exchangers is low (Alonso et al., 2015). This type of heat exchanger is troubled with frost formation. Warm and humid exhaust will condense and freeze on surfaces with a temperature below 0 °C. Frost will eventually block the air flow through the heat exchanger on the exhaust air side and hamper heat transfer. Frost formation problems may be solved by preheating the outdoor air or by-passing some of the outdoor air, at the expense of recovery efficiency. The efficiency of the heat exchanger can be controlled by bypassing a share of the supply air.

Tube heat exchangers are much the same as plate heat exchangers. Instead of being separated by plates, the two air flows are separated by tubing. Supply air flows through tubes, while the exhaust air flows

on the outside of the tubes. Thus, it has a lower risk of freezing (Novakovic et al., 2007). Efficiency and frost protection mechanisms can be controlled similarly to the plate heat exchanger.

Run-around

Run-around heat exchangers have one large advantage: The supply air duct can be placed remotely from the exhaust air duct (to some extent). One heat exchanging coil is placed in the supply air duct and another in the exhaust air duct, connected by pipes. A heat transfer fluid (usually a glycol—water mixture) is flowing in the closed circuit. Heat is given off from the exhaust air to the heat transfer liquid flowing in the pipes. Heat is given off from the heat transfer liquid to the supply air in the supply air duct. The heat transfer liquid can be self-circulating due to density differences or driven by a circulation pump.

Efficiency can be controlled by installing a three-way valve in the liquid circuit. This valve can also be used for avoiding frost formation. This heat exchanger type has a rather low efficiency. However, a heat pump using the heat transfer liquid as heat source can easily be used to improve the total heat recovery efficiency.

Heat pipe

Heat pipe heat exchangers share the working principle of the run-around heat exchanger. However, they use heat pipes to transfer heat between the ducts. A pipe is placed between the exhaust air and the supply air. A fluid on the inside of the pipe, usually some kind of refrigerant, is evaporated by the warm exhaust air. Due to the reduced density, it moves towards the top of the pipe. The top of the pipe is placed in the supply air duct. Heat is transferred to the supply air from the refrigerant, which condenses and flows down to the bottom of the pipe where it is once more evaporated. Temperature efficiency and frost protection mechanisms can be controlled by bypassing some of the supply air.

2.1.3 Membrane energy exchangers (MEE)

Membrane energy exchangers make use of a semi-permeable membrane material which allows for moisture in the air to pass, but not air itself. Thus, both sensible and latent energy can be recovered. This type of energy exchangers are rather new, and much effort has recently been put into research within this field from research institutions in mainly Canada, China and Italy (Abdel-Salam et al., 2014). Differences in temperature and moisture content is the motive power of heat and mass transfer. Several types of membrane energy exchangers have been developed. Two of the most promising solutions are *Flat plate energy exchanger* and *Run-around membrane energy exchanger*.

Flat plate

The flat plate energy exchanger has the same size and shape as the plate heat exchanger. However, the materials separating the air flows are made of a semi-permeable membrane material. Heat and moisture are transferred from the exhaust air to the supply air.

Run-around membrane energy exchanger (RAMEE)

The build-up of this energy exchanger is the same of the run-around heat exchanger. Instead of air–water heat exchangers placed in the supply and exhaust air duct, the RAMEE energy exchanger has liquid-to-air membrane energy exchangers (LAMEE). A LAMEE is a membrane plate exchanger with air and a desiccant solution flowing alternately (Abdel-Salam et al., 2014). Heat and moisture are transferred from the exhaust air to the desiccant solution in the LAMEE. The desiccant solution circulates to the supply air duct, where heat and moisture are given off to the supply air, before circulating back to the exhaust air LAMEE.

2.1.4 Comparison of heat exchangers

The different kinds of heat/energy exchangers have different advantages and disadvantages. The heat recovery methods made mention of in this chapter are compared in table 2.1.

Three out of eight heat exchangers do not demand adjacent ducts. These solutions are convenient when retrofitting balanced ventilation in older buildings. However, adjacent ducts are not a challenge when building a new residential house.

All of the regenerative heat exchangers have high sensible efficiencies, and experience no or only limited problems related to frost formation. The energy wheel has the highest latent heat recovery efficiency. However, all three heat exchangers are, to some extent, troubled with transfer of odour from exhaust air to supply air.

The traditional recuperative heat exchangers, where membrane is not made use of, experience large troubles with regard to frost formation in cold climates. Even though the maximum efficiency for a plate heat exchanger can be as high as 90%, the yearly efficiency will drop when measures are taken to avoid frost formation during cold periods. Thus, these heat exchangers are not suited for use in cold climates.

Table 2.2 from NS 3031 (2014) lists the minimum discharge air temperature for different heat exchangers. Recuperative heat exchangers (not membrane based) in residential buildings have a frost protection temperature of +5 °C to +9 °C, which is well above the freezing point. Some parts of the heat exchanger, called "cold corners", may have a temperature which is somewhat lower than the average temperature. Thus, it is not enough to have a minimum leaving air temperature just barely above the freezing point.

The membrane based heat exchangers show promising figures, but are not yet commercialised. The heat wheel is the most used heat exchanger for residential buildings, and non-residential buildings where a small leakage from exhaust air to supply air can be accepted. Its properties with regard to frost formation and efficiency are also satisfactory. Thus, this is the most interesting case to look into in the heat recovery simulations.

Table 2.1: Comparison of different heat/energy exchangers, based on information from Alonso et al. (2015) unless stated otherwise.

Type of heat exchanger	Adjacent ducts	Sensible efficiency	Latent efficiency	Frost formation	Transfer of odour
Regenerative:					
Fixed matrix ¹	✓	70 – 80	–	Minor	✓
Heat wheel	✓	50 – 80	–	Minor	✓
Energy wheel	✓	80 – 85	80 – 85	✗	✓
Recuperative:					
Plate/tube	✓	60 – 90	–	✓	✗
Run-around	✗	65 – 70	–	✓	✗
Heat pipe ¹	✗	50 – 60	–	✓	✗
Membr. plate	✓	80 – 85	46 – 76	✗	✗
RAMEE	✗	60 – 80	50 – 65	✗	✗

¹ Novakovic et al. (2007).

Table 2.2: Minimum allowed discharge air temperature from heat exchanger, according to NS 3031 (2014)

Heat exchanger type	Min. temp. °C
Rotating wheel and fixed matrix, all buildings	–10 °C
Recuperative (plate, etc.), non-residential	+0 °C
Recuperative (plate, etc.), residential (optimum)	+5 °C
Recuperative (plate, etc.), residential (conservative)	+9 °C

2.2 Heat recovery using exhaust air heat pumps

Heat pumps are the most common alternative to heat exchangers for ventilation heat recovery. In addition to recovery of ventilation heat, the heat pump can also supply additional energy to the building. The heat pump may use for example outdoor air and/or energy from the ground as additional heat source, but this is not considered as heat recovery from ventilation air (see chapter 2.4, p. 20).

Using a heat pump for heat recovery has both advantages and disadvantages compared to the heat exchangers mentioned in chapter 2.1. The supply air and exhaust air duct do not have to be adjacent, which can be an important aspect when retrofitting heat recovery in existing buildings.

Depending on the system solution, the heat pump is able to supply energy for both DHW, space heating and preheating of the supply ventilation air. The heat pump evaporator is usually able to remove more energy from the exhaust air, compared to a heat exchanger. Small, residential passive houses have a very low yearly heat demand. Thus, a heat pump could be able to cover a considerable amount of the yearly heat demand in such buildings.

Some system designs are able to provide cooling of the supply air during periods with high outdoor temperatures. However, NS 3700 (2013) states that residential passive houses should achieve thermal comfort without mechanical cooling. There are usually no need for space heating or pre-heating of the supply air during the summer season, though there is still a demand for DHW. Some system solutions can heat DHW and at the same time provide cooling of the supply air. During the same period, a heat exchanger would not recover any useful energy.

Heat pumps are dependent on electrical energy for the compressor in order to recover heat. Thus, heat pumps use energy in order to recover heat that could be recovered with no or only limited energy consumption by a ventilation heat exchanger. That is one of the major drawbacks of using a heat pump for ventilation heat recovery.

An exhaust air heat pump increases the noise level from the technical room, seeing that the compressor normally is placed within the

building envelope, as opposed to heat pumps using outdoor air as only heat source. Thus, a higher requirement for sound insulation of the AHU cabinet or the technical room is required.

2.2.1 Thermodynamic basis for CO₂ heat pumps

Heat pumps are able to move energy from an energy source with low temperature to an energy sink with higher temperature, using heat exchangers, a compressor, an expansion device and a suitable refrigerant. The most basic components are illustrated in figure 2.2.

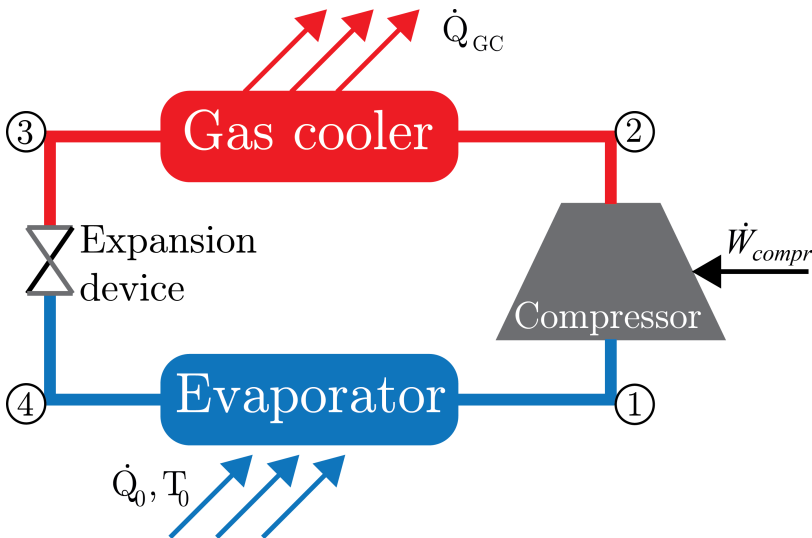


Figure 2.2: Illustration of the most basic components in a heat pump

Heat pumps operate in thermodynamic cycles. These cycles are usually drawn in log P-h diagrams or T-s diagrams. An additional diagram, the T-h diagram, is much used for CO₂ heat pumps. An illustration of a T-h diagram for a transcritical CO₂ heat pump cycle is shown in figure 2.3.

Dry saturated gas from the evaporator is compressed in the compressor. An ideal reversible compressor would result in condition 2_{is} . Condition 2_{ad} is a state representing adiabatic compression, where the isentropic efficiency is considered. The last state, 2_r , is the real state

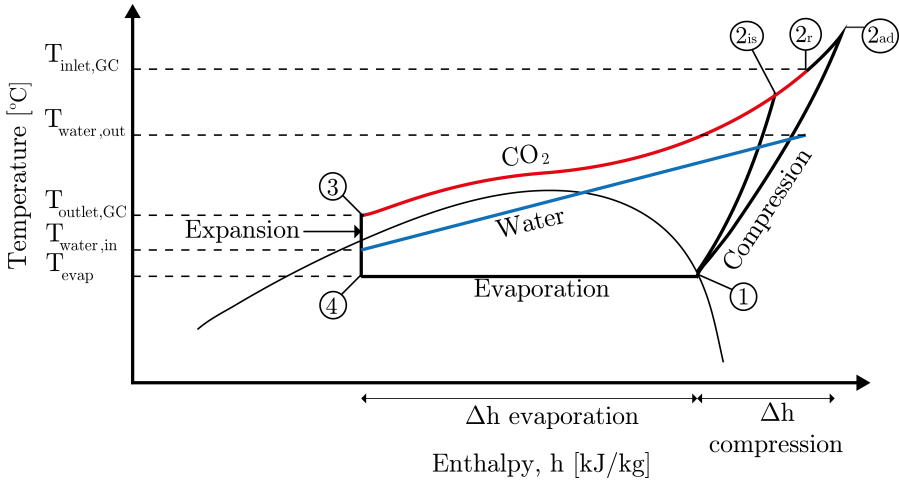


Figure 2.3: T-h diagram showing a general transcritical heat pump cycle. 2_{is} equals isentropic compression, 2_{ad} equals adiabatic compression, while 2_r is the real compression process, including heat loss from the compressor. Heat is given off from CO₂ (red line) to water (blue line). GC is short for "gas cooler".

of the refrigerant after compression. This process point has lower enthalpy than 2_{ad} due to heat loss from the compressor to the surroundings. However, the enthalpy can be both higher and lower than 2_{is} , depending on the heat loss rate. The equations and correlations used to calculate thermodynamic states are presented in chapter 5.3.2 (p. 67).

Heat is given off from CO₂ to water in the gas cooler, after the compression process. As distinct from subcritical heat pumps, heat is given off at a large temperature glide. This results in a good temperature adaptation between the CO₂ being cooled and the water being heated. The difference between heat rejection in a condenser (subcritical) and a gas cooler (transcritical) is illustrated in figure 2.4. Heat rejection at a large temperature glide results in a higher COP compared to heat rejection at a constant temperature. The heat transfer properties of CO₂ is also excellent (Stene, 2004). Thus, a transcritical CO₂ heat pump is a good choice for heating of DHW.

CO₂ differs strongly from refrigerants for subcritical heat pump

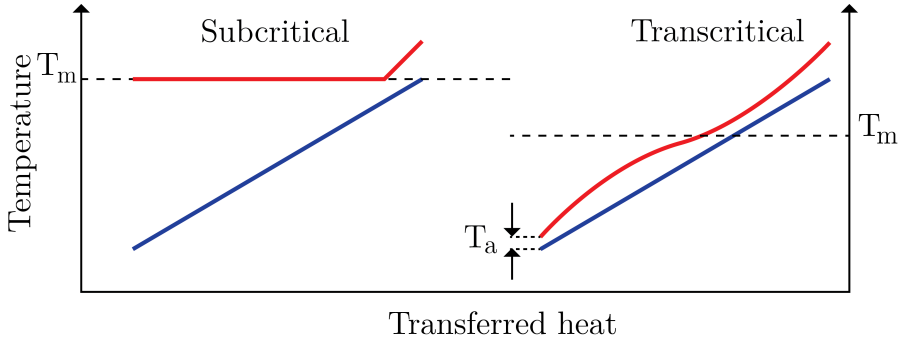


Figure 2.4: Comparison of average temperature during heat rejection for subcritical and transcritical heat pump. T_a is the temperature approach.

cycles. Subcritical cycles often use ammonia, HFCs or hydrocarbons (usually R290). The major difference between CO_2 and subcritical refrigerants is the critical point. The critical point of CO_2 is at $31.1\text{ }^\circ\text{C}$ and 73.8 bar , making it suited for transcritical operation.

Transcritical pressure lines (isobars) for CO_2 are shown in figure 2.5. Components for subcritical heat pump cycles often have a pressure rating of 25 bar to 40 bar . Some industry standard heat pumps operate at 60 bar . CO_2 heat pump components have a pressure rating of 120 bar to 150 bar on the high pressure side Stene (2014).

Increased gas cooler pressure results in a more linear isobar, which is advantageous for heat transfer in the gas cooler. The CO_2 gas behave more and more like an ideal gas at high pressures. Higher gas cooler pressures also increase the required compression work and the CO_2 discharge gas temperature. Thus, finding the ideal gas cooler pressure is not easily done.

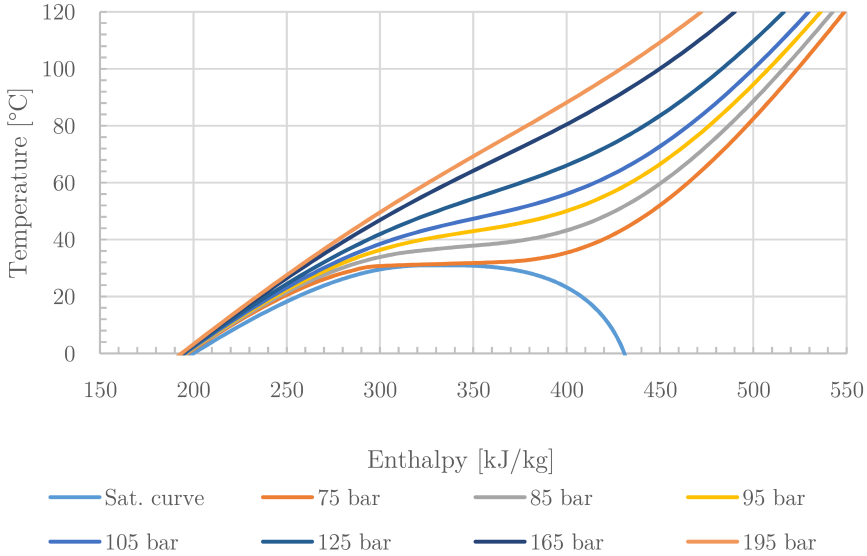


Figure 2.5: Transcritical pressure lines for CO_2 in a T-h diagram. The data was generated using NIST REFPROP.

2.2.2 System configurations

There are several different possible system configurations for heat pumps recovering energy from the exhaust air. The next sections assess the most common system configurations for exhaust air heat pumps. All configurations will experience frost formation on the evaporator when used in cold climates. Defrosting is required regularly, which reduces the SPF of the heat pump .

Air–air configuration

The air–air system configuration has an evaporator placed in the exhaust air duct and a condenser placed in the supply air duct. Heat is transferred directly from the exhaust air to the supply air. Heat cannot be stored, and all required heat must be produced instantaneously. The configuration can provide cooling of the supply air, if equipped with a four-way valve. Energy removed from the supply air is not utilized, but rejected to the exhaust air leaving the building.

The heat pump cannot be used for heating of DHW. During periods with high outdoor temperatures, the heat pump is thus not used (except for cooling). Efficient rotating wheels have efficiencies between 80% and 85%, which most of the year results in a sufficiently high supply air temperature in normal or mild Norwegian climates. An air–air exhaust air heat pump uses electrical energy in order to recover the same energy, and is thus much less efficient.

This heat pump configuration may be used for space heating. Warm air, heated by the heat pump, is supplied to the zones. Space heating through ventilation air has low investment costs compared to hydronic heating, but is not much used in Norway due to reduced ventilation efficiency and reduced thermal comfort. However, a recent study indicates that ventilation heating in Norwegian passive houses in could be feasible, due to the low heating demands (Holte, 2013).

Air–water configuration

Air–water exhaust air heat pumps reject the energy in the condenser or gas cooler to water. The condenser or gas cooler may transfer heat directly to a thermal storage, or to water circulating between the condenser/gas cooler and the thermal storage. Heat may also be given off directly to water in a hydronic heating circuit. The heated water may be used for DHW, space heating or ventilation heating, and is thus much more flexible than the air–air configuration.

Products with this system configuration are usually not able to provide cooling of the supply air, seeing that they do not have a heat exchanger (CO₂–air) placed in the supply air duct. However, a solution proposed by Renedo et al. (2007) enables cooling of the supply air and heating of DHW at the same time. Dampers are used to switch the flow direction through the evaporator. Thus, the supply air is guided to the heat pump evaporator, while the exhaust air bypasses the evaporator.

Air–air/water configuration

This heat pump configuration is able to give off heat to both water and to the ventilation supply air. This system configuration is used by the Danish AHU and heat pump manufacturer Nilan (see chapter 3.3.3,

p. 35), among others. The advantage of air–air/water configurations is the possibility to cool the supply air and heat DHW simultaneously. This is made possible by placing a heat exchanger (CO_2 –air) in the supply air duct, together with a CO_2 –water heat exchanger in the storage tank. A simplified sketch of this system configuration is shown in figure 2.6.

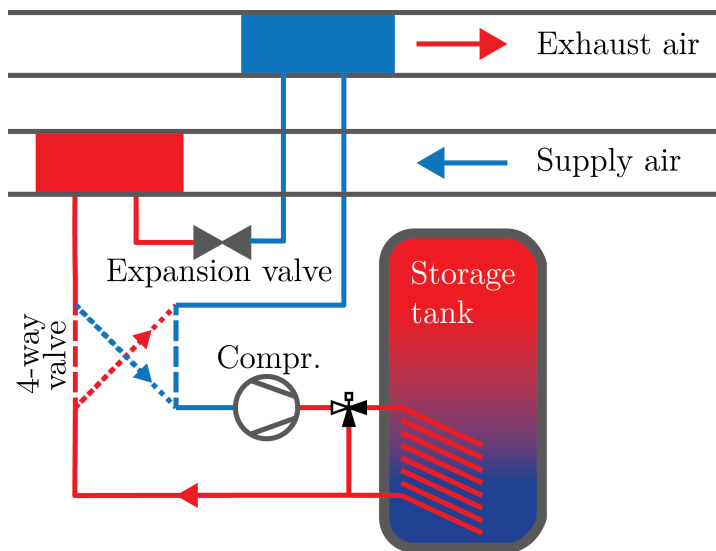


Figure 2.6: System configuration sketch for air–air/water systems in heating mode. The dotted lines illustrate the refrigerant flow in cooling mode. The illustration does not take optimum flow directions in the heat exchangers into consideration.

When running in cooling mode, a four-way valve changes the refrigerant flow through the heat exchangers in the exhaust and supply air duct. Heat is given off to the DHW tank. Any surplus energy is given off in the exhaust air duct.

This system configuration is often used for space heating through ventilation air. The basic model from Nilan (chapter 3.3.3) is only able to provide space heating through warm supply air, and not through hydronic heating in the zones.

2.3 Hybrid heat recovery

Hybrid heat recovery solutions use a ventilation heat exchanger (chapter 2.1), often plate or heat wheel, and one of the heat pump configurations mentioned above (chapter 2.2.2). The exhaust air passes through a ventilation heat exchanger and gives off heat to the supply air. Thereafter, exhaust air passes through the heat pump evaporator before leaving the building. A ventilation heat exchanger have an efficiency of less than 100%, resulting in an air temperature after the ventilation heat exchanger above the outdoor air temperature. The difference in temperature between the discharge air after the heat exchanger and the outdoor air is illustrated in figure 2.7 for different heat exchanger efficiencies and outdoor temperatures.

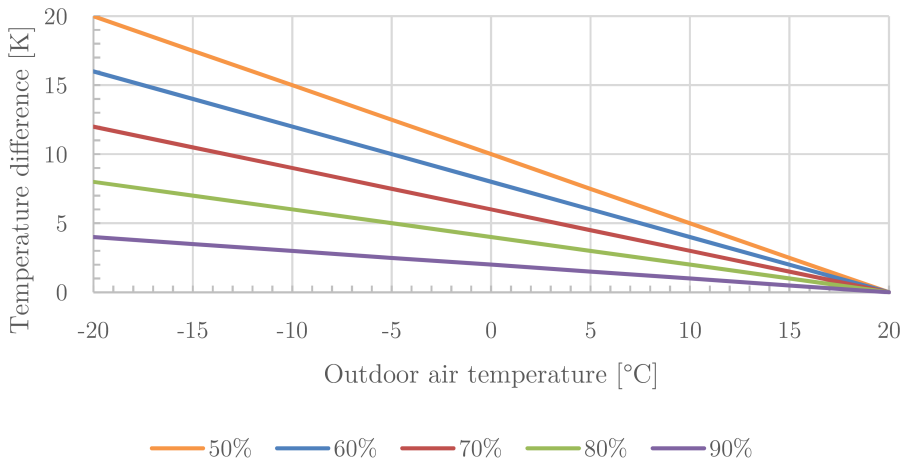


Figure 2.7: Temperature difference between discharge air and outdoor air for different heat exchanger efficiencies. The indoor temperature is set to 20 °C.

The difference in temperature between the air after the ventilation heat exchanger and outdoor air is taken advantage of by the exhaust air heat pump. The increased temperature of the heat source is beneficial for the heat pump performance, seeing that more energy can be removed from the air before reaching the minimum temperature.

Alternatively, the heat pump will be able to operate at an increased evaporation temperature.

The products from Genvex, Nilan and Exvent (chapter 3.3, p. 31) are examples of products for hybrid heat recovery. The products from Genvex and Nilan are based on the air–air/water system configuration, using plate heat exchangers for ventilation heat recovery. The product from Exvent is based on the air–air system configuration, using a heat wheel for ventilation heat recovery. According to Fabrizio et al. (2014), the main advantage for hybrid heat recovery systems is the packed configuration and its easy assembly and installation in residential buildings.

2.4 Heat pumps for ventilation heat recovery in NS 3031 (2014)

The revised edition of NS 3031 from 2014 contains a supplement for calculation of the performance for exhaust air heat pumps. Recovered energy from the exhaust air can be used for preheating of the supply air, but also DHW and space heating, and still be regarded as *recovered* energy. Figure 2.8 illustrates the energy flows in an exhaust air heat pump.

The amount of recovered energy equals energy removed from the exhaust air down to outdoor temperature. Removal of energy from the exhaust air beneath the outdoor temperature is *not* regarded as recovered energy. The useful energy from the exhaust air heat pump consists of three parts:

- Recovered energy
- Compressor energy used to recover the above energy
- Energy removed from exhaust air below the outdoor temperature, plus the compressor energy used to obtain that energy

The first part, the recovered energy, is calculated according to equation 2.1. η equals the combined efficiency for heat distribution, heating control and heat emission. Equation 2.2 calculates the amount of energy used by the compressor for heat recovery. Equation 2.3 calculates

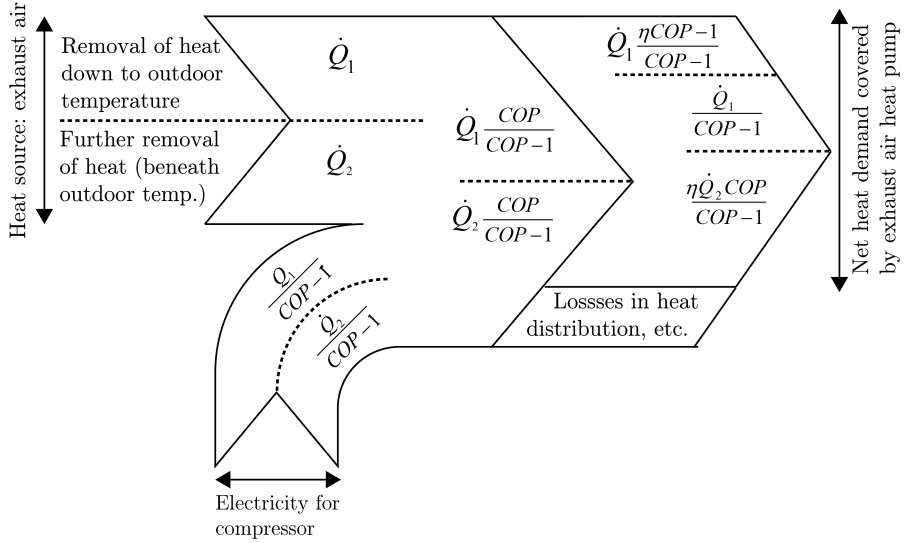


Figure 2.8: Energy flows in an exhaust air heat pump, according to NS 3031 (2014).

the third share of energy from the exhaust air heat pump. The annual amount of recovered energy is thus calculated according to equation 2.4, where a time step of one hour or less should be used. The *recovered* energy from the exhaust air is subtracted from the annual energy demand for heating in the building. The energy used by the compressor is added to the net energy heating demand.

$$\dot{Q}_1 \frac{\eta COP - 1}{COP - 1} \quad (2.1)$$

$$\frac{\dot{Q}_1}{COP - 1} \quad (2.2)$$

$$\frac{\eta \dot{Q}_2 COP}{COP - 1} \quad (2.3)$$

$$Q_{\text{rvd, hp}} = \sum_{i=1}^{8760} \dot{Q}_{1,i} \frac{\eta_i COP_i - 1}{COP_i - 1} \quad (2.4)$$

Chapter 3

Literature

Relevant literature on heat exchangers and heat pumps for ventilation heat recovery were presented in the project report (Solberg, 2014). This chapter will provide some additional literature on heat pumps for ventilation heat recovery, including hybrid heat recovery. The following scientific databases and research publication websites were used in the search for relevant literature:

- AIVC Publications
- DAIM
- DiVA portal
- Fraunhofer Publica
- Google Scholar
- Purdue e-Pubs
- REHVA Publications & Resources
- ResearchGate
- ScienceDirect
- Scopus
- Web of Science

Different combinations of the following keywords were used in the search for relevant publications. In addition, the bibliography of relevant publications was looked over in search for other useful publications. Some employees at SINTEF and NTNU were also asked for relevant publications.

- Carbon dioxide
- CO₂
- CVHD
- EAHP
- Energy recovery
- Exhaust air
- Heat pump
- Heat recovery
- Ventilation air

Only a limited number of relevant publications were found. Most of the reports have investigated the performance of an exhaust air heat pump or a hybrid recovery unit at a constant heat demand and constant temperatures, for example at winter or summer conditions. No reports were found where the annual energy performance of a residential building equipped with a heat pump for heat recovery was assessed. In the following sections, publications regarding exhaust air heat pump solutions and hybrid solutions are looked into and discussed.

3.1 Exhaust air heat pump heat recovery

Ott (2006) set up and tested an exhaust air CO₂ heat pump for combined space heating and hot water heating. The heat pump used active control of both gas cooler pressure, super heating and water mass flows in order to maximize the COP. The gas cooler pressure was altered according to operating mode: tap water heating mode or space heating mode. The prototype heat pump had a heating capacity of 2 kW, removing energy from 150 m³/h exhaust air initially at 20 °C. Water

was heated from 25 °C to 35 °C in space heating mode. Corresponding numbers for heating of DHW were 17 °C and 70 °C. The evaporation temperature was -1 °C, while the optimum super heating was chosen in a tolerated range from 3 K to 9 K.

Results from the prototype CO₂ heat pump experiments showed that the gas cooler pressure resulting in the highest COP (3.22) for space heating was 82 bar. The optimum gas cooler pressure for heating of domestic hot water was 100 bar, resulting in a COP of 3.19. Ott also compared these results to a propane (R290) heat pump. The propane heat pump achieved a COP of 4.2 and 2.7 for space heating and heating of DHW respectively.

The space heating and DHW heating COP values are approximately the same. The inlet water temperature in the case of space heating is lower than the corresponding value for heating of DHW, but the required compression work for heating of DHW is higher due to higher gas cooler pressure. These two factors seems to level each other out.

The experiments performed by Ott show that a CO₂ heat pump is a rational choice for heating of DHW, but not necessarily for space heating. Three blocks of flats located in Oslo (Tveita housing cooperative) were recently refurbished, including the DHW and space heating plant (Borge, 2014). A large CO₂ heat pump was installed for heating of DHW, and an additional heat pump using R134a was installed in order to cover the space heating demands. Both heat pumps were using exhaust air as heat source. The dedicated DHW heat pump achieved a SPF of 4.5. The performance of the R134a heat pump was not investigated.

These two reports show that a CO₂ heat pump is an excellent choice for heating of DHW, though not necessarily for space heating. However, Stene (2004) looked into a CO₂ heat pump for *combined* space heating and heating of DHW, and compared it to a heat pump using a HFC as refrigerant. The results showed that the CO₂ heat pump performed better than the HFC heat pump in cases where the yearly delivered energy for DHW production was more than 25% to 30% of the total yearly delivered heat from the heat pump. The main reason for the high CO₂ heat pump performance was the use of a tripartite gas cooler. A tripartite gas cooler consists off three parts. The last part of the gas

cooler gives off heat to preheat the DHW, the middle part gives off heat to space heating, and the third part reheats the DHW to the setpoint temperature. The tripartitioning results in an excellent temperature adaptation for water being heated and CO₂ being cooled down. The COP for combined mode (DHW *and* space heating) was thus higher than the COP for heating of DHW only. For a single-unit dwelling, it would normally not be economically feasible to install one CO₂ heat pump for heating of DHW and another HFC based heat pump for space heating. Therefore, a solution with a tripartite gas cooler should be used – both with regard to life-cycle costs and environmental aspects.

Stavset et al. (2014) performed simulations on a CO₂ exhaust air heat pump for DHW, space heating and heating of ventilation air. The simulations were carried out for 5 consecutive winter days with an outdoor temperature of -10 °C. The heat pump used in the simulations consisted of a standard evaporator, suction gas heat exchanger, tripartite gas cooler, compressor and expansion valve. The gas cooler pressure was set to 85 bar constantly. The ventilation air flow rate was set to 2.1 m³/hm² when occupied, and 1.2 m³/hm² when not occupied. Five different scenarios with different occupant behaviour models and heat pump controllers were assessed, where the DHW, SH and VH energy demands were set to constant values, depending on the occupant behaviour (home, not home or sleeping). The resulting COP for the different scenarios ranged from 4.1 to 4.5 for combined DHW, space and ventilation heating on a winter day. The heat pump was able to cover the entire heating demand (DHW, SH and VH) for the building.

The simulations were only performed for a constant outdoor climate, resulting in a constant heat demand depending on whether the occupants are home and awake, not at home, or sleeping. The model does therefore not assess the performance during different seasons. The average daily ventilation air flow rates used in the model vary from 1.8 m³/hm² to 2.1 m³/hm². This is 50% to 75% more than the minimum air flow rate according to the Norwegian building code (Technical Regulations, 2010), which may increase the COP of the heat pump, but also increase the total demand of delivered energy to the building.

Based on the numbers stated in the report, the average outlet air temperature from the evaporator is equal to about -8 degC or less

(for scenario #1). However, the report concludes that there was no need for active defrosting of the heat pump evaporator. This is caused by periods with a lower heat demand, resulting in outlet temperatures from the evaporator above the freezing point (Alonso, 2015).

The results from the report show that an exhaust air CO₂ heat pump can obtain high COP values when operating in winter mode. In addition, the report shows that the system losses due to defrosting of the evaporator may be low or non-existent.

3.2 Hybrid heat recovery

Kluge (2008) investigated the performance of "Vitotres 343", a CVHD (compact ventilation and heating device) from Viessmann. The device was the first of its sort from Viessmann for residential passive houses (Viessmann, 2014), and could use both exhaust air and outdoor air as heat source for the heat pump. The refrigerant used in the heat pump was R134a. Measurements on the device were carried out with an outdoor temperature of 3.5 °C to 5°C and a room temperature of 26 °C. The supply air temperature from the CVHD was 22.5 °C. The CVHD operated with an exhaust and supply air flow rate of about 137 m³/h. The fan supplying the evaporator with outdoor air was not activated during the measurements. Therefore the measurements were performed with exhaust air as only heat source. The measurements showed an heat exchanger efficiency of 83.3%. The COP of the heat pump was measured to 2.06. At these conditions, the heat pump provided a heating power of 1.28 kW.

Kluge (2008) also looked into different ways of improving the performance of the heat pump. Use of a suction gas heat exchanger (SGHX) was estimated to increase heat pump COP by 2.8% at summer conditions and 3.2% at winter conditions for the R134a heat pump. The performance is increased, but the investment cost of the CVHD is also increased. Stene (2004) performed calculations on a CO₂ heat pump showing that an increasing superheat of the CO₂ before compression had a *very* limited impact on the COP. Thus, a suction gas heat exchanger should only be used in cases where it is necessary to evaporate liquid CO₂ in the suction line, in order to avoid compressor failure.

Kluge (2008) also estimated that substituting R134a with CO₂ would increase the COP by 18% at summer conditions and 9.8% at winter conditions, which substantiates the advantage of using CO₂ as refrigerant in such applications.

Calay and Wang (2013) proposed a hybrid heat recovery system consisting of an energy wheel and a reversible air–air heat pump. Isentropic compression and a constant temperature difference of 15 °C in heat exchangers were assumed. Between 64% and 73% of the heat energy could be saved using the energy wheel and the heat pump, compared to a system with an electric heater. Though not stated clearly in the report, it is assumed that it is the space heating and ventilation heating demand that are reduced by the given percentage.

The solution proposed by Calay is not able to reduce the amount of delivered energy for heating of DHW. The total energy saving is thus limited in passive houses with a low energy consumption for space heating and ventilation heating, compared to energy for heating of DHW. The calculations performed in the report are of limited accuracy and value due to isentropic compression, very simplified heat exchanger modelling and calculations only for selected operating conditions. The choice of refrigerant is not stated.

Fraunhofer ISE proposed a CVHD solution for high performance buildings, for space heating, heating of DHW and heating of the ventilation air (Bühning, 2005). The solution provides space heating using hot ventilation supply air. The CVHD uses a heat exchanger for passive ventilation heat recovery, and is thus a hybrid solution. The Fraunhofer CVHD also had an earth–air heat exchanger to preheat the ventilation air, and a solar collector to heat the storage tank whenever possible. Such solutions have a market share of 30% to 50% in the German market for residential passive houses and low energy houses, according to the report.

Three different commercialized products were tested according to the NS-EN 255-3 (2008) test procedure (now replaced by NS-EN 16147 (2008)). Product A had a solar collector and an earth–air heat exchanger, in addition to a passive air–air heat exchanger and an exhaust air heat pump. One condenser was located in the storage tank and another condenser was placed in the supply air duct. Product B was the

same solution as product A, but without the earth–air heat exchanger. Product C used both exhaust air and outdoor air as heat source, seeing that the product is meant for buildings with a higher heat demand than passive houses. The outdoor air was constantly mixed in with the exhaust air before the evaporator. The heat pump condenser transfers all heat to an internal brine loop. The brine may also be heated by heat from solar collectors or electrical resistance heaters. The heat is subsequently given off to the supply air and/or the thermal storage. The most relevant results from the tests are presented in table 3.1. The measurements were performed without solar collectors activated.

Table 3.1: Test results for three different commercialized products.

Parameter	Prod. A	Prod. B	Prod. C
Exhaust air flow rate [m ³ /h]	146	132	140
Outdoor air flow rate [m ³ /h]	–	–	144
COP after drawing of tank [–]	3.02	2.64	2.26 ¹
COP heating days [–]	3.39	3.15	–

¹ A more efficient brine pump would result in a COP of 2.7.

It is difficult to compare the different products, seeing that they are dimensioned differently. The COP of an exhaust air heat pump is to a large degree depending on the amount of energy removed from the exhaust air in the gas cooler. It is assumed that the test was carried out under as equal conditions as possible, in order to be able to compare the different products. The test showed that product A performed better than product B. However, product A had a higher evaporator air flow rate *and* an earth–air heat exchanger. It is likely to assume that most of the increased performance is due to the earth–air heat exchanger. Product C performed worse than product A and B. However, if a more energy efficient brine pump had been used, the COP would rise to 2.7, which is about the same as product B. It is likely that the brine circuit would result in a somewhat reduced performance, but the extra outdoor air energy for the evaporator seems to even out the differences.

50 detached single family passive houses equipped with a CVHD

were monitored for three years by Fraunhofer ISE (Bühning, 2005). 23 of the houses used a ventilation device with an earth coupled heat pump. The remaining 27 used a ventilation device with an exhaust air heat pump. Both systems were equipped with solar collectors. The buildings equipped with an exhaust air heat pump consumed in average about 3000 kWh/m²yr, compared to 3600 kWh/m²yr for buildings with earth coupled heat pumps. The relatively high energy consumption of the earth coupled heat pump system was caused by interaction problems between different controllers, energy for the brine pump, and controller parameters for the storage tank that were not optimized. Even though the earth coupled heat pumps were not controlled ideally, the results shows that a hybrid heat recovery system utilizing an exhaust air pump may achieve a high performance.

3.3 Available commercialized products

There are several commercialized products providing heat recovery using heat pumps for residential buildings. This chapter presents some commercialized solutions for *balanced* ventilation, offering recovery with heat pump technology with or without additional passive heat recovery. Many products for exhaust ventilation exist. Such products are dominant in residential buildings in Sweden. However, only products for balanced ventilation are taken into consideration. System solution, advantages, drawbacks and technical information are presented for each product. No products using R744 as refrigerant were found. Equivalent systems using other refrigerants are interesting and relevant nevertheless. The information written in this chapter is based on information found on the manufacturers' websites, unless stated otherwise.

3.3.1 NIBE – heat pump recovery

NIBE, founded in Sweden, is the largest manufacturer of domestic energy products in the Nordic countries. They offer several solutions using heat pumps for heat recovery from exhaust air in exhaust ventilation systems. NIBE also has a product for balanced ventilation called "*NIBE F470*" (NIBE, a,b). The product does not have a heat exchanger for passive heat recovery. Heat is transferred from exhaust air to water in a tank-in-tank. The system design of "*NIBE F470*" is shown in figure 3.1. The system cannot provide cooling of the supply air. Heat can only be recovered using the heat pump. This is a large disadvantage compared to hybrid solutions where a passive heat exchanger is used to recover heat with close to no energy consumption, before the heat pump recovers additional energy.

Advantages:

- Natural refrigerant
- Possible with high supply water temperature at low pressure rating (PN25), due to using R290

Drawbacks:

- No passive heat recovery
- Cooling of supply air not possible

NIBE also has another product called "NIBE F750". The product is originally for exhaust ventilation, but can be used for balanced ventilation with supplementary equipment. The required supplementary equipment for balanced ventilation (supply air fan, filter, heating coil, etc.) is placed in a separate unit due to lack of space in the standardized NIBE cabinet (Solsem, 2015b). This product does not offer passive heat recovery neither. The refrigerant is R407C, and the compressor used in the product is a larger frequency controlled rolling piston compressor (ABK Klimaprodukter, 2015).

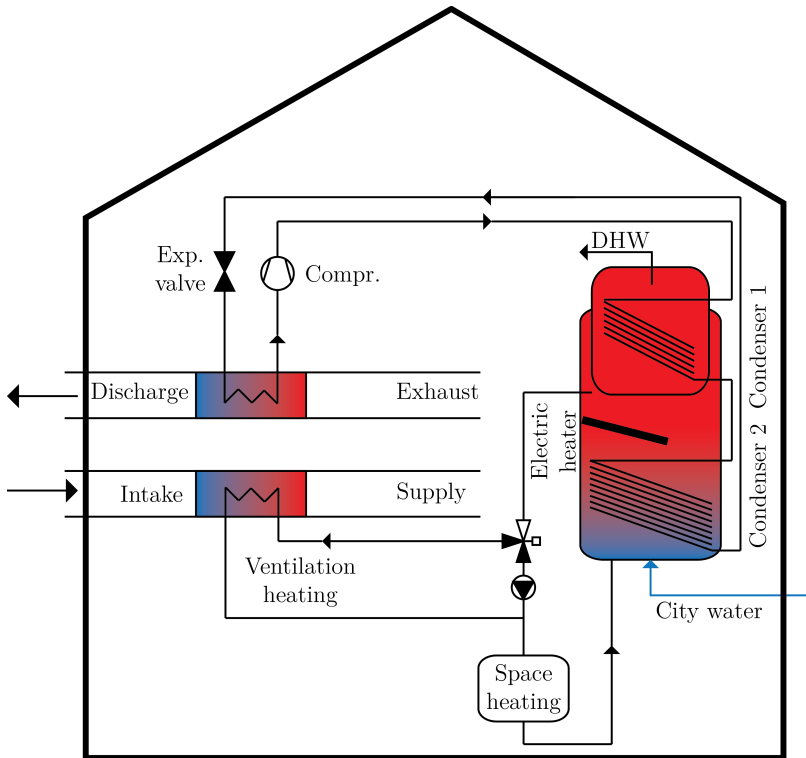


Figure 3.1: System solution of NIBE F470 (Solsem, 2015a).

3.3.2 Genvex – hybrid recovery

Genvex is a Danish manufacturer of air handling units, owned by NIBE. "Genvex COMBI 185 S/LS" is an air handling unit offering hybrid heat recovery using an aluminium plate heat exchanger and an air–water/air heat pump. The AHU comes in two different compressor sizes, hence the "S/LS" in the product name. The system solution does not offer active cooling, even though it has a condenser placed in the supply air duct and therefore could achieve active cooling by using a four-way valve. An illustration of the "COMBI 185 S/LS" is shown in figure 3.2.

Heat is given off to a storage tank and to the supply air in order to provide heating of the building. According to Madsen (2015), service coordinator at Genvex, the maximum supply air temperature is set to

45 °C. The supply air flow is increased if the supply air temperature exceeds the limit.

According to Madsen (2015), a counter-current plate heat exchanger is used due to its efficiency of up to 90%, and the fact that the heat wheels are usually not efficient enough to satisfy Danish building codes.

Advantages:

- Hybrid recovery
- Prepared for solar collectors
- R134A has the lowest GWP value of the most common HFC refrigerants, together with other attractive thermodynamic properties

Drawbacks:

- Drain from heat exchanger required
- Active cooling not possible, though having a condenser in the supply air duct
- Plate heat exchanger for passive heat recovery
- Heating of DHW and ventilation air only
- Space heating with ventilation air
- Intermittent control of compressor

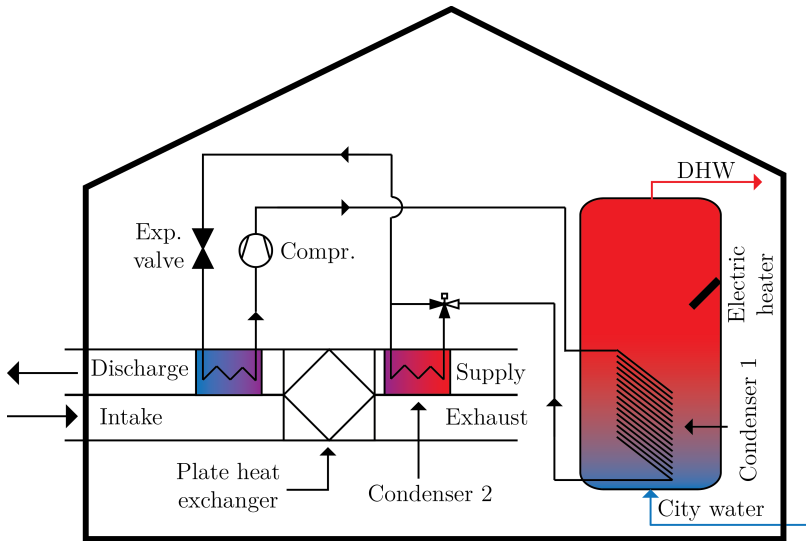


Figure 3.2: System solution of Genvex 185 S/LS (Solsem, 2015a).

3.3.3 Nilan – hybrid recovery

The Danish manufacturer Nilan produces ventilation units for both exhaust ventilation and balanced ventilation. Several different solutions for balanced ventilation are available. Only solutions able to provide hydronic heating and heating of domestic hot water are taken into account in this report. The *”Compact P Nordic”* series is a series of hybrid heat pumps with different possibilities for additional heat sources. *”Compact P Nordic”* is the basic model providing heat recovery using a polystyrene counterflow heat exchanger for passive heat recovery and a heat pump for active heat recovery. *”Compact P Nordic GEO”* has an additional heat pump extracting heat from bore hole(s) or the soil around the house. *”Compact P Nordic UVP”* has an additional heat pump extracting heat from the outdoor air. Since the two solutions are using an additional heat pump in order to utilize the additional heat source, only *”Compact P Nordic”* is allowed for in the continuation.

”Compact P Nordic” has two condensers, as illustrated in figure 3.3: One is placed in the DHW storage tank, while the second condenser is placed in the supply air duct. The condenser in the supply air duct

makes active cooling of the supply air possible by utilizing a three-way valve. Heat removed from the supply air, together with compressor energy, can be used to heat the DHW tank. Excess energy is released to the exhaust air. A damper may bypass the passive heat exchanger if desired.

Advantages:

- Passive heat recovery
- Cooling of supply air and heating of DHW at the same time
- Prepared for additional heat source (geothermal or outdoor air), solar heating and extra storage tank
- Bypass of passive heat exchanger possible
- Variable speed drive

Drawbacks:

- Drain from heat exchanger required
- Heating of supply air before heat exchanger required in order to avoid freezing. Reduces thermal efficiency.
- Heating of DHW and ventilation air only.
- Space heating with ventilation air.
- Refrigerant has high GWP

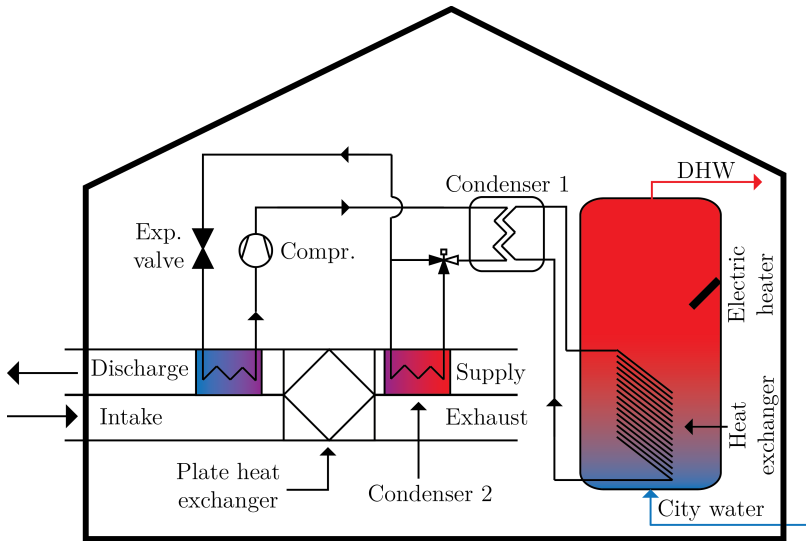


Figure 3.3: System solution of Nilan Compact P Nordic. The illustration represents the unit operated in heating mode.

3.3.4 Enervent/Exvent – hybrid recovery

The Finnish air handler unit manufacturer Exvent has developed a hybrid heat recovery solution called *"Greenair HP"*. *"Greenair HP"* is the brand name for AHUs equipped with a heat wheel and an integrated exhaust air to supply air heat pump. There are three different AHU models with the *"Greenair HP"* technology. The heat pump has a four-way valve in order to utilize the heat pump for both heating and cooling of the supply air. The heat pump transfers heat directly from the exhaust air to the supply air. Thus, heat cannot be accumulated and the solution cannot provide heating of DHW. Condenser energy is not made use of when operated in cooling mode. Hot air heating is utilized when the building has a heating demand. The system solution for the Exvent heat recovery solution is illustrated in figure 3.4.

Advantages:

- Passive heat recovery
- Rotating heat exchanger (high efficiency, less troubled with frost formation)
- Cooling of supply air possible
- Variable speed drive

Drawbacks:

- Heat pump energy can only be used for heating/cooling of supply air, not DHW
- Hot air heating may reduce thermal comfort
- Heat cannot be accumulated
- Refrigerant has high GWP

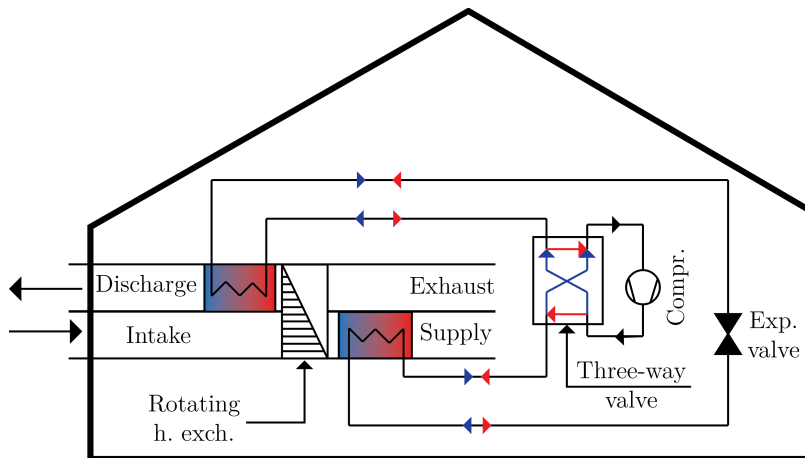


Figure 3.4: System solution of Exvent Greenair HP. Red (heating mode) and blue (cooling mode) arrows illustrate refrigerant flow direction.

3.3.5 Comparison of commercialized products

A table comparing some of the most important parameters of the different heat recovery solutions is presented in table 3.2. Nilan and Exvent both use R410A as refrigerant. R410A is an unnatural refrigerant with a GWP value of 2090 (Forster. et al., 2007), compared to 1300 for R134a (Stene, 2014) and 3 for the natural refrigerant R290 (Lampugnani and Zgliczynski, 1996).

The product from NIBE has no possibility for passive heat recovery. All heat recovery is done utilizing the heat pump. Much heat could be transferred from the exhaust air to the supply air without any energy consumption, as in the solutions from Nilan and Exvent.

Exvent uses a rotating wheel for passive heat recovery, which is advantageous with regard to frost formation. Heat from the heat pump can only be given off to the supply air, which is a large disadvantage for this solution. Heating of DHW amounts to a large part of the total heating demand, and cannot be covered by the Exvent heat recovery solution. In addition, space heating with hot supply air is often not desired.

All solutions, except the product from NIBE, have a condenser placed in the supply air duct. The purpose of this condenser is to provide space heating through the supply air. This heating method is not much utilized in Norway, due to reduced ventilation efficiency and reduced thermal comfort. The solution from NIBE, where water from a storage tank may be used to preheat the supply air, seems like a more rational solution for Norwegian conditions.

The air handling unit from Nilan has the best system configuration for heat recovery in a passive house, compared to the alternative products presented in this chapter. A large advantage, compared to NIBE, is the passive heat exchanger. Compared to the solution from Genvex, it has a VSD controlled compressor, and is able to provide cooling of the supply air and at the same time heat DHW.

The solution from Nilan is not an ideal solution. The largest disadvantage is the choice of heat exchanger. A heat wheel would be a choice for Norwegian conditions due to strongly reduced frost formation at low outdoor temperatures and easy control of heat exchanger efficiency. CO₂ should be the preferred refrigerant for exhaust air heat

pumps in residential passive houses, considering the large share of energy used on heating of DHW.

Table 3.2: Comparison of the different heat recovery products

	NIBE	Genvex	Nilan	Exvent
Passive heat exchanger type	None	Aluminium plate h.ex.	Polystyrene plate h.ex.	Rotating h.ex.
Heat source(s)	EA	EA	EA	EA
Heat sink(s)	Water	Water/air	Water/air	Air
Cooling option	✗	✗	✓	✓
Refrigerant	R290	R134a	R410A	R410A
Tank volume [dm ³]	170 + 70	185	175	N/A
Compressor type	Piston	Piston	Piston	Scroll
Compr. control	On/off	On/off	VSD	VSD

Chapter 4

Basis for simulations

A well-insulated detached residential building is used to investigate energy efficiency and energy consumption for the different heat recovery solutions. Residential buildings amounts to 38% of the total Norwegian building stock. 52% of these buildings are detached houses (Dar, 2014). The most important properties of the building, together with different occupant behaviour models and climates are presented in this chapter. The different heat recovery and/or energy supply cases are also explained.

4.1 Building used in simulations

The single-unit dwelling used in this thesis is rectangular, consisting of two floors, with hipped cold roof. The building, named "Karita" is one of Mesterhus' most popular houses. The GIA of the building is 172.6 m², which is a normal size for single-unit dwellings in Norway. An illustration of the building is shown in figure 4.1.

The drawings of "Karita", provided by Mesterhus, are intended for houses in accordance with the prevailing building code (Technical Regulations, 2010). Thus, only internal measures with regard to floor area, window and door areas, plus placing of doors, windows, internal walls and internal doors are kept. Other parameters, such as wall thickness and other thermal properties, are changed in order to fulfil the Norwegian passive house standard for residential buildings (NS 3700, 2013).



Figure 4.1: Illustration of "Karita", used with authorization from Mesterhus.

The thermal properties and energy efficiencies of the building and the building envelope are listed in table 4.1.

Table 4.1: Thermal properties and energy efficiencies of "Karita"

Parameter	Value	Unit
U-value, external walls	0.15	W/m ² K
U-value, window panes	0.6	W/m ² K
U-value, window frames	0.9	W/m ² K
U-value, roof	0.09	W/m ² K
U-value, ground floor	0.08	W/m ² K
Thermal bridges, normalized	0.03	W/m ² K
Solar heat gain coefficient	0.55	–
Air leakage number, n ₅₀	0.6	h ⁻¹
Specific fan power	1.5	kW/ m ³ /s

The values used in table 4.1 are based on either minimum requirements or typical values for residential passive houses, according to NS 3700 (2013). Conformity with the passive house standard has been verified using Simien, a software developed by "ProgramByggerne".

The passive house standard also contains requirements regarding energy supply sources, which is not taken into account. A heat wheel with a maximum efficiency of 80%, which is the minimum requirement, was used in Simien when verifying the fulfilment of NS 3700 (2013). Heat loss from thermal bridges are assumed evenly distributed over the total building envelope area.

4.2 Occupants' behaviour

The occupants' behaviour may have a large impact on yearly energy use. Heat loss from the building envelope is reduced to a minimum in residential passive houses. Thus, energy consumed by the occupants (DHW and electrical appliances) dominate the total energy consumption. The simulations in this report are carried out with three different occupant behaviours in order to examine the influence and sensitivity of occupants' behaviour with regard to energy. The three different models differ particularly in means of DHW consumption, but also with regard to presence within the building body, use of electrical appliances and rooms not in use. A doctoral thesis by Dar (2014) emphasize the importance of the occupants' behaviour when dimensioning and designing the heating system. Using different occupant behaviour models in the simulations can be used to assess the sensitivity of the results with regard to the occupants' behaviour.

It is assumed that the temperature setpoints in the different rooms are the same for all occupants behaviours, unless stated otherwise. The assumption is the same for indoor lighting, which use values from NS 3031 (2014).

The three occupant behaviour models mentioned below have 2, 4 and 5 members. The occupants' presence in the building are assumed to be as shown in appendix A.2.

4.2.1 Standardized occupant behaviour model (NS3031)

The standardized occupant behaviour is based on NS 3031 (2014). The standard contains standardised figures per square metre for DHW consumption and internal loads (lighting, occupants and appliances).

These figures are listed in table 4.2. It is assumed that 100% of the energy used for lighting and 60% of the energy used for equipment are heating up the surrounding air. The remaining 40%, in addition to energy for DHW, is not contributing to heating of the indoor air (NS 3031, 2014). The standardized behaviour model is situated in between the two other behaviours with regard to DHW consumption and energy consumption for electrical appliances.

Table 4.2: Standard figures from NS 3031 (2014) for DHW, lighting and equipment. 16 operating hours a day.

	Yearly energy consumption kWh/(m ² yr)	Share of energy converted to heat in zone
DHW	29.8	0%
Lighting	11.4	100%
Equipment	17.5	60%

4.2.2 "Small" occupant behaviour model

The "Low" occupant behaviour model is represented by an elder couple, and is meant to be a behaviour model with low energy consumption. The heating setpoint is reduced to 10 °C in rooms not in use, and the lights are turned constantly off in the same rooms. It is assumed that the two bedrooms on the western side of the building are not in use (see figure 5.2, p. 56). The doors to these rooms are constantly closed, and do not follow the same door schedule as the two other occupant models illustrated in appendix A.3.

The energy consumption of electrical appliances is reduced to 25%, compared to the value from NS 3031 (2014), due to fewer occupants and fewer appliances.

The main parting matter is the consumption of DHW, as the occupants are assumed to take one shower each, every second day. Table 4.3 shows the basis for the calculation of assumed DHW consumption for this occupant behaviour model.

Table 4.3: Calculation of DHW consumption for "Small" occupant behaviour model. "Spec. energy" equals yearly energy per square metre GIA.

	No.	Mass flow	dT	Time	E. per op.	Energy
	–	kg/s	K	min	kWh	kWh/yr
Showering	365	13	32	6	–	1058
Dishwashing	122	–	–	–	2.5	304
Hand wash	2190	13	35	0.5	–	578
Misc.	–	–	–	–	–	150
Total energy						2090
Spec. energy						12.1

4.2.3 "Large" occupant behaviour model

The "Large" occupant behaviour model represents a family of two adults and three children with a high energy consumption. The energy consumption of electrical appliances and DHW is set to be evidently higher than the two others. Table 4.4 shows the basis for the calculation of assumed DHW consumption for "Large" occupant behaviour model. It is assumed that all five members of the family shower once a day. The average time per shower is increased by two minutes, compared to the calculations for the "Small" model.

The energy consumption of electrical appliances is increased by 25% compared to the standard number from NS 3031 (2014), due to more inhabitants.

Table 4.4: Calculation of DHW consumption for "Large" occupant behaviour model. "Spec. energy" equals yearly energy per square metre GIA.

	No.	Mass flow	dT	Time	E. per op.	Energy
	–	kg/s	K	min	kWh	kWh/yr
Showering	1825	13	32	8	–	7052
Dishwashing	183	–	–	–	2.5	456
Hand wash	5475	13	35	0.5	–	1446
Misc.	–	–	–	–	–	200
Total energy						9155
Spec. energy						53.0

4.2.4 Comparison of occupant behaviour models

The most important differences between the three three different occupant behaviour models are shown in table 4.5. They differ widely, especially with regard to the consumption of DHW. "Small" and "Large" DHW consumptions are respectively 60% less and 78% larger than the standard DHW consumption value from NS 3031 (2014).

Table 4.5: Comparison of energy posts for the three occupants behaviour models

Occupant model	DHW consumption kWh/(m ² yr)	Appliances kWh/(m ² yr)	Lighting kWh/(m ² yr)
Small	12.1	4.8	11.4
NS3031	29.8	17.5	11.4
Large	53.0	21.9	11.4

Another large difference is that the two bedrooms on the western side of the building are not in use, and the temperature setpoint is strongly reduced in those rooms. This leads to a reduced space heating power demand.

The difference in internal loads from equipment, lighting and people

cause the net energy demand for space heating to differ between all three occupant behaviour models. Increased internal loads will result in a reduced need for space heating. Hence, less energy has to be covered by the heat pump. This will in turn result result in improved running conditions for the heat pump.

4.3 Heat recovery cases

There are several possible methods for heat recovery utilizing heat wheels and/or heat pumps. This section presents the different heat recovery cases that are looked into and simulated in this report. All cases use the same reference building, and are simulated for different climates, represented by different locations in Norway (see chapter 4.4).

The different heat recovery cases are presented in table 4.6. All seven combinations of heat wheel, exhaust air heat pump and outdoor air heat pump are taken into account. "*oHP*" does not recover any energy, seeing that no exhaust air energy is made us of before the air is discharged from the building. Thus, the exhaust air and the discharge air will have the same temperature for this heat recovery case. The case is still simulated in order to compare its performance to the true heat recovery cases.

The different cases are given short names that makes referring to them easier. The name gives information about how heat is recovered in that specific case. E.g. "*HWeoHP*" represents a configuration where a heat wheel (*HW*) and a heat pump (*HP* using both exhaust air and outdoor air (*eo*)) are used to recover ventilation heat and supply energy to the building.

All energy from the heat pump is given off to water in tanks. The water is used for hydronic heating and heating of DHW. Direct-acting electricity is used to supply the remaining heat demand not covered by the different heat recovery cases (see figure 5.5, p. 67).

Table 4.6: Overview of the different heat recovery cases in the report. Only *Heat wheel* and *Exhaust air* are associated with heat recovery. *HW* = heat wheel, *HP* = heat pump, *e* = exhaust air and *o* = outdoor air.

Case name	Heat wheel	Heat pump energy source	
		Exhaust air	Outdoor air
eHP		✓	
oHP ^{a)}			✓
eoHP		✓	✓
HW	✓		
HWeHP	✓	✓	
HWoHP	✓		✓
HWeoHP	✓	✓	✓

^{a)} This option does not recover heat, but is included for comparison purposes.

4.4 Climates

The outdoor climate has a large influence on the heat loss from the building. It also has a significant impact on the performance of heat pumps using outdoor air as heat source. The weather data used when checking compliance to the Technical Regulations (2010) is equal to the climate in Oslo, Norway. Heat recovery simulations are performed for two cities with a characteristic climate, in addition to Oslo.

Stavanger, located on the western coast of Norway, has mild winters, providing good conditions for using outdoor air as heat source. Kautokeino, located in the northern part of Norway, has very low outdoor temperatures most of the year. An overview of the selected locations, together with yearly mean temperatures, are shown in table 4.7.

Stavanger, and especially Kautokeino, can be regarded as the extremes of the Norwegian climate. The mean temperature in Oslo is not much lower than the corresponding temperature for Stavanger. However, the winters months are clearly colder, and the summer months

somewhat warmer, compared to Stavanger.

The local climate should be employed when designing a residential building according to NS 3700 (2013). Thus, the properties of the building envelope (thickness, U-value, etc.) would be different for a building located in Stavanger compared to Kautokeino. However, the same building with its thermal properties is used in all simulations in this report.

Table 4.7: Climate data used in the simulations. Yearly mean temperatures [$^{\circ}\text{C}$] and coldest day temperatures [$^{\circ}\text{C}$] from Kvande et al. (2012).

Location	Yearly mean temperature	Coldest day	Climate data source
Oslo	6.2	-21.8	ASHRAE IWEC
Stavanger, Sola	7.8	-15.5	ASHRAE IWEC 2
Kautokeino	-2.1	-46.9	ASHRAE IWEC 2

Chapter 5

Heat recovery simulations in IDA ICE and Matlab

This chapter describes the architecture of the simulation model, and the reasoning for choosing IDA ICE and MATLAB as simulation platform. It also describes the building model that was used in IDA ICE and the heat pump model developed in MATLAB.

5.1 Simulation platform and architecture

Several simulation platforms were assessed in the project report (Solberg, 2014): TRNSYS, Modelica, MATLAB, EnergyPlus, IES VE and IDA Indoor Climate and Energy (IDA ICE). A combination of IDA ICE and MATLAB was regarded as the best simulation platform for this specific purpose.

The IDA ICE software is good at simulating air flows, temperatures, heating and cooling loads, etc. The software has built-in components that may be used to build a customized plant. However, the range of components is limited. Components for exhaust air heat pumps are not yet available, and the possibilities for doing modifications on existing components are limited. A CO₂ heat pump model has thus been developed in MATLAB in order to estimate the performance of the CO₂ heat pump. A new MATLAB CO₂ heat pump model was made in

order to develop a transparent model tailored for the purpose of this report. Making a new model from scratch will also contribute to a greater learning potential.

The architecture of the simulation model is shown in figure 5.1. The following data for each time step from IDA ICE is used by the MATLAB code:

- Heat demand (DHW, space heating and ventilation heating) [W]
- Air temperature *before* IDA ICE heat exchanger [°C]
- Air temperature *after* IDA ICE heat exchanger [°C]
- Exhaust air, air flow rate [m³/h]
- Temperature of water at bottom of DHW tank [°C]
- Mass flow of incoming water from DHW tank [kg/s]
- Temperature of water at bottom of space heating tank [°C]
- Mass flow of incoming water from space heating tank [°C]
- Temperature of outdoor air [°C]

The data from IDA ICE is imported into MATLAB using an Excel file as connecting link. Ventilation air flow rate, discharge air temperature and outdoor temperature are used to describe the evaporator heat source. The outdoor temperature is used in cases *oHP*, *eoHP*, *HWoHP* and *HWeoHP*, where outdoor air is used as heat source.

The heat demand includes energy for DHW, space heating and pre-heating of ventilation air, and is used to control the compressor and the expansion valve. The heat pump will try to cover as much energy as possible within the defined limitations. The heat demand is calculated in IDA ICE using two electrical boilers as stand-in for the CO₂ heat pump – one boiler for DHW and one boiler for ventilation heating and space heating.

Temperatures from the DHW tank and space heating tank, combined with their respective mass flow rates, are used to calculate the inlet water temperature to the gas cooler.

Ideally, the amount of heated water and the temperature of the water should be reported back to IDA ICE (indicated by dotted line).

IDA ICE and MATLAB are not able to communicate for the time being, though EQUA is working on such a feature, according to Sahlin (2015), CEO at EQUA Simulation AB. Thus, all CO₂ heat pump simulations must be post-processed in MATLAB, based on input data from IDA ICE. The MATLAB model is further explained in chapter 5.3 (p. 65).

The NIST REFPROP software (Lemmon et al., 2013) is used to calculate the thermodynamic states of CO₂. The REFPROP MATLAB function "refprop.m" is called to from the MATLAB script, returning the desired properties of CO₂ for the given input properties (e.g. pressure, temperature, entropy, enthalpy, etc.)

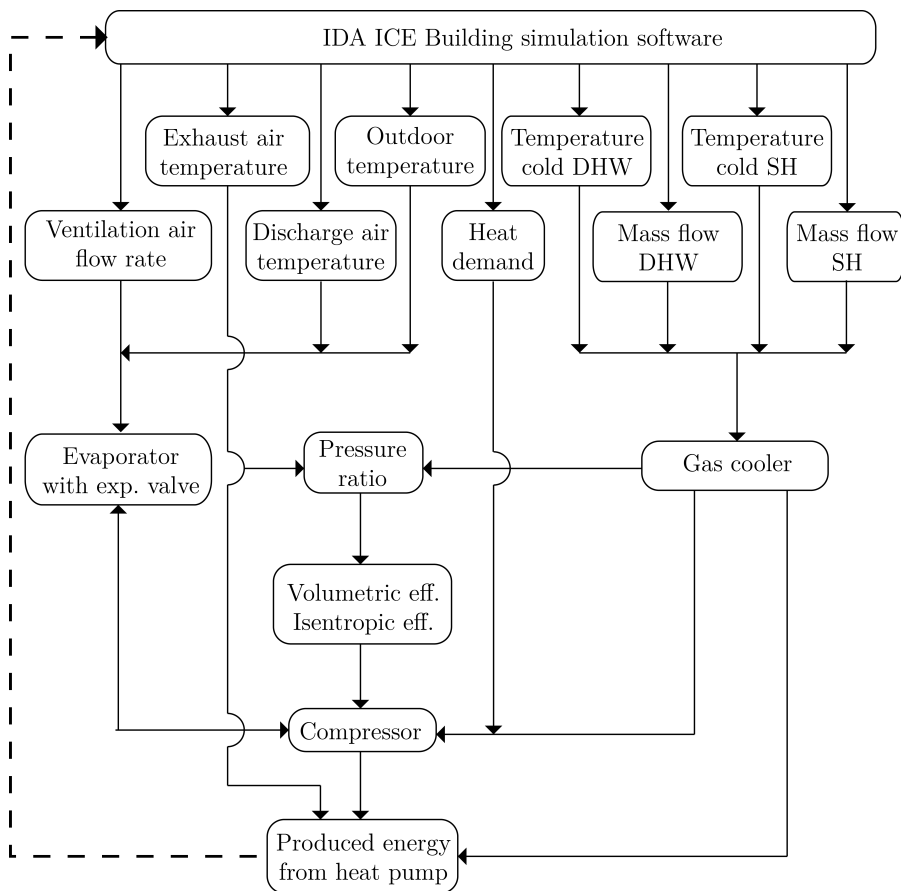


Figure 5.1: Architecture of the simulation model, connection between IDA ICE and MATLAB. Dotted line indicates continuous communication between IDA ICE and MATLAB.

5.2 Building simulation and heat rec. in IDA ICE

”Karita” was modelled and simulated in IDA ICE in order to find the building’s energy consumption, heat demands, air temperatures and temperature levels in the DHW tank and the space heating tank. The building model is based on the residential building described in chapter 4.1 (p. 41). This chapter describes the IDA ICE model, deviations from the standard setup, and assumptions that have been made. All properties and parameters are as default, unless stated otherwise.

5.2.1 Zone division

The building has been divided into a total of 11 zones, with one zone for each room. Illustrations of the zones, including area, internal doors and ventilation air flows are shown in appendix A.1. A less detailed floor plan is shown in figure 5.2. The staircase between 1st and 2nd floor has modelled by inserting a horizontal opening in the floor, allowing air to be exchanged between the zone below and above the horizontal opening.

5.2.2 Internal doors

Internal doors affect the air flow between zones in the building. A complete table with an overview of the internal doors is shown in appendix A.3. The table contains size, leak area and opening schedule for all internal doors. Ventilation air is balanced in the building as a whole, but not in each zone. Thus, some doors have a larger leak area than others, in order to allow air to pass through an air-gap below the door.

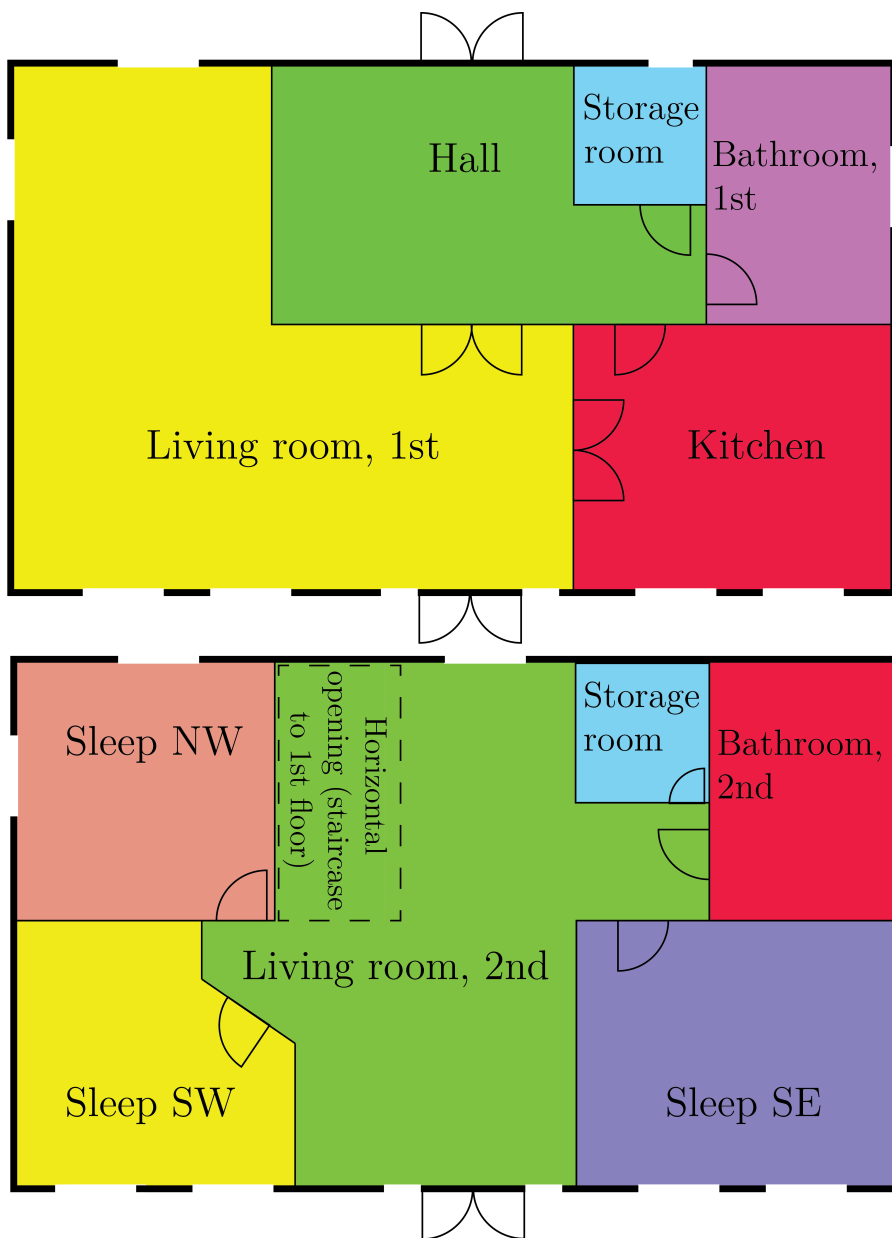


Figure 5.2: Floor plan of the building "Karita"

5.2.3 Windows, opening of windows and shading

The window frame area is assumed to constitute 20% of the total window area for all windows. Windows located on the same facade within the same zone are merged into one large window in order to save simulation time, as recommended by EQUA Simulation AB (2013).

It is assumed that the building is located in a housing estate, where nearby buildings provide shadow. Thus, buildings of the same size and height have been placed around the building as illustrated in figure 5.3. No shading from the horizon has been applied.

Window blinds (© *External blind (BRIS)*) are applied in the interest of reducing excessive indoor temperatures. A control macro has been made, which activates the window blinds when the zone temperature exceeds 23 °C. The macro is illustrated in appendix A.4.

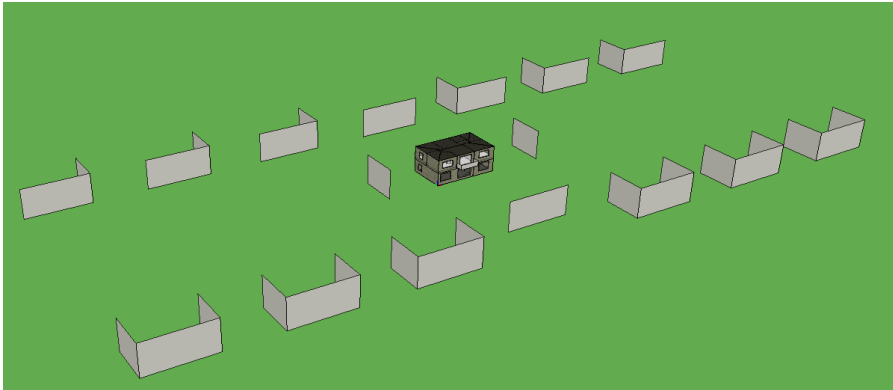


Figure 5.3: Shading objects from nearby buildings illustrated

Opening of windows is also required in order to reduce excessive indoor temperatures. This is done by selecting "PI temperature control AND schedule" as control strategy in IDA ICE. Windows may be opened from May to August, from 7 AM to 23 PM. The opening area of the windows is equal to 100% and 20% of window width and height respectively. A window will open if the temperature in its zone is too high. Window opening for windows located on the northern facade is not enabled.

5.2.4 IDA ESBO plant

The plant used in the IDA ICE model is based on a standard ESBO (Early Stage Building Optimization) plant. The ESBO plant was generated with "Topup heating" as only eligible option. "Generic hot water tank" and "Generic cold water tank" are mandatory choices. This default plant was modified to include a secondary storage tank and an additional electrical standard boiler, as illustrated in appendix A.5.

The generic cold water tank, the two brine tanks, and pumps and pipes for zone and AHU cooling, are not easily removed from the plant. Thus, they are disabled, and not removed from the plant drawing.

The two hot water tanks with accompanying boilers, serve two different purposes. One tank and boiler are intended for DHW production, while the other tank and boiler are intended for space heating purposes. These two tanks have different temperature setpoints. Both tanks are modelled as non-ideal, which means that both mixing losses and stratification losses occur within the tanks. The two standard electrical top-up heaters and the accompanying pumps are controlled using PI controllers. The two heaters in IDA ICE act as stand-ins for the heat pump. The heat pump performance must be post-processed in MATLAB (see chapter 5.1).

Inlet and outlet fittings on the tanks are placed in heights resulting in the lowest water inlet temperature to the boiler and the highest outlet temperature to the consuming unit (see table 5.1 and 5.2).

All tanks and boilers are dimensioned to cover the occupant behaviour model with the highest demand. Thus, the DHW tank and boiler are dimensioned to cover the large demand of the "Large" occupant behaviour model. The space heating tank and boiler are dimensioned to cover the demand of the normalized occupant behaviour model, seeing that it is the model with the highest power demand for space heating and preheating of ventilation air.

DHW tank and boiler

The DHW tank and boiler are located in the upper-left corner of the figure in appendix A.5. The non-default parameters for the tank and boiler are listed in table 5.1. All these parameters will affect the results

of the simulations to some extent. Thus, a parameter study is performed, which looks into the sensitivity of some of the most important parameters. These results are presented in chapter 6.2 (p. 86).

The low value of "Nominal mass flow at no external dp" may seem very low. IDA ICE has no built-in support for calculation of pressure loss in pipes and components. What IDA ICE does best is the thermal part of the building simulations. Thus, this value (called "*MFNOM*" in IDA ICE) is set to a sufficiently low value in order to limit the maximum mass flow rate of the pump supplying water from the DHW tank to the boiler.

Table 5.1: Deviations from default tank and boiler parameters for DHW system.

Parameter	Value	Unit
Tank:		
Ideal tank	False	(logical value)
Number of tank layers	12	–
Tank volume	0.30	m ³
Inner tank radius	0.25	m
Inlet height city water	0.0	m
Inlet height from boiler	1.5	m
Outlet height DHW	1.5	m
Outlet height to boiler	0.0	m
Height of temperature reader	1.0	m
Boiler:		
Temperature setpoint	70.0	°C
Max heating power	3.5	kW
Min. temperature out	70.0	°C
Max. temperature out	75.0	°C
Pump:		
Nominal mass flow rate at no external dp	0.0001	kg/s

DHW distribution

The DHW consumption is not uniformly dispersed during the day. It is assumed that there are three peak periods during the day:

- Morning, before work/school
- Afternoon, after work/school
- Evening, after activities and before bed

The DHW distribution schedule is illustrated in figure 5.4. The DHW consumption can be set to 0%, 50% or 100% for a chosen time resolution. The total yearly DHW consumption is dispersed equally on each day, according to the daily schedule. The DHW distribution schedule is employed in order to get a more realistic distribution of the DHW consumption, which will affect the heating power of the DHW boiler.

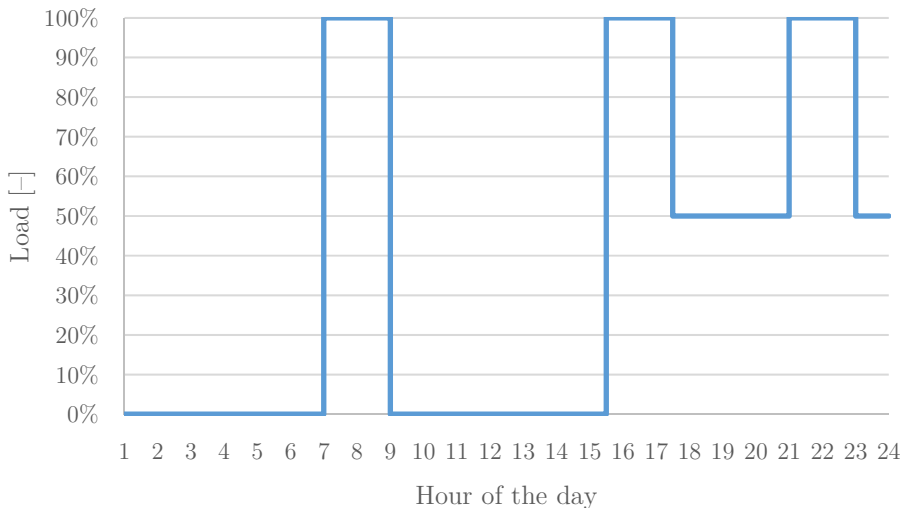


Figure 5.4: DHW distribution schedule used in the IDA ICE model.

Space heating tank and boiler

The space heating tank, together with its electrical boiler, is located in the middle of the figure in appendix A.5. The non-default parameters

for the tank and boiler are listed in table 5.2. The height of the temperature reader is set to 0.9 meters in all simulation cases, unless stated otherwise.

Table 5.2: Deviations from default tank and boiler parameters for the space heating and ventilation heating system. *AHU* = air handling unit, *SH* = space heating.

Parameter	Value	Unit
Tank:		
Ideal tank	False	(logical value)
Tank volume	0.10	m ³
Inner tank radius	0.25	m
Inlet height return AHU	0.0	m
Inlet height return SH	0.0	m
Inlet height return boiler	0.56	m
Outlet height supply AHU	0.56	m
Outlet height supply SH	0.56	m
Outlet height supply boiler	0	m
Height of temperature reader	0.4	m
Boiler:		
Temperature setpoint AHU	35.0	°C
Max temperature setpoint SH	40.0	°C
Max heating power	3.0	kW
Min. temperature out	70.0	°C
Max. temperature out	75.0	°C

5.2.5 Hydronic heating and dimensioning of radiators

Space heating and preheating of ventilation air are both based on low-temperature hydronic heating, achieved by floor heating and a heating coil placed in the AHU. The supply and return temperatures are 40 °C and 30 °C respectively at maximum power. Each heated zone has a standard "WatRad" IDA ICE object, which supplies hydronic heating to the zone.

The indoor temperature setpoint is set to 21 °C during the day. Night set-back is used, reducing the temperature setpoint to 19 °C from 23:00 to 07:00.

The required maximum heating power for each zone is found by running a "Heating load" simulation in IDA ICE. The maximum heating power for each zone is set to an exaggeratedly value before running the heating load simulation. The resulting required heating power for each zone is used when subsequently dimensioning the "WatRad" object for each zone. The supply temperature and return temperature at maximum power for space heating is set to respectively 40 °C and 30 °C for all simulations. The supply water temperature is changed with regard to the outdoor temperature. The radiators are dimensioned according to the local climate.

The "Alternative input data" option is used when designing the "WatRad" object. Maximum power, and supply and return temperature, are entered in the dialogue box. IDA ICE thereafter calculates the required heat emission properties for the given radiator size. The occupant behaviour model resulting in the highest maximum heat load value for each "WatRad" is used.

5.2.6 Ventilation and air handling unit

The building is designed with a balanced mechanical ventilation system. Ventilation is provided with the standard air handling unit in IDA ICE. Deviations from the standard setup is listed in table 5.3. Logging of the following parameters in the AHU are enabled, seeing that they are being used in the post-processing in MATLAB:

- Air intake temperature (outdoor temperature)
- Discharge air temperature
- Exhaust air temperature

"Minimum allowed leaving temperature" is set to -10 °C, in accordance with NS 3031 (2014) (see chapter 2.1.4, p. 9). This parameter is used to protect the heat exchanger from frost formation on the heat exchanger surfaces.

Ventilation air flow rates was determined according to §13-2 in the Technical Regulations (2010), which is based on four different criteria. The method resulting in the highest air flow rate is the method that should be employed:

- 1) Rooms in use demand $1.2 \text{ m}^3/\text{hm}^2$, while rooms not in use demand $0.7 \text{ m}^3/\text{hm}^2$.
- 2) Bedrooms must be supplied with a minimum of $26 \text{ m}^3/\text{h}$ per bed when in use.
- 3) Rooms that are not intended for continuous occupancy should be supplied a total of $0.7 \text{ m}^3/\text{hm}^2$
- 4) Kitchens, toilets and washrooms demand $36 \text{ m}^3/\text{h}$, while bathrooms demand $54 \text{ m}^3/\text{h}$.

The building has three bedrooms, where the two largest bedrooms have air flow rates dimensioned for two persons. This legislation results in a total ventilation air flow rate of $220 \text{ m}^3/\text{h}$ when occupied, and $117 \text{ m}^3/\text{h}$ when the building is not occupied. However, the *average* daily ventilation air flow rate must be equal to $220 \text{ m}^3/\text{h}$ (NS 3031, 2014). Thus, a constant ventilation air flow rate is used in the simulations. The impact of reducing the ventilation air flow when the building is unoccupied is investigated in chapter 6.2.6 (p. 97). The ventilation air flow rate is changed from $220 \text{ m}^3/\text{h}$ to $117 \text{ m}^3/\text{h}$ by altering the fan operation schedule in IDA ICE.

Ventilation air flow rates for each room/zone are written on the floor plan in appendix A.1. Numbers in parenthesis equal air flow rates when the ventilation system is running at minimum air flow rates. Air is supplied to rooms with high air quality requirements (bedrooms, living rooms), and drawn off in rooms with lower requirements for air quality (bathrooms, kitchen, storage rooms). All exhaust air from the building, including air from bathrooms and kitchen, are assumed to pass the heat wheel. Forced exhaust air from the kitchen ventilator is not taken into account in the simulations.

Table 5.3: Deviations from default air handling unit setup in IDA ICE.

Parameter	Value	Unit
Heat exchanger:		
Capacity	220	m ³ /h
Efficiency at capacity	80%	–
Minimum allowed leaving temperature	-10	°C
Fans:		
Specific fan power	1.5	kW/(m ³ /s)
Air temperature rise	100%	of fan energy
Supply temperature setpoint:		
Constant temperature	18	°C

5.2.7 Simulation of heat wheel heat recovery

Heat recovery using a heat wheel is done with the built-in heat exchanger in IDA ICE. The maximum efficiency is set to 80% at maximum air flow (220 m³/h). The efficiency is somewhat higher at lower ventilation air flows, due to lower velocities through the heat exchanger. The efficiency is reduced at elevated outdoor temperatures in order to achieve the desired supply air temperature of 18 °C. Deviations from the default IDA ICE setup are listed in table 5.3.

5.3 Heat pump simulations in Matlab

This chapter describes how the different heat pump heat recovery cases are simulated in MATLAB. The heat pump simulations are based on data from the building and heat wheel simulations in IDA ICE.

5.3.1 Matlab files overview

The MATLAB heat pump script consists of 8 scripts/functions of varying complexity. The main file (*main.m*) uses the other 7 files in order to return the desired information. The different files are presented in table 5.4.

An additional file, called *input.xlsx*, is necessary to run the MATLAB script. This Excel file contains the data exported from IDA ICE, which is imported to MATLAB in the *main.m* file. Each column contains different output data from IDA ICE, with 8760 rows of data. Thus, the time step of the MATLAB simulations are 1 hour.

The MATLAB script uses data from IDA ICE to calculate the amount of energy that can be covered by the heat pump for each time step. The heat pump simulations are based on the heat pump cycle illustrated in figure 2.3 (p. 14) and equations 5.3 to 5.15, presented in chapter 5.3.2.

Table 5.4: Description of the different MATLAB files

File name	Description
main.m	The main file connecting the rest of the files. Imports data from IDA ICE via Excel. Contains the script running iterations for each time-step. Calculates output values (SPF, energy coverage, etc.).
parameters.m	Script defining parameters regarding: <ul style="list-style-type: none"> • Convergence • Heat source(s) of the heat pump • Compressor properties (compressor volume, operating range, heat loss, motor efficiency, maximum CO₂ discharge temp, etc.) • Evaporator properties (UA value, minimum evaporation temperature) • Gas cooler properties (temperature approach, pressure) • Fan properties (SFP, efficiencies, air flow)
constants.m	Script defining constants.
thermo-dynamics.m	Function handling thermodynamic relations. Input: Temperature after IDA ICE heat exchanger, temperature of inlet water on gas cooler, evaporator air flow. Output: Gas cooler energy, evaporator energy, compressor energy, discharge CO ₂ temperature, evaporation temperature, required compressor volume
eta_is.m	Function with pressure ratio as input argument, returning isentropic efficiency
eta_vol.m	Function with pressure ratio as input argument, returning volumetric efficiency
pre-allocations.m	Script preallocating parameters.
clear_var.m	Script clearing irrelevant parameters.

5.3.2 Heat pump model system solution

The MATLAB script calculates the amount of energy, given input data from IDA ICE, that can be covered by the heat pump for each time step. Any remaining energy not covered by the heat pump is covered by an electric resistance heater. Figure 5.5 presents a sketch of the system solution used in the simulations. The heat pump is dimensioned for "Large" occupant behaviour model, seeing that the building is designed for a maximum of five persons.

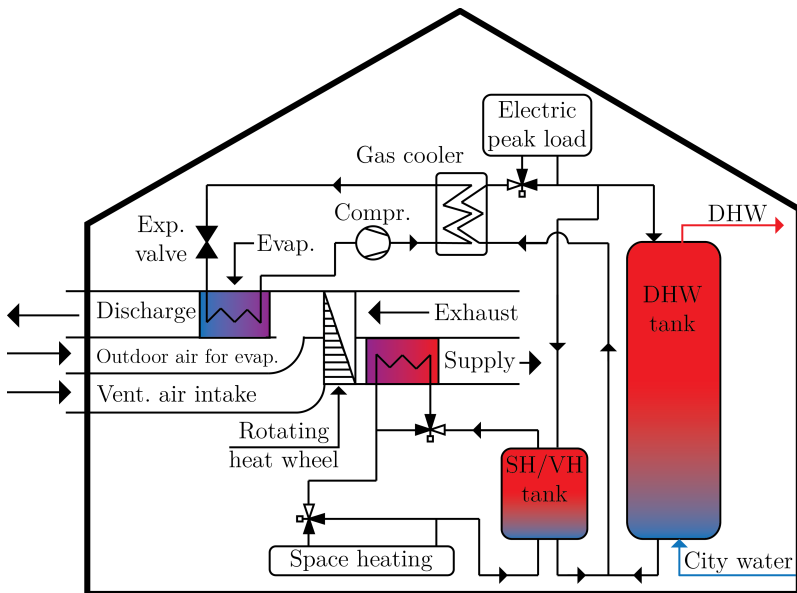


Figure 5.5: Simplified sketch of system solution simulated in MATLAB.

5.3.3 Operating modes

The heat pump model may be run in three different modes, separated by the heat source in use:

- Exhaust air
- Outdoor air
- Exhaust air and outdoor air

The desired operating mode is chosen in *parameters.m*. Use of a passive heat exchanger is enabled or disabled in IDA ICE. The heat exchanger is disabled by setting the efficiency of the heat exchanger to zero. When the heat wheel is disabled, the discharge air temperature from the building will be equal to the exhaust air temperature from the zones in the building.

The temperature and air flow rate on the evaporator inlet correspond to the discharge air temperature and the air ventilation air flow rate from the building in IDA ICE, when using exhaust air as heat source.

The temperature of the air at the evaporator inlet equals the outdoor air temperature when using outdoor air as heat source. Air is provided by an outdoor air fan. The air flow rate of this fan is defined in *parameters.m*. An outdoor air flow rate of 250 m³/h is used unless stated otherwise. This value is based on results from the parameter study (see chapter 6.2.3, p. 92).

An intermittently operated outdoor air fan is used when running in combined mode. The fan is used only if it is beneficial. Each time step is calculated with and without running the outdoor air fan. The alternative with best performance, in terms of delivered energy to the building for heating, is preferred. Energy consumed by the outdoor air fan is taken into account (see chapter 5.3.9). Exhaust air and outdoor air are mixed when the outdoor air is used, according to equation 5.1 and 5.2.

$$T_{\text{evap,inlet}} = \frac{T_{\text{exhaust}} \cdot \dot{V}_{\text{EA}} + T_{\text{outdoor}} \cdot \dot{V}_{\text{outdoor}}}{\dot{V}_{\text{EA}} + \dot{V}_{\text{outdoor}}} \quad (5.1)$$

$$\dot{V}_{\text{total}} = \dot{V}_{\text{EA}} + \dot{V}_{\text{outdoor}} \quad (5.2)$$

5.3.4 Evaporator

Heat is transferred from air to CO₂ in the evaporator. A constant UA value is assumed for the evaporator. This value is set to 160 W/K, based on results from the parameter study (see chapter 6.2.2, p. 90). The amount of energy removed from the air passing the evaporator is calculated according to equation 5.3. Thereafter, the LMTD for the

evaporator is calculated using equation 5.4. The heat pump evaporation temperature is found using equation 5.6, which is derived from the standard LMTD equation (equation 5.5).

$$\dot{Q}_{\text{evap}} = \dot{V}_{\text{air}} c_{p_{\text{air}}} (T_{\text{ahe}} - T_{\text{disch}}) \quad (5.3)$$

$$\text{LMTD} = \dot{Q}_{\text{evap}} / UA \quad (5.4)$$

$$\text{LMTD} = \frac{T_{\text{ahe}} - T_{\text{evap}} - (T_{\text{disch}} - T_{\text{evap}})}{\ln \left(\frac{T_{\text{ahe}} - T_{\text{evap}}}{T_{\text{disch}} - T_{\text{evap}}} \right)} \quad (5.5)$$

$$T_{\text{evap}} = \frac{T_{\text{disch}} \cdot \exp \left(\frac{T_{\text{ahe}} - T_{\text{disch}}}{\text{LMTD}} \right) - T_{\text{ahe}}}{\exp \left(\frac{T_{\text{ahe}} - T_{\text{disch}}}{\text{LMTD}} \right) - 1} \quad (5.6)$$

5.3.5 Compressor

Dry saturated CO₂ gas is compressed to a gas cooler pressure defined in *parameters.m*. The MATLAB code takes isentropic losses, heat loss (non-adiabatic) and motor loss into account when calculating the compression process.

At first, an isentropic compression process is calculated. $h_{2\text{is}}$ is defined by the gas cooler pressure and an entropy equal to dry saturated steam at evaporation temperature (s_1). REFPROP (see chapter 5.1, p. 51) calculates the CO₂ enthalpy after isentropic compression based on these two input parameters, according to equation 5.7. p_{gc} equals the gas cooler pressure and s_1 equals the CO₂ entropy after the evaporator.

$$h_{2\text{is}} = \text{refpropm}('H', 'P', p_{\text{gc}}, 'S', s_1, 'co2'); \quad (5.7)$$

An adiabatic compression process is calculated according to equation 5.8. η_{is} is returned by the *eta_is.m* MATLAB function, having gas cooler

pressure and evaporation pressure as input parameters (see chapter 5.3.5).

$$h_{2\text{ad}} = h_1 + \frac{h_{2\text{is}} - h_1}{\eta_{\text{is}}} \quad (5.8)$$

The real condition of the CO₂ after compression ($h_{2\text{r}}$) is found using equation 5.9. This equation takes heat loss from the compressor into account based on the constant k , which is defined in *parameters.m*. This value is set to 24% unless stated otherwise, based on information from Rekstad (2015a). Thus, the heat loss from the compressor equals 24% of the compressor shaft power.

$$h_{2\text{r}} = h_1 + (1 - k)(h_{2\text{ad}} - h_1) \quad (5.9)$$

The compressor work is calculated using equation 5.10. η_{motor} is a constant motor efficiency defined in *parameters.m*, including the motor efficiency, transmission efficiency and the frequency converter efficiency. It is assumed that the motor efficiency is *not* included in the isentropic compressor efficiency. The motor efficiency is set to a constant value of 87%, assuming an IE4 class motor (de Almeida et al., 2009).

$$\dot{W}_{\text{compr}} = \frac{\dot{m}_{\text{CO}_2}(h_{2\text{ad}} - h_1)}{\eta_{\text{motor}}} \quad (5.10)$$

Isentropic and volumetric efficiency

The calculation of isentropic and volumetric compressor efficiencies are based on information from Berntsen (2013) and Rekstad (2015b). Curves showing efficiencies at different pressure ratios are shown in figure 5.6. It is assumed that the efficiency curves are the same for all frequencies.

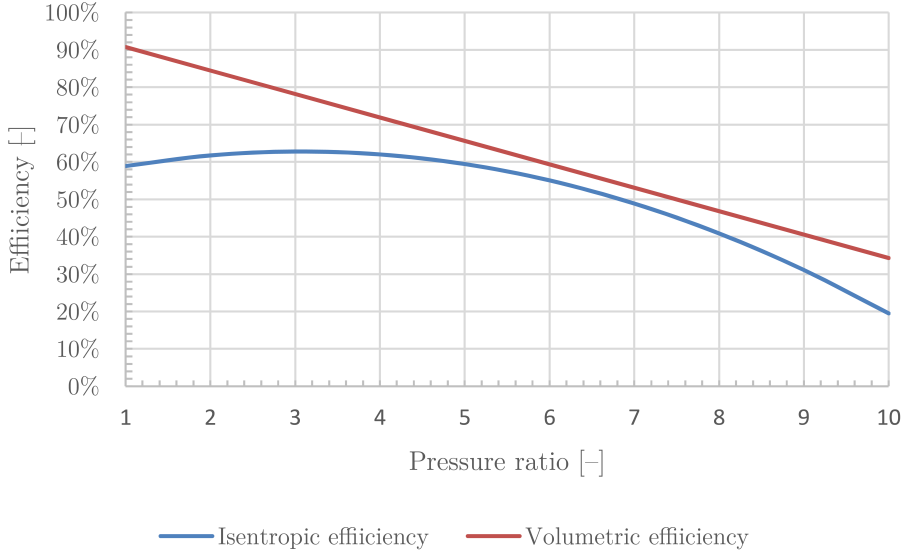


Figure 5.6: Isentropic and volumetric compressor efficiencies as a function of the pressure ratio (Berntsen, 2013; Rekstad, 2015b).

Compressor volume

The compressor volume [m^3/h] at full load is defined in *parameters.m*, together with a minimum compressor volume flow. The minimum compressor volume flow is defined as a percentage of the maximum flow. This value is by default set to 30% (Rekstad, 2015b), but may be changed in *parameters.m*. These two volume flows represent the operating range of the compressor using VSD (full capacity and minimum part load).

The compressor volume used in the simulations is changed according to which heat recovery case is being simulated. The different heat recovery cases have different optimum compressor volumes. The optimum compressor volume for each case is found in chapter 6.2.1 (p. 86).

The compressor can only be operated within these limits. The heat pump is run intermittent if the required heat demand is lower than the heat pump heating power at minimum part load.

Intermittent drive is not desired, seeing that heat is only recovered

by the heat pump when the compressor is running. Thus, a compressor designed with a somewhat small volume *may* prove more efficient than a compressor with a larger volume.

If too big a compressor volume is chosen, the compressor may not be able to run at all due to limitations put on the discharge CO₂ gas temperature. A large compressor volume removes more energy from the air, and the evaporation temperature will be low. Low evaporation temperatures result in high discharge CO₂ gas temperatures.

5.3.6 Gas cooler

Heat is given off from CO₂ to water in the gas cooler. Modelling a gas cooler for CO₂ heat pump applications is more advanced than modelling a condenser for a subcritical heat pump. Heat is rejected from CO₂ to water over a large temperature glide in a gas cooler, whilst heat is rejected at a constant temperature in a condenser for a subcritical heat pump. The gas cooler should be modelled using a discretization method, in order to know the temperature development within the gas cooler for both water and CO₂.

The heat transfer coefficient will be strongly dependant on the CO₂ mass flow (i.e. velocity), but also mass flow of water. The complexity of such a gas cooler model is not consistent with the scope of this report. Implementation of such a gas cooler model would also increase the simulation time considerably. Thus, a much simpler gas cooler model is used. Several assumptions have been made when modelling the gas cooler:

- No pressure loss
- Constant gas cooler pressure, defined in *parameters.m*
- Constant water outlet temperature
- Constant temperature approach value

Pressure losses in heat exchangers are inevitable, causing the temperature to decrease. The pressure loss is strongly dependant on the gas cooler mass flow. A pressure drop has lower significance for CO₂ than for other common refrigerants, according to Stene (2014). Pressure loss in the gas cooler is thus not allowed for.

The gas cooler pressure should ideally be changed continuously according to the conditions in the gas cooler and water temperature demands. Seeing that the temperature development in the gas cooler is not known, a constant gas cooler pressure is applied. The heat transfer could be hampered if the gas cooler pressure is set to an insufficient value.

Stene (2004) performed experiments and simulations on a tripartite gas cooler for preheating of DHW, space heating and reheating of DHW. Three different operation modes were assessed: Space heating, heating of DHW, and combined operation (both SH and DHW). The results from the simulations showed that a constant gas cooler pressure could be applied with only a minor reduction in COP for all three operating modes. This conclusion was based on a DHW temperature of 70 °C. For higher DHW temperatures, the advantage of being able to have a variable gas cooler pressure becomes more vital. In addition to the numbers presented in 5.5, Stene found an optimum gas cooler pressure of 85 bar to 95 bar for combined operation, at DHW temperatures of 60 °C to 80 °C and turn/return SH temperatures of 40/35 °C. Stene also found that the COP is quickly reduced when the heat pump is operating below the optimum gas cooler pressure. Thus, the gas cooler pressure should be equal to, or somewhat higher than, the optimum value. Based on this information, the gas cooler pressure is set to a constant value of 100 bar in all simulations.

Table 5.5: Optimum CO₂ gas cooler pressure at an evaporation temperature of −5 °C (Stene, 2014).

Application	Water temperature setpoint [°C]	Optimum pressure [bar]
Space heating	30	80
Space heating	35	85
Space heating	45	95
Hot water heating	60	90
Hot water heating	70	100
Hot water heating	80	110

A constant water temperature of 70 °C leaving the gas cooler is assumed. This is achieved by controlling the water pump. The pump control is set to adjust its volume flow in order to achieve the desired water setpoint temperature.

A constant temperature difference between water at the gas cooler inlet and CO₂ at the gas cooler outlet is assumed. This value is set to 4 K in *parameters.m*. Thus, the outlet CO₂ temperature will vary according to the inlet water temperature. This assumption will in some cases be advantageous, and in other cases disadvantageous, for the heat pump performance. The outlet CO₂ enthalpy is thus calculated in MATLAB according to equation 5.11. T_{cw} equals gas cooler water inlet temperature for that time step, p_{gc} equals gas cooler pressure, while t_a equals the temperature approach. p_{gc} and t_a are defined in *parameters.m*.

$$h_3 = \text{refpropm}('H', 'T', T_{cw} + t_a, 'P', p_{gc}, 'CO_2'); \quad (5.11)$$

5.3.7 Expansion device

The expansion process is assumed to be isenthalpic. The CO₂ enthalpy after expansion is calculated using equation 5.12.

$$h_4 = h_3 \quad (5.12)$$

5.3.8 Mass flow and volume flow

With all four process points calculated, the CO₂ mass flow and volume flow can be calculated. CO₂ mass flow is calculated using equation 5.13:

$$\dot{m}_{CO_2} = \frac{\dot{Q}_{rem}}{h_1 - h_4} \quad (5.13)$$

Specific volume for the suction gas (v_1) and CO₂ volume flow \dot{V}_{CO_2} are calculated according to equations 5.14 and 5.15. t_1 equals the evaporation temperature, while 'Q' defines the gas quality (1 at saturated vapour).

$$v_1 = 1/\text{refpropm}('D', 'T', t1+\text{kkelvin}, 'Q', 1, 'co2'); \quad (5.14)$$

$$\dot{V}_{\text{CO}_2} = \frac{\dot{m}_{\text{CO}_2} \cdot v_1}{\eta_{\text{vol}}} \quad (5.15)$$

5.3.9 Fan energy

An extra fan is required in order to transport outdoor air to the evaporator. In addition, the evaporator placed in the air duct leaving the building is causing an increased pressure loss, which increases the energy consumption of the exhaust air fan in the AHU.

Based on calculations performed using the air handling unit calculator for *"SAVE VTR 300/B venstre"* on the Systemair (nd) website, the increase in fan power due to increased pressure loss over the evaporator can be neglected. Thus, the extra energy consumption and the negligible heating of the exhaust air is not taken into account.

The total pressure loss for the air provided by the outdoor air fan is calculated to about 120 Pascal at 200 m³/h, based on diagrams for components from Lindab (nd). The fan *"K125XL"* from ebm-papst (nd) is close to matching this operating point, with a resulting SFP of 1.3 kW/(m³/s) and a total efficiency of 34.5%. This SFP value is used by the MATLAB script to calculate the energy consumption for fans with various air flow rates. It is assumed that only the motor and fan wheel losses (65.5%) heat up the air before passing the heat pump evaporator.

5.3.10 Solving the system of equations

All equations, relations and limitations are defined in the MATLAB script, leaving only one unknown parameter. This parameter is the discharge air temperature from the evaporator. A half-interval search algorithm (binary search) finds the optimum discharge air temperature resulting in the lowest demand for delivered energy for heating for each time step. The demand for delivered electrical energy to the building is minimized. The efficiency of the search algorithm is illustrated in

figure 5.7. dt_{min} is the parameter used to define the accuracy of the simulations. A larger dt_{min} value implies a less accurate simulation and vice versa. A dt_{min} value of 0.01 is chosen in all heat recovery simulations.

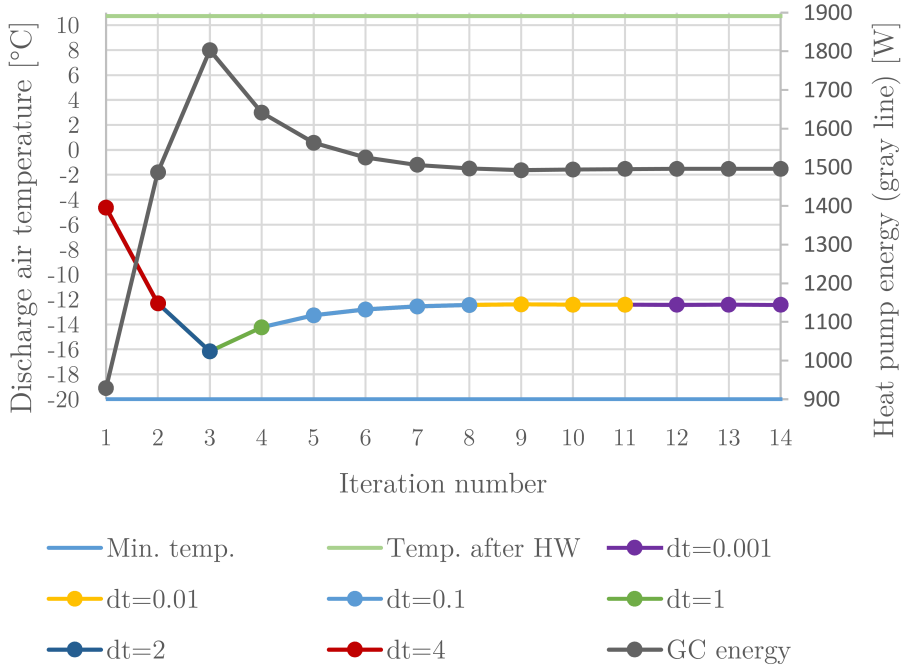


Figure 5.7: Example of how the half-interval search algorithm works. The numbers in the illustration are for a random time step with actual values.

A valid discharge air temperature must satisfy the following conditions:

- Discharge CO₂ gas temperature below 115 °C
- CO₂ volume flow *below* the maximum value
- CO₂ volume flow *above* the minimum value

In addition, the discharge air temperature should result in a gas cooler heating power equal to or below the required heat demand from

IDA ICE. The heat pump will be operated intermittent if the heat pump delivers *more* energy than required at minimum part load.

An evaporator with an infinitely high UA value will result in equal evaporation temperature and discharge air temperature. An evaporation temperature close to, or lower than, $-20\text{ }^{\circ}\text{C}$ will result in a compressor discharge gas temperature exceeding the limit of $115\text{ }^{\circ}\text{C}$ at 100 bar gas cooler pressure. Hence, the MATLAB script uses $-20\text{ }^{\circ}\text{C}$ as the minimum possible discharge air temperature. A valid discharge air temperature must thus have a value between $-20\text{ }^{\circ}\text{C}$ and the temperature after the IDA ICE heat exchanger.

The initial guess value for the discharge air temperature from the evaporator is the average of $-20\text{ }^{\circ}\text{C}$ and the discharge air temperature from the heat wheel (from IDA ICE). This temperature difference is called dt . The heat pump cycle for this specific discharge air temperature is calculated. Information from the cycle is analysed in order to determine whether the guessed temperature was too high or too low. This is determined by investigating the discharge CO_2 gas temperature, required compressor volume, and the amount of gas cooler heat compared to the heat demand.

If the guessed value was too high, the dt value is multiplied by 0.5 and *subtracted* from the initial guess. If too low, the dt value is multiplied by 0.5 and *added* to the initial guess. This procedure is repeated until the difference between the old dt value and the new dt value is less than dt_min (set to 0.01).

At low heat source temperatures and/or in periods where the discharge CO_2 temperature at minimum part load is higher than 115°C , the heat pump is turned off.

The MATLAB script uses this approach on each time step, using a MATLAB `for` loop. This means that each time step is calculated separately, independent of the previous and the next time step.

Chapter 6

Results

This chapter presents the results from simulations performed in IDA ICE and MATLAB. The main focus is on the results from the heat recovery cases, but some results from the building itself are also presented.

The different heat recovery cases, climates or occupant behaviour models are in this chapter often compared in terms of delivered energy for heating. In this report, "delivered energy for heating" is defined as the delivered electrical energy to the building used for heating of DHW, space heating and ventilation heating. Thus, the amount of delivered energy for heating is usually *lower* than the net energy demand for heating.

6.1 Building simulations

The building has been simulated for three different climates and three different occupant behaviour models. The significance of climate and occupant behaviour for the building's energy consumption are assessed.

6.1.1 Heating energy

Figure 6.1 shows the required heating energy for Oslo, Stavanger and Kautokeino climate, for the "NS3031" occupant behaviour model and heat recovery case *HW* (heat wheel only).

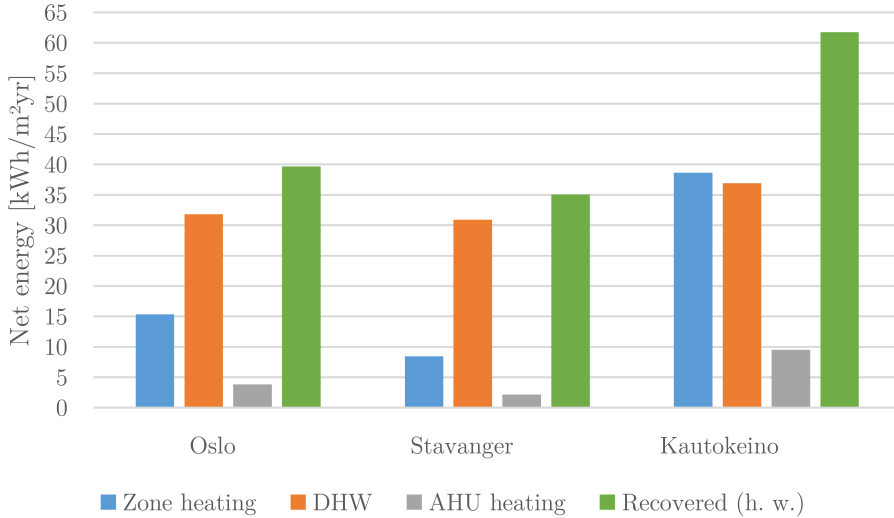


Figure 6.1: Net heating energy for "NS3031" occupant behaviour model and heat recovery case "HW" (heat wheel only).

The results show large differences for the building using different climates. The heating demand for this building located in Kautokeino is more than twice the heating demand when located in Oslo. This will have a considerable impact on the performance of the heat pump. The minimum allowed leaving temperature from the AHU, set to $-10\text{ }^{\circ}\text{C}$ (see chapter 5.2.6, p. 62), limits the heat recovered by the heat wheel for Kautokeino climate. Compared to the much more extreme temperatures, the amount of recovered energy by the heat wheel is only 56% larger than the equivalent number for Oslo climate. The corresponding increase in zone heating energy demand is however 151%.

According to the Norwegian passive house standard (NS 3700, 2013), this building located in Oslo has a maximum net energy demand for space heating of $19.2\text{ kWh/m}^2\text{yr}$ (zone heating and AHU heating). The results from the simulation in IDA ICE show a required heat demand of $19.2\text{ kWh/m}^2\text{yr}$, while the simulations performed in Simien (see chapter 4.1, p. 41) show a heat demand of $19.1\text{ kWh/m}^2\text{yr}$. The building is therefore in accordance with NS 3700 (2013) when heat recovery case "HW" is used, disregarding the requirements for renewable energy. The

results also show good coherence between Simien and IDA ICE, and increase the redundancy of the building simulation results.

The consumption of energy for DHW differs between climates. This is caused by IDA ICE changing the city water temperature according to the climate used in the simulations. The difference in inlet water temperature is especially decisive for the DHW energy consumption in Kautokeino. The city water temperature in Kautokeino is calculated by IDA ICE to -1.88 °C. The DHW tank in IDA ICE is modelled with a heat loss from the tank to the surroundings that also contributes to an increased DHW energy consumption compared to the standard DHW consumption from NS 3031 (2014) of 28.9 kWh/m²yr.

6.1.2 Space heating and ventilation heating power

Figure 6.2, 6.3 and 6.4 show the duration curves for the space heating and heating of ventilation air boiler power for Oslo, Stavanger and Kautokeino respectively. Curves for different occupant behaviour models are shown for the building, with and without a heat wheel for ventilation heat recovery.

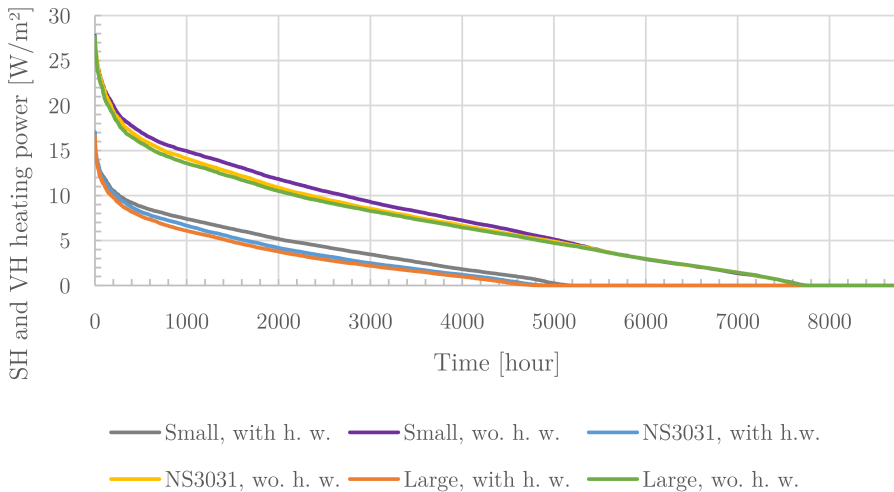


Figure 6.2: Duration curve for space heating and ventilation heating power for Oslo climate ("h. w." = "heat wheel, wo. = "without").

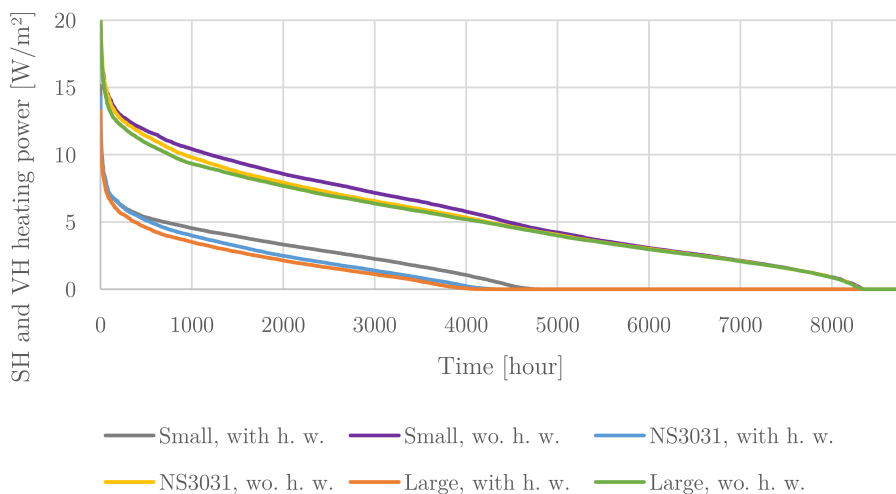


Figure 6.3: Duration curve for space heating and ventilation preheating power for Stavanger climate ("h. w." = "heat wheel, wo. = "without").

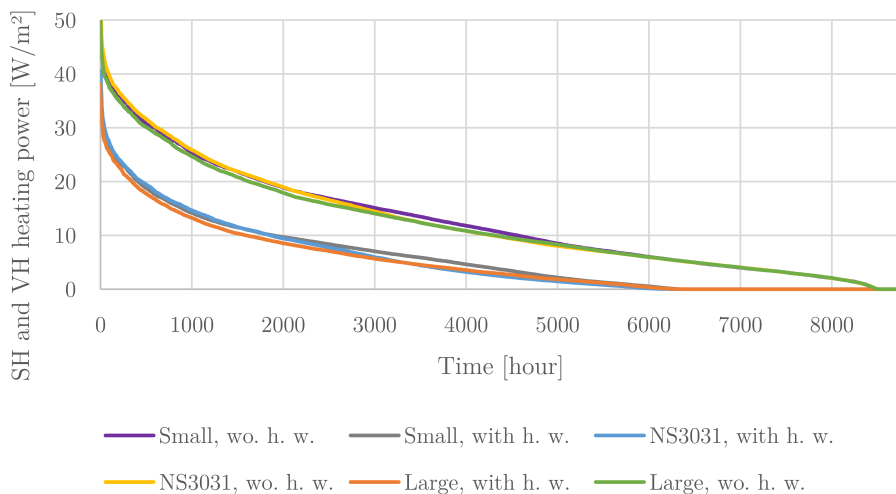


Figure 6.4: Duration curve for space heating and ventilation preheating power for Kautokeino climate ("h. w." = "heat wheel, wo. = "without").

The occupant behaviour models have a low impact on the space heating and ventilation air heating power. The significance is lowest for the Kautokeino climate, seeing that the difference in internal loads (people, equipment and lighting) between the models are very small compared to the total required heating power. "Small" always have the highest SH and VH heating demand, followed by "NS3031" and "Large".

6.1.3 DHW tank temperatures and boiler power

The temperature profile and boiler power of the DHW tank are almost independent of the local climate. Small deviations occur due to different city water temperatures for different climates. The properties of the tank and boiler, plus the DHW consumption distribution over the day, can be found in chapter 5.2.4 (p. 58). Figure 6.5 presents duration curves for the temperature in the bottom layer of the DHW tank for the different occupant behaviour models and storage tank volumes (Oslo climate). The temperature reader in the tank is placed at the same relative height for all simulations, $\frac{1}{3}$ from the top.

The temperature profile for "Small" and "NS3031" are close to equal. The temperature profile of "Small" is somewhat more affected by the heat loss *from* the surroundings, seeing that there is less circulation of water in the tank. Thus, the temperature for "Small" is a little higher than "NS3031" for temperatures up to 20 °C. At higher temperatures than 20 °C, "Small" and "NS3031" are close to equal. The temperatures at the bottom of the tank for the "Large" model reaches up to 70°C, depending on storage tank volume. It is not beneficial to run the CO₂ heat pump close to this temperatures. The heat pump will be turned off during such operating conditions.

All curves, except "Small", are uneven and jagged. Increased DHW consumption and reduced storage volume results in more uneven curves. It is natural to assume that a larger storage tank results in better tank stratification, though a higher heat loss. This is also the case for the "Large" occupant behaviour model, where simulations have been performed for three different storage volumes. However, there is a period of about 700 hours where the temperatures are higher in the 400 liter tank compared to the 300 liter tank. It is not known what

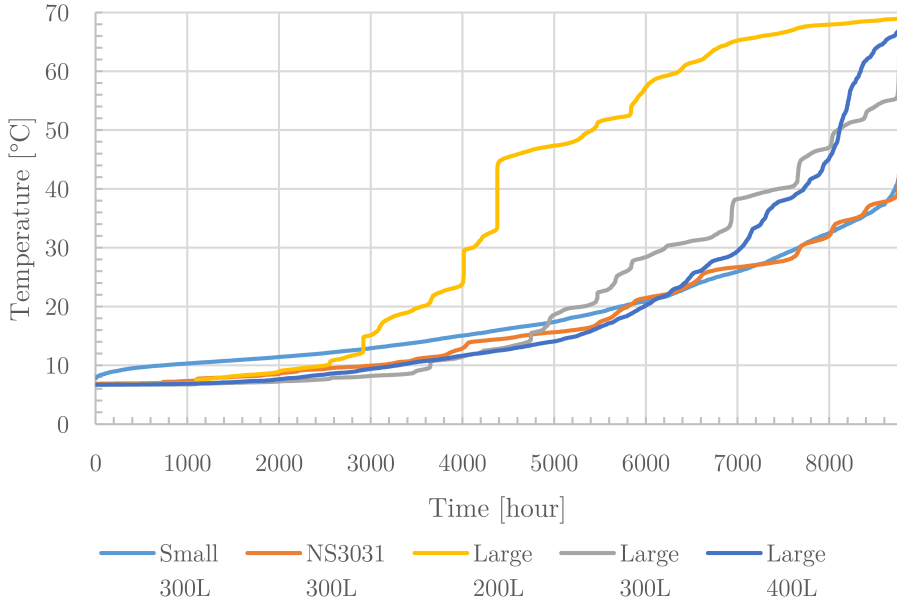


Figure 6.5: Duration curve for temperature at the bottom of the DHW tank for the different occupant behaviour models and storage tank volumes (Oslo climate).

is causing these two phenomena (uneven curves and the increased temperature) for the IDA ICE storage tank.

Duration curves for the DHW boiler power are shown in figure 6.6. Even though there is a large DHW consumption in the "Large" model, it is still possible to provide the required amount of energy without very high boiler power. It is essential to avoid large power fluctuations and intermittent operation of the boiler, in order to achieve good operating conditions for the heat pump. This is made possible by having a large DHW tank volume.

The smallest tank (200 liter) for "Large" occupant behaviour is not able to keep the DHW water temperatures in the upper tank layers at the desired setpoint temperature at the evenings, due to the large DHW consumption after 15:30. The temperature of the DHW leaving the tank drops to about 55 °C at 23:00. This is, however, a sufficient

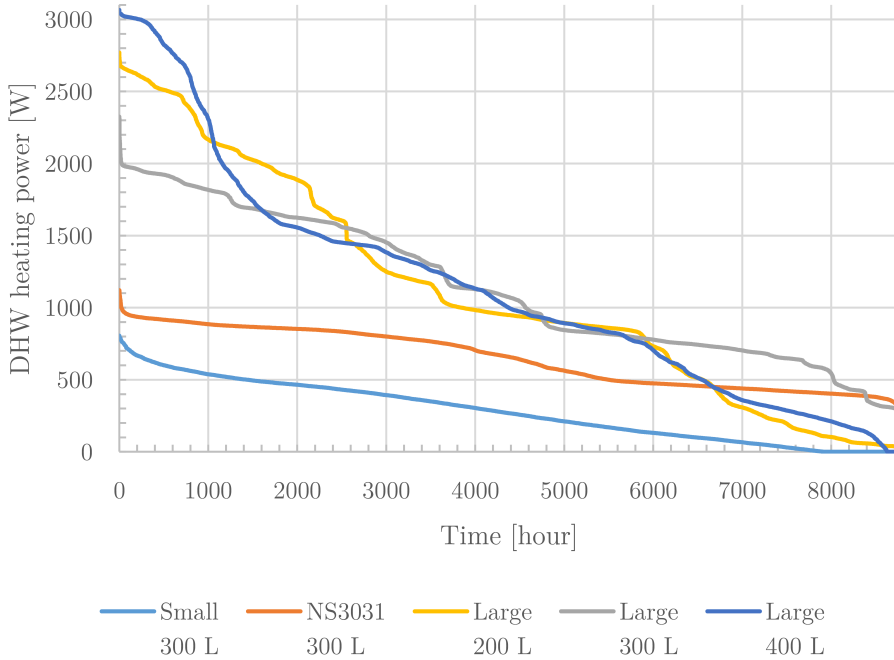


Figure 6.6: Duration curve for DHW boiler power for the three different occupant behaviour models and storage tank volumes (Oslo climate)..

temperature for most purposes. The tank is able to recharge during the night, when there is no DHW consumption. The main drawback with the 200 liter tank is the high temperature in the bottom of the tank, reducing the heat pump performance significantly (see chapter 6.2.4).

The largest tank has a generally lower heating power compared to the 300 liter tank, but from hour 0 to 1000 in figure 6.6, the heating power is evidently higher. It is not known what is causing this behaviour in the IDA ICE storage tank model. Chapter 6.2.4 (p. 94) looks into what impact the choice of storage tank volume has on the delivered energy for DHW, SH and VH to the building.

6.2 Parameter study

This chapter looks into several of the most important parameters used in the heat recovery models, and assesses their influence on the heat recovery performance. The results from the parameter study are used to design a more optimized building and heat recovery model, used when comparing the different heat recovery cases in chapter 6.4.

6.2.1 Compressor size

The heat pump compressor has a maximum volume flow. The minimum compressor volume flow is equal to 30% of the maximum value, achieved by using an inverter controlled motor (see chapter 5.3.5, p. 71). Figure 6.7 shows the optimum compressor volume for each heat recovery case for "Large" occupant behaviour model and Oslo climate. "Large" is used in the comparison, seeing that the building is dimensioned for five people.

A compressor with low maximum volume flow compared to the demand will run continuously, but can only partially cover the demand in periods with a high energy demand. A compressor with a high maximum volume flow is able to cool down the evaporator air to the minimum possible temperature. However, the lowest part load volume flow is equal to 30% of the maximum compressor volume flow. A large compressor will have a correspondingly large minimum volume flow. This will force the heat pump to be run intermittently in periods with low energy demands. The heat pump may also be turned off, if running the compressor on the minimum capacity results in a too low evaporation temperature. The discharge CO₂ gas temperature is strongly dependant on the evaporation temperature, which limits the lower possible evaporation temperature.

The optimum full load compressor volume flow varies from 0.75 m³/h to 1.0 m³/h. The heat recovery cases that do not involve using a heat wheel (*eHP* and *eoHP*) remove large amounts of heat from the exhaust air. Hence, the optimum compressor volumes are larger. Cases *oHP*, *HWeHP*, *HWeoHP* and *HWeoHP* remove less energy from the air, seeing that much heat has already been recovered by the heat wheel, and/or the available heat source is limited. Thus a smaller compressor should

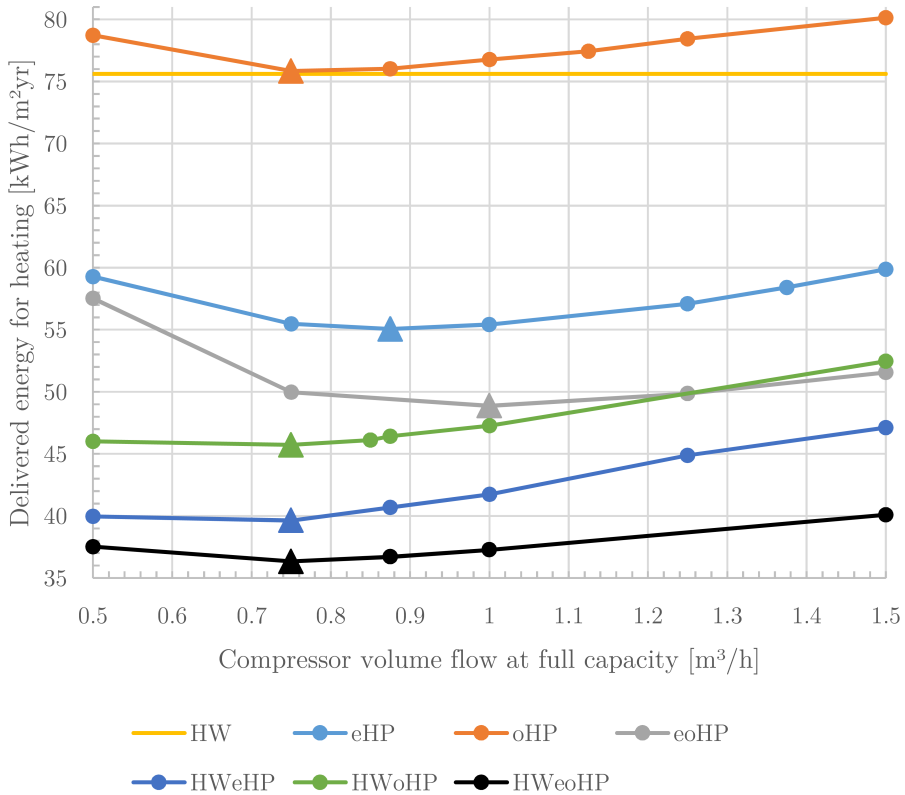


Figure 6.7: Optimum compressor volume at full capacity for "Large" occupant behaviour model, for building located in Oslo climate. The optimum compressor volume for each heat recovery case is marked with a triangle. Heat recovery case *HW* (heat wheel only) does not involve using a heat pump, but is shown to compare the performance to the other cases.

be used.

The impact of compressor volume on the heat recovery performance is rather small for heat recovery cases utilizing a heat wheel. However, installing a too small compressor volume for *eHP*, *oHP* and *eoHP* will hamper the performance of the heat pump.

eoHP and *HWeoHP* utilize exhaust air *and* outdoor air. A small compressor size results in less heat removed from the air, and thus the advantage of being able to use outdoor air is reduced. Therefore, at low compressor sizes, the performance of *eoHP* and *HWeoHP* are getting closer to the corresponding heat recovery case not utilizing outdoor air (*eHP* and *HWeHP*).

The same figure was made for "Large" occupant behaviour model, using Kautokeino climate. The result is shown in figure 6.8. The building located in Kautokeino has a larger demand for space heating and ventilation heating. More heat is removed from the exhaust air, and a slightly larger compressor should be installed for *eHP* and *eoHP*.

The optimum compressor sizes for Oslo and Kautokeino climates are compared in table 6.1. The differences in compressor size are small, and the influence on delivered energy for heating is also small, seeing that the curves for both Oslo and Kautokeino are close to flat in the area close to the optimum size. The climatic differences between Oslo and Kautokeino are larger than between Oslo and Stavanger. Thus, optimum compressor sizes for Stavanger are assumed to be close to the optimum sizes for Oslo. The optimum compressor size for each case in Oslo is therefore also used for Stavanger and Kautokeino in all simulations.

The compressor sizes mentioned in table 6.1 are rather small. CO₂ has a high vapour density compared to other common refrigerants. This results in a high volumetric heating capacity (VHC), and thus small compressor sizes. The available range of CO₂ compressors today is limited in the small volume segment. However, it must be expected that available compressor sizes will increase in the near future, making the compressor sizes found in this report available at a reasonable cost.

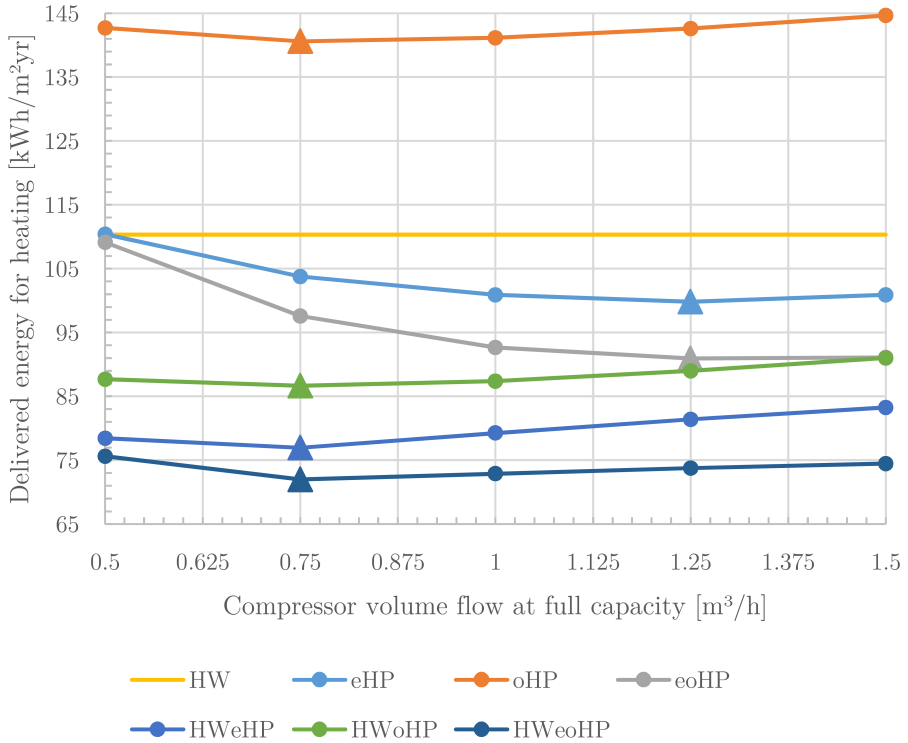


Figure 6.8: Optimum compressor volume at full capacity for "Large" occupant behaviour model, for building located in Kautokeino climate. The optimum compressor volume for each heat recovery case is marked with a triangle. Heat recovery case *HW* (heat wheel only) does not involve using a heat pump, but is shown to compare the performance to the other cases.

Table 6.1: Comparison of optimum compressor volume flow at full capacity for Oslo and Kautokeino climate.

	Oslo [m ³ /h]	Kautokeino [m ³ /h]
eHP	0.875	1.25
oHP	0.75	0.75
eoHP	1.0	1.25
HW	–	–
HWeHP	0.75	0.75
HWoHP	0.75	0.75
HWeoHP	0.75	0.75

6.2.2 Evaporator UA value

It is important to have a large UA value on the heat pump evaporator in order to achieve high heat pump performance. A large UA value reduces the temperature difference between the outlet air temperature of the evaporator and the CO₂ evaporation temperature. Figure 6.9 illustrates the significance of the UA value for the "Large" occupant behaviour model in Oslo climate. Figure 6.10 shows the same curves for heat recovery cases *eHP* and *HWeHP* for Oslo, Stavanger and Kautokeino climate. Occupant behaviour model "Large" is used seeing that the building is dimensioned for five people.

Achieving a low temperature difference is especially important for heat pump applications with a limited heat source, such as exhaust air heat pumps. As much as possible of the heat source must be exploited. One of the main limitations of the exhaust air heat pump is the maximum discharge CO₂ gas temperature from the compressor, which limits the lower possible evaporation temperature. A low UA value will reduce the amount of energy that can be removed from the exhaust air, before the evaporation temperature reaches the lower limit. Thus, the evaporator should be designed with a large UA value in order to ensure a low temperature difference between the CO₂ and the outlet air temperature from the evaporator.

Heat recovery case *eHP* and *eoHP*, together with *HWeHP* and *HWeoHP*, achieve the same performance at low UA values. At these

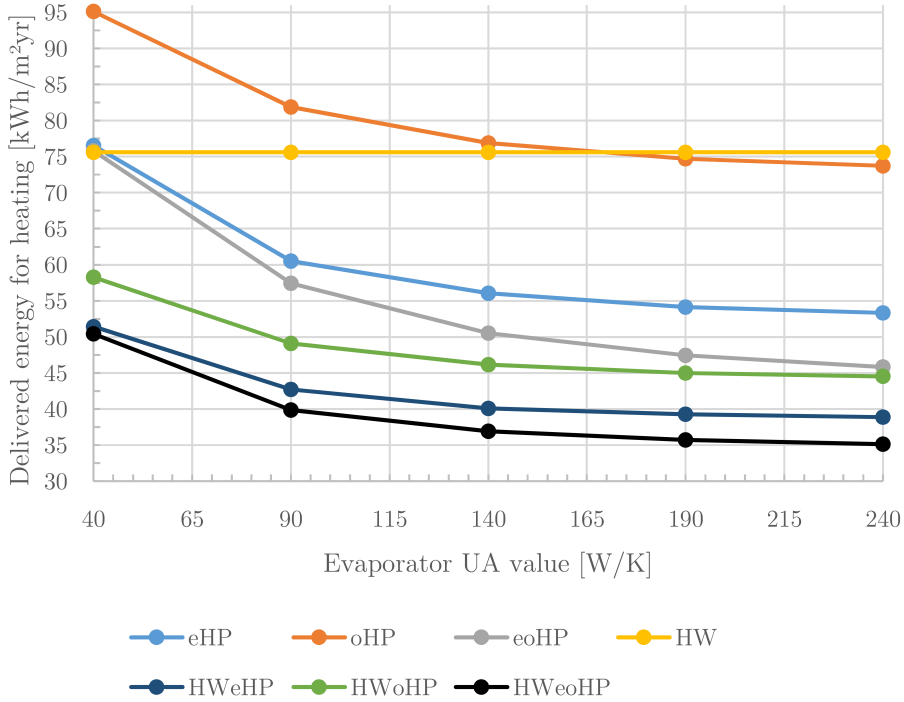


Figure 6.9: Delivered energy for heating at different UA values for all heat recovery cases. "Large" occupant behaviour in Oslo climate is used. Heat recovery case *HW* is included for comparison.

conditions, the heat pump does not benefit from being able to use outdoor air as an additional heat source.

The UA value is a trade-off between reduced temperature differences between air and CO₂, investment costs, space limitations, and pressure loss on both CO₂ and air side of the evaporator. Only the temperature difference is taken into account in the MATLAB heat pump model.

An UA value of 160 W/K is used in all simulations. This fixed value is somewhat high for some heat recovery cases and more suitable for others. A more in depth study of the evaporator is required in order to choose the ideal UA value where all aspects are taken into account, including a variable heat transfer coefficient. The heat transfer coefficient is strongly depending on volume flow of air and especially

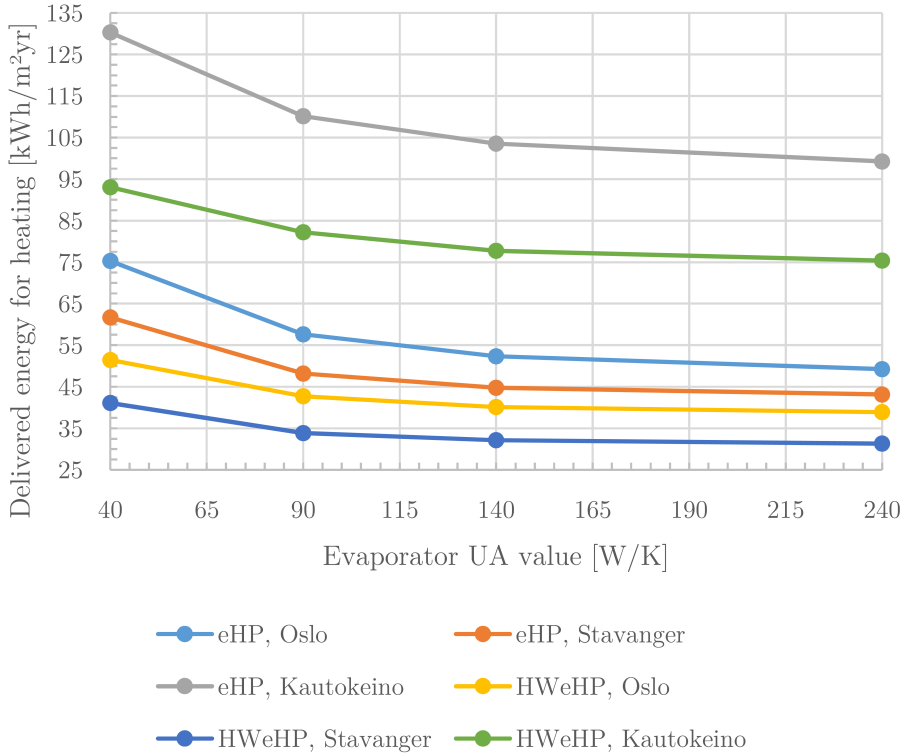


Figure 6.10: Delivered energy for heating at different UA values for heat recovery cases *eHP* and *HWeHP* for Oslo, Stavanger and Kautokeino. "Large" occupant behaviour model is used.

CO₂. Seeing that a VSD compressor is used in the model, the CO₂ volume flow will vary and thus also the heat transfer coefficient.

6.2.3 Outdoor air fan volume flow

Four out of the seven heat recovery methods are using outdoor air as main or additional heat source. The influence of the outdoor air volume flow is illustrated in table 6.11, simulated for "Large" occupant behaviour model using Oslo climate. All heat recovery cases where outdoor air is made use of as heat source are shown. Optimum compressor sizes from 6.2.1 are used in the simulations.

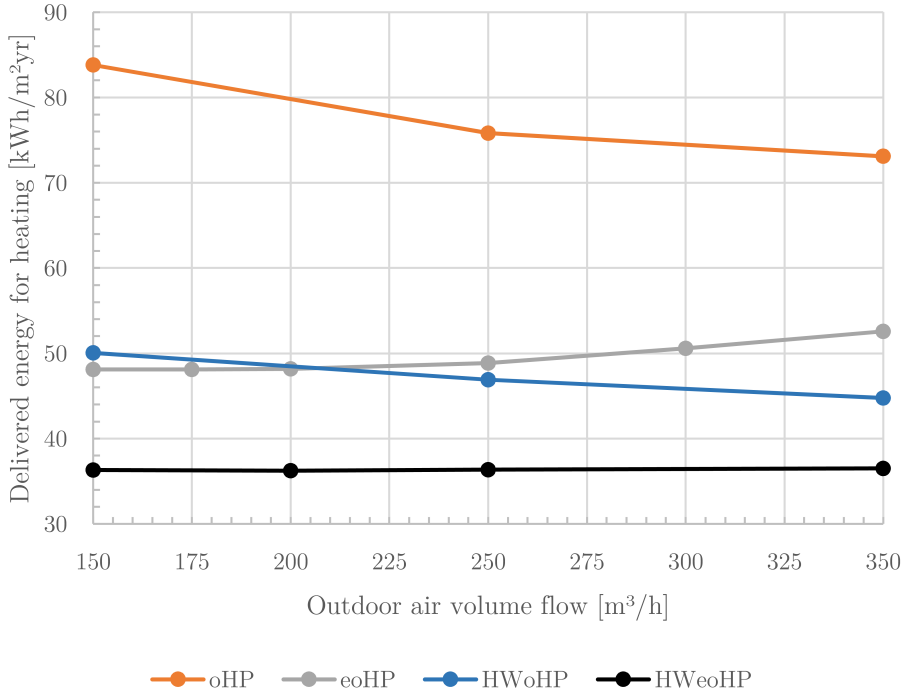


Figure 6.11: Outdoor air fan volume flow influence on delivered energy for heating. Simulated for "Large" occupant behaviour model using Oslo climate.

Heat recovery cases *oHP* and *HWoHP* have outdoor air as only evaporator heat source, and are more dependent on having a sufficiently large volume flow of outdoor air. Though not illustrated in figure 6.11, the curves for these two heat recovery cases have a global minimum. If the outdoor air fan volume flow is increased above this level, the required fan work will increase more than the performance of the heat pump. This will result in an increased amount of delivered energy for heating to the building. The global minimum occurs at an air flow rate of around 550 m³/h for *oHP*, resulting in 72.5 kWh/m²·yr delivered energy for heating.

eoHP and *HWeoHP* use exhaust air as main heat source for the heat pump, and the performance is thus less influenced of the outdoor air fan

volume flow. The curves are close to linear, though global minimums exist ($175 \text{ m}^3/\text{h}$ and $200 \text{ m}^3/\text{h}$ for *eoHP* and *HWeoHP* respectively).

The ideal outdoor air fan volume flow is a trade-off between heat pump performance and installation costs. Increased volume flow calls for a larger fan and increased duct diameter, together with increased work on the building. The aesthetics of the building may also be affected. Thus, an outdoor air fan volume flow of $250 \text{ m}^3/\text{h}$ is considered adequate, and is used in all simulations.

Heat recovery case *oHP* and *HWoHP*, where an outdoor air–water heat pump is used, would in most cases be installed with a larger volume flow of air. The compressor and the evaporator would be placed in a box outside the building, resulting in less air side pressure loss and reduced noise requirements. However, these two cases are also simulated with an air flow of $250 \text{ m}^3/\text{h}$ for better comparison with the other cases. The improved performance of higher air flow rates is in any case limited.

6.2.4 Influence of DHW storage tank volume

The storage tank volume may influence strongly on the required heating power and on the efficiency of the stratification of water in the tank. Simulations were performed for the "Large" occupant behaviour model. The influence on the temperature on the bottom of the tank and the required DHW heating power is shown in figure 6.5 and 6.6 respectively. The influence on the yearly delivered energy for heating (DHW, SH and VH) is shown in figure 6.12.

A storage tank volume of 200 liters increases the temperature at the bottom of the space heating tank considerably. The required DHW heating power vary much more during the day, which also reduces the heat pump performance. The yearly amount of delivered energy for DHW, SH and VH increases by 18%, 14% and 20% for heat recovery cases *HWeHP*, *HWoHP* and *HWeoHP* respectively, compared to a storage tank of 300 liters.

A storage tank of 400 liters results in a slightly increased amount of delivered energy for DHW, SH and VH. This is caused by increased heat loss from the storage tank, together with occasionally higher required heating power. The reason for the occasionally increased DHW heating power, calculated by IDA ICE, is not known. A DHW storage tank

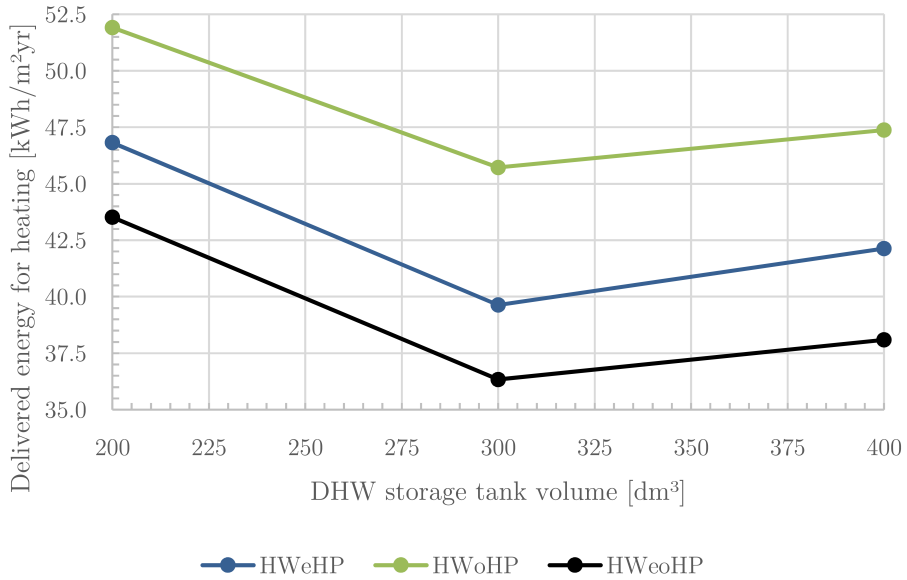


Figure 6.12: Influence of DHW storage tank volume on delivered energy

volume of 300 liters is used in all other simulations.

6.2.5 Influence of night time set-back

Night time set-back is used to lower the energy for heating during the night when the occupants are asleep. This is achieved by lowering the heating setpoint from 21 °C to 19 °C in the period from 23:00 to 07:00.

The net yearly energy demand for the building is reduced, due to the reduced heat loss at night time. However, the required heating power increases seeing that the building must be heated from 19 °C to 21 °C in a short period of time every morning. This increased power will affect the performance of the heat pump negatively. After 23:00, the required space heating and ventilation heating power will be *reduced*, which will affect the performance of the heat pump positively. The average space heating and ventilation heating demand over the year is also lowered.

Simulations were carried out in order to estimate the real impact of night time set-back, using the "Large" occupant behaviour model for a building located in Oslo. Table 6.2 compares the yearly amount of delivered energy for heating with and without night time set-back for each heat recovery case.

Table 6.2: Influence of night time set-back on delivered energy for DHW, SH and VH. "Large" occupant behaviour model and Oslo climate. The reductions are calculated for a period of one year.

Heat rec. case	With set-back <i>kWh/m²yr</i>	Without set-back <i>kWh/m²yr</i>	Energy saving
No heat rec.	115.1	117.3	1.8%
eHP	55.1	57.2	3.8%
oHP	75.8	78.1	2.9%
eoHP	48.9	50.5	3.1%
HW	75.6	77.2	2.1%
HWeHP	39.6	41.6	4.8%
HWoHP	45.7	47.5	3.8%
HWeoHP	36.3	37.9	4.2%

Despite the increased power consumption for heating caused by the temperature rise from 19 °C to 21 °C every the morning, night time set-back is still profitable for all heat recovery cases. Night time set-

back is most profitable for *eHP* among the solutions without a heat wheel, and *HWeHP* among the solutions with a heat wheel. These two heat recovery solutions benefit the most from the lowered average space heating power, due to the limited heat source. The DHW boiler is working on a high capacity in the first part of the night, and on low capacity early in the morning when the tank is close to fully loaded. Using night time set-back will therefore even out the required amount of energy for DHW, SH and VH. This will in turn especially benefit the heat recovery cases with a limited heat source.

6.2.6 Influence of reduced ventilation air flow when unoccupied

Air handling units for residential buildings often have an option of three different air flow rates operation modes. One air flow rate for normal operation, one low air flow rate for use when the building is unoccupied, and a third air flow rate for special occasions (e.g. high moisture production and/or many people).

Some house owners use the low air flow rate mode at daytime when the building is left empty. This will reduce the ventilation heat loss and fan energy, but at the same time reduce the heat source energy for heat pumps utilizing the exhaust air.

Simulations were carried out using "Large" occupant behaviour model in Oslo climate for all heat recovery cases. The air flow rate was reduced from $1.45 \text{ m}^3/\text{hm}^2$ to $0.7 \text{ m}^3/\text{hm}^2$, which is the minimum air flow rate for an unoccupied residential building in the prevalent Technical Regulations (2010). The AHU is assumed to run at low air flow rates from 08:00 to 16:00 every day, including weekends. The reduction in delivered energy for heating for each heat recovery case is shown in table 6.3. The reductions are calculated by comparing, for each case, the delivered energy for the building with and without reduced ventilation air flow rates at daytime. Figure 6.13 shows the impact of reducing the ventilation air flow during daytime on the heat pump. The impact is shown for a time period of 24 hours on the 1st of January.

A building with no heat recovery system will have a large benefit of reducing the ventilation air flow rate when the building is not occu-

Table 6.3: Influence of a 52% reduction of the ventilation air flow rate in a period from 08:00 to 16:00 every day, for "Large" occupant behaviour model in Oslo climate. The reductions are calculated for a period of one year. The numbers are delivered energy for DHW, SH and VH.

Heat rec. case	Const. vent. kWh/m ² yr	Red. vent. daytime kWh/m ² yr	Energy saving
No heat rec.	115.1	108.9	5.5 %
eHP	55.1	54.3	1.3 %
oHP	75.8	70.9	6.5 %
eoHP	48.9	47.4	3.1 %
HW	75.6	74.7	1.3 %
HWeHP	39.6	41.2	-4.1 %
HWoHP	45.7	44.9	1.8 %
HWeoHP	36.3	36.4	-0.1 %

ped. *oHP* will also experience a large reduction in delivered energy for heating, seeing that it is the solution with the lowest energy coverage. Reduced ventilation when unoccupied will reduce the ventilation heat loss considerably, while the heat pump heat source is unchanged.

eHP will experience only a minor energy saving. The available heat source is reduced by 52%. The available heat source for *HWeHP* is reduced by more than 52%, seeing that the heat wheel achieves higher efficiencies at reduced air flow rates. Hence, the heat pump will operate at a very low COP, or it will not be able to operate at all at minimum part load, due to high resulting discharge CO₂ gas temperatures. *HWeHP* will experience an *increased* energy consumption of about 4%. The performance of *HWeoHP* is close to unaltered.

As can be seen in figure 6.13, the compressor volume flow is clearly reduced when the ventilation air flow rate is reduced for case *HWeHP*. This reduction of compressor volume is necessary in order to maintain a discharge CO₂ gas temperature below 115 °C. The heat from the gas cooler is reduced by 40% to 50%. The occupants have a large DHW consumption from 07:00 to 09:00, according to figure 5.4 (p. 60).

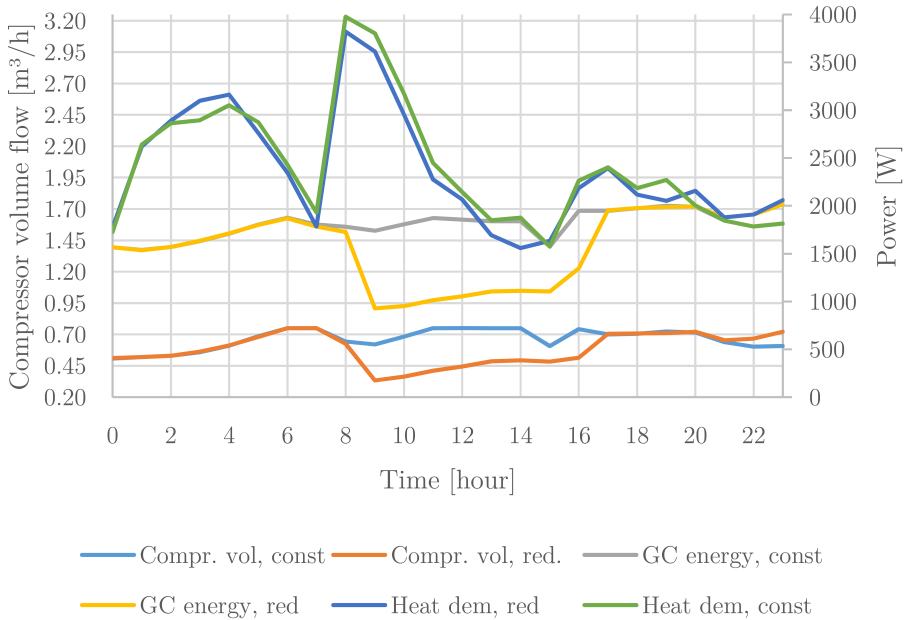


Figure 6.13: Influence of a 52% reduction of the ventilation air flow rate in a period from 08:00 to 16:00 every day. The numbers are for *HWeHP* for "Large" occupant behaviour model in Oslo climate, 1st of January. *GC* = gas cooler.

This is why the required energy increases rapidly in this time period, in addition to heating the building from 19 °C to 21 °C (see chapter 6.2.5).

6.2.7 Heat wheel efficiency

Figure 6.14 illustrates the impact of the ventilation heat exchanger efficiency on the yearly amount of delivered energy to the building. An efficiency of 80% is used in all other simulations in this report.

HWeHP experiences a reduction in delivered energy for DHW, SH and VH of 17% when going from 60% to 90% heat exchanger efficiency. *HW* has a reduction of 14%, while *HWeHP* and *HWeoHP* experience a reduction of 10%. The reduction is larger for *HWeHP* than for *HWeoHP*. This is because of the low energy coverage of the heat

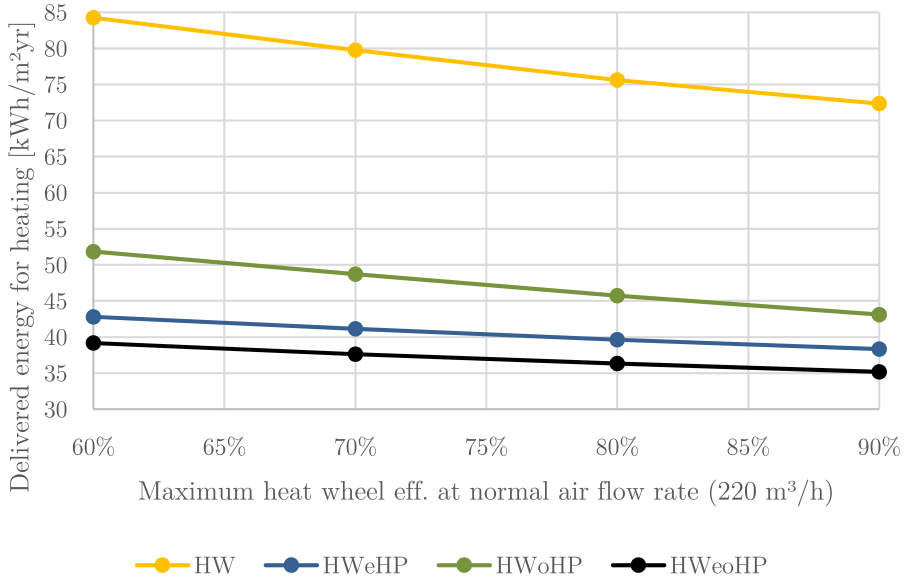


Figure 6.14: Heat wheel efficiency influence on delivered energy for "Large" occupant behaviour model, using Oslo climate.

pump and the unchanged evaporator heat source. For all other heat recovery cases, the evaporator heat source is reduced at higher heat wheel efficiencies. This would influence the dimensioning of the compressor, but that it not accounted for.

6.3 Sensitivity analysis

In this section, the sensitivity of different parameters are investigated. The investigated parameters are not parameters that can be designed freely, but rather parameters that have been assumed when making the model (e.g. isentropic and volumetric efficiency, gas cooler temperature approach value, compressor operating range, etc.).

6.3.1 Isentropic efficiency and compressor heat loss factor

The isentropic efficiency curve used in the model is shown in figure 5.6 (p. 71). The heat loss from the compressor is based on experiments on a real CO₂ compressor. The isentropic efficiency and the compressor heat loss factor are, together with the evaporation temperature, determining for the discharge gas CO₂ temperature. Figure 6.15 illustrates the influence of the isentropic efficiency and the heat loss factor on the yearly demand for delivered energy for heating, for the *HWeHP* heat recovery case. In the simulations, the isentropic efficiency curve is displaced with +10 and -10 percentage points from the original isentropic efficiency curve.

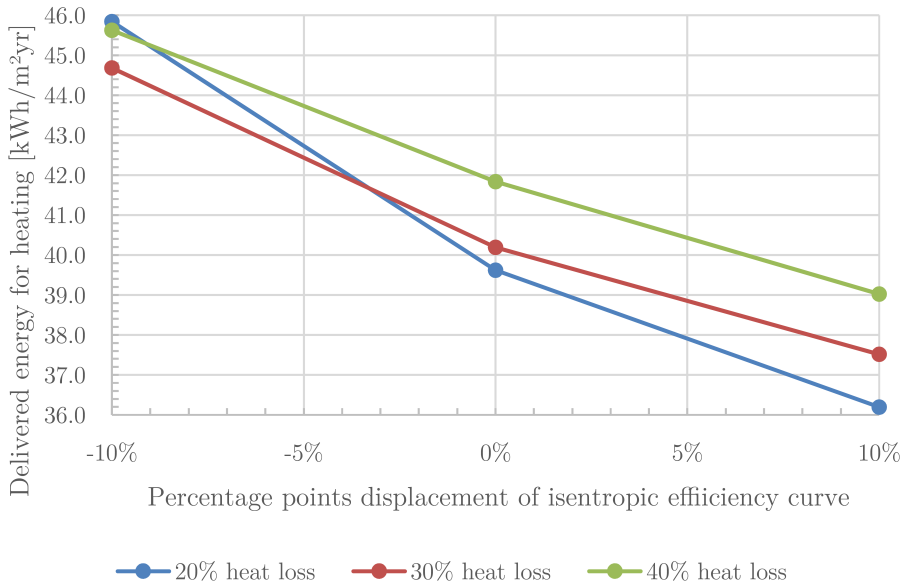


Figure 6.15: Sensitivity of isentropic efficiency and compressor heat loss factor on the amount of delivered energy for heating for heat recovery case 5. "Large" occupant behaviour model for Oslo climate was used in the simulations.

The isentropic efficiency has a large impact on the yearly amount of delivered energy for heating. A compressor with 10 percentage points increased isentropic efficiency reduces the delivered energy for heating by approximately 7% for 20%, 30% and 40% compressor heat loss. A reduced efficiency increases the amount of delivered energy by 16%, 11% and 9% for 20%, 30% and 40% compressor heat loss factor respectively.

A low heat loss from the compressor is generally desirable. However, figure 6.15 shows that a heat loss of 30% is more desirable than 20% for poor isentropic compressor efficiencies. The compressor heat loss reduces the discharge CO₂ gas temperature, according to equation 5.9 (p. 70). The increased heat loss results in a lower minimum evaporation temperature, and more heat can be removed from the exhaust air before exceeding the maximum discharge CO₂ gas temperature. The advantage of having lower possible evaporation temperatures is larger than the disadvantage of increased compressor heat loss, at low isentropic efficiencies. The figure also illustrates the importance of using high quality compressors with high isentropic efficiencies.

6.3.2 Temperature approach value

The gas cooler is modelled with a constant temperature difference (temperature approach value) between incoming water and the outgoing CO₂. The sensitivity of the parameter is illustrated in figure 6.16 for "Large" occupant behaviour model in Oslo climate.

The demand for delivered energy increases linearly at increasing temperature approach values. The curve gradients for all heat recovery cases are small and close to equal. Thus, the sensitivity of the choice of temperature approach value in the gas cooler model is rather low.

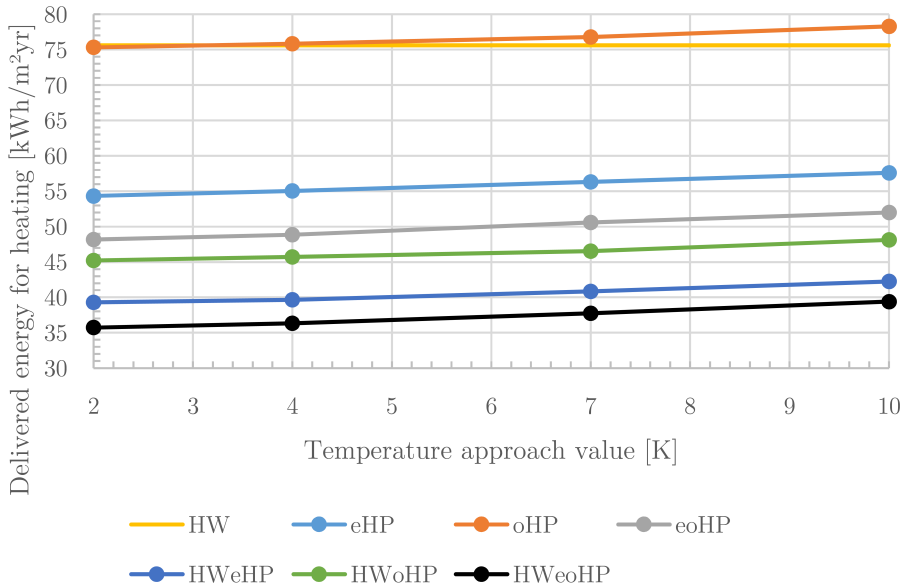


Figure 6.16: Sensitivity of the temperature approach value on the amount of delivered energy for heating for heat recovery case 5. "Large" occupant behaviour model for Oslo climate was used in the simulations..

6.3.3 Compressor operating range

A frequency controlled compressor has a limited operation range. The lowest possible part load volume flow is defined as a percentage of the compressor volume flow at full capacity (see chapter 5.3.5, p. 69).

Figure 6.17 illustrates the sensitivity of the parameter defining the minimum part load compressor load, for "Large" occupant behaviour model in Oslo climate. Figure 6.18 illustrates the same parameter for "Small" occupant behaviour model in Stavanger climate.

The minimum volume flow parameter has a low significance for small compressor sizes, seeing that the compressor is running above the minimum limit most of the time. The large consumption of DHW for the "Large" occupant model results in steady operation of the heat pump, with a heat demand all year round.

In figure 6.18, heating of DHW constitutes to a smaller amount of

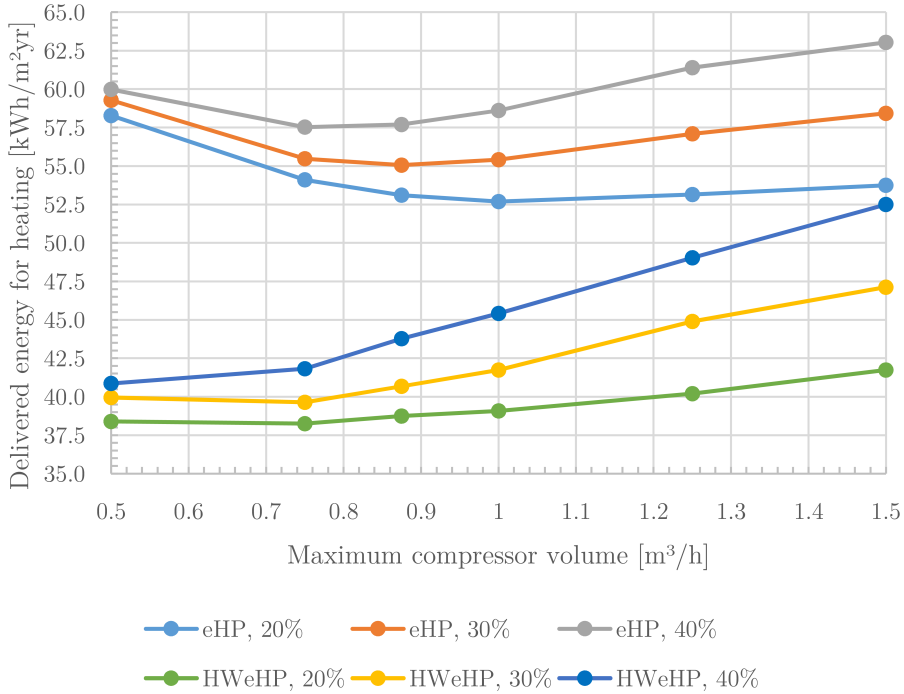


Figure 6.17: Significance of minimum compressor volume for "Large" occupant behaviour model, Oslo climate. The percentage number is the compressor volume flow at minimum capacity, compared to full capacity.

the total heat demand. Therefore, there is a larger fluctuation in the total heat demand throughout the year. This results in a significant difference in the performance for the different operating ranges (20%, 30% and 40%), also at lower compressor sizes.

A larger compressor size results in more intermittent operation of the heat pump, or no operation at all in some periods. A compressor with a limited operation range should therefore have a lower maximum volume flow, compared to a compressor with a larger operation range.

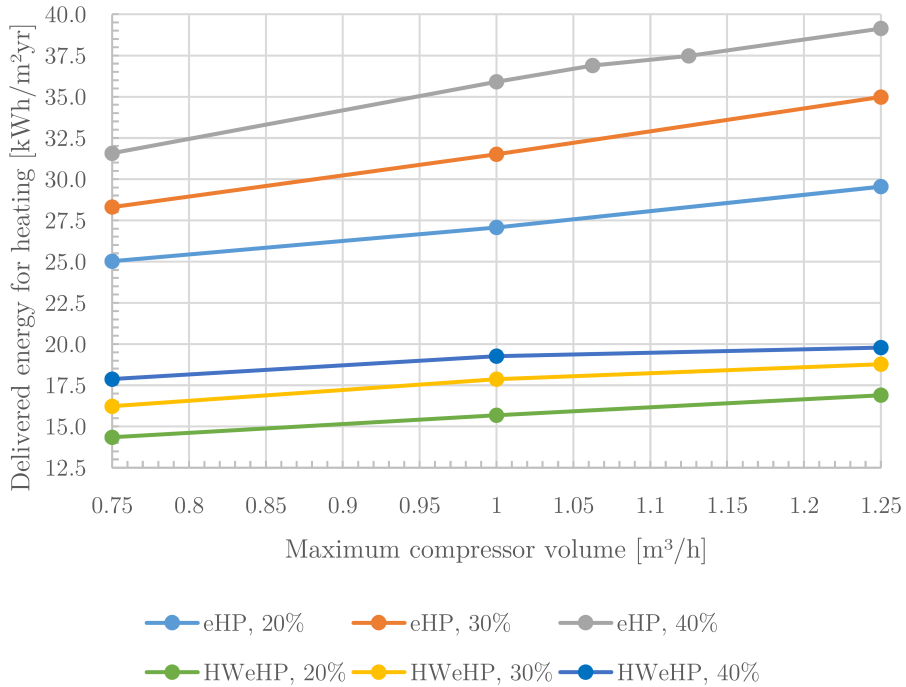


Figure 6.18: Significance of minimum compressor volume for "Small" occupant behaviour model, Stavanger climate. The percentage number is the compressor volume flow at minimum capacity, compared to full capacity.

6.4 General performance

This chapter will present the main results for the different heat recovery cases for different climates and occupant behaviour models. Table 6.4 compares each heat recovery method to the worst case scenario with no heat recovery.

Table 6.4: All heat recovery solutions, for all climates and occupant behaviour models, compared to the worst case scenario with no heat recovery.

	Case	Small	NS3031	Large
Oslo	eHP	52%	53%	52%
	oHP	35%	36%	34%
	eoHP	56%	57%	58%
	HW	51%	43%	34%
	HWeHP	73%	68%	66%
	HWoHP	68%	63%	60%
	HWeoHP	76%	72%	68%
Stavanger	eHP	52%	54%	56%
	oHP	43%	45%	43%
	eoHP	56%	58%	59%
	HW	55%	45%	35%
	HWeHP	74%	69%	68%
	HWoHP	71%	65%	64%
	HWeoHP	78%	73%	71%
Kautokeino	eHP	44%	44%	40%
	oHP	18%	19%	18%
	eoHP	47%	48%	46%
	HW	47%	42%	36%
	HWeHP	63%	59%	55%
	HWoHP	57%	53%	49%
	HWeoHP	65%	62%	58%

6.4.1 Comparison of cases with and without outdoor air

Exhaust air is a limited heat source for a heat pump. Outdoor air may be used to increase the available energy for the evaporator. Heat recovery case *eHP* and *eoHP* are identical, except that *eoHP* may use outdoor air as an additional heat source if beneficial. The same applies

for *HWeHP* and *HWeoHP*. Figure 6.19 and figure 6.20 compare the performance of heat recovery for a heat pump with and without outdoor air as additional heat source, for "Small" and "Large" occupant behaviour respectively.

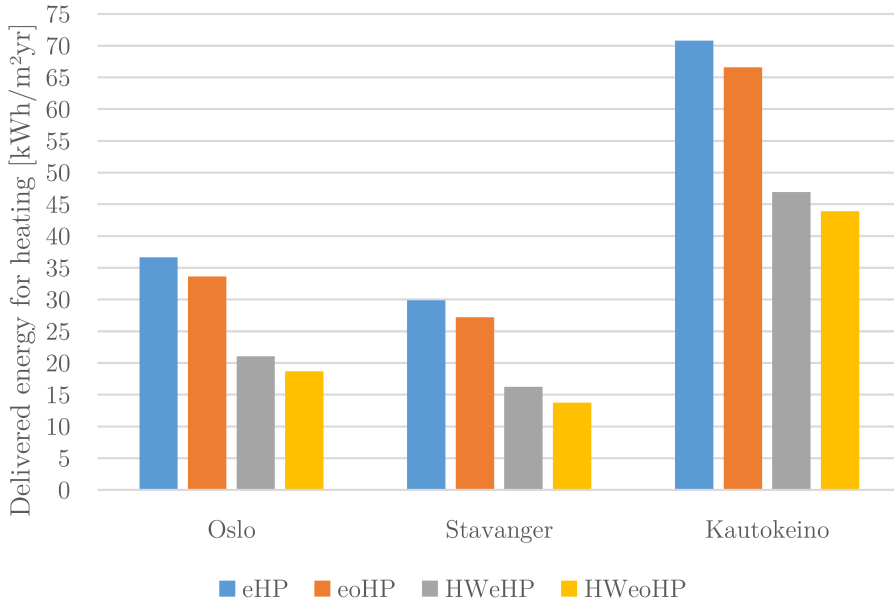


Figure 6.19: Comparison of solutions with and without outdoor air as additional heat source for "Small" occupant behaviour model.

Figure 6.19 shows that an exhaust air heat pump in a residential building with a low DHW consumption has limited use of being able to use outdoor air as an additional heat source. The advantage is larger for solutions without a heat wheel. In more extreme climates, such as in Kautokeino, the extra heat source is somewhat more useful. The differences in delivered energy for heating in Kautokeino climate for *eHP* and *eoHP*, and for *HWeHP* and *HWeoHP*, are 4.2 kWh/m²·yr and 3.0 kWh/m²·yr respectively.

Figure 6.20 compares the same heat recovery cases for "Large" occupant behaviour model. The advantage of being able to use outdoor air as an additional heat source is increased, due to the high DHW con-

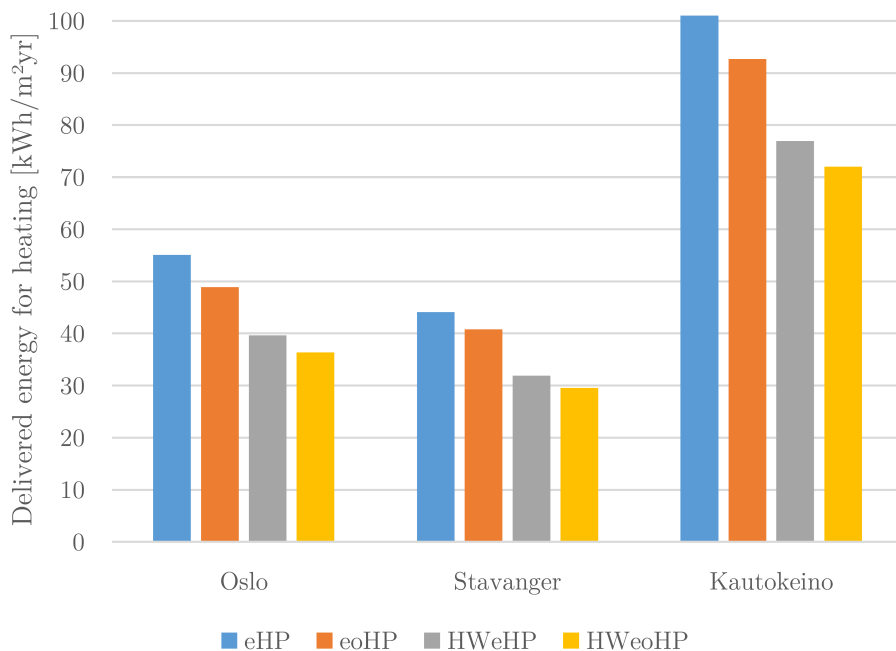


Figure 6.20: Comparison of solutions with and without outdoor air as additional heat source for "Large" occupant behaviour model.

sumption. However, in mild climates, such as in Stavanger, the benefit is very limited, even with a high DHW consumption. The differences in delivered energy for heating in Kautokeino climate for *eHP* and *eoHP*, and for *HWeHP* and *HWeoHP*, are 9.4 kWh/m²yr and 5.0 kWh/m²yr respectively.

6.4.2 Comparison of cases in different climates

Figure 6.21, 6.22 and 6.23 show the heat recovery cases' performance for Oslo, Stavanger and Kautokeino climate, with regard to delivered electrical energy for DHW, SH and VH.

Heat recovery case *eHP* can be compared to the exhaust air heat pumps for exhaust ventilation that are much used in Sweden, though they normally use a HFC refrigerant. Its performance is better than *HW* (typical for modern residential buildings in Norway) for all cli-

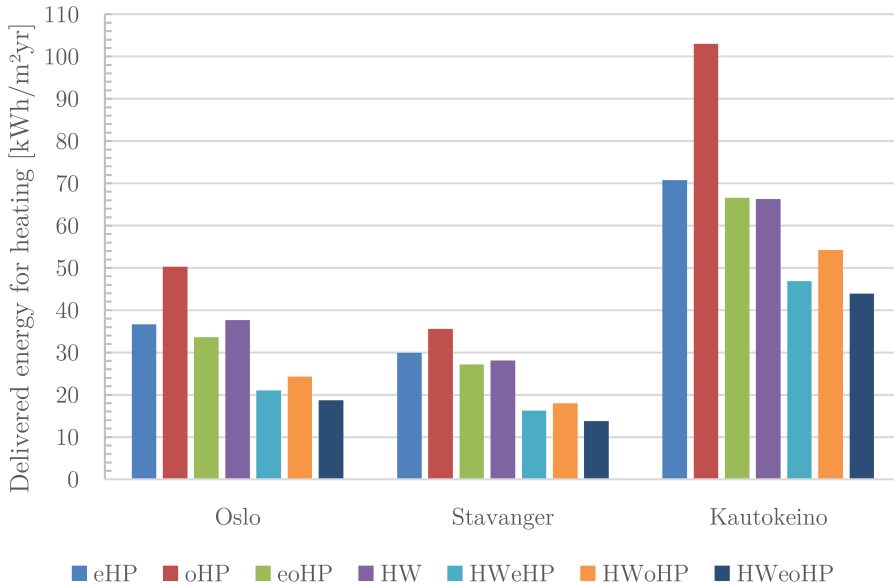


Figure 6.21: Comparison of heat recovery cases for "Small" occupant behaviour model.

mates, for "NS3031" and "Large" occupant behaviour. Though the performance of *eHP* is better than *HW*, the investment cost is higher, and the thermal comfort and ventilation efficiency may decrease in exhaust ventilation systems.

Heat recovery case *oHP*, a heat pump using outdoor air as heat source, does not actually recover ventilation heat. However, it could be an alternative to *eHP*, seeing that both cases consist of a heat pump only. *eHP* performs significantly better than *oHP*, due to the high temperature of the exhaust ventilation air. The total investment cost for *eHP* is assumed to be lower than for *oHP*. The exhaust air heat pump is sold as a complete unit together with the AHU, and does not need a heat pump technician for the assembly. *oHP* would normally consist of a AHU and a separate heat pump unit, which should be installed by a professional. However, *eHP* is dependent on exhaust ventilation or balanced ventilation.

eoHP uses exhaust air, together with outdoor air if beneficial, as

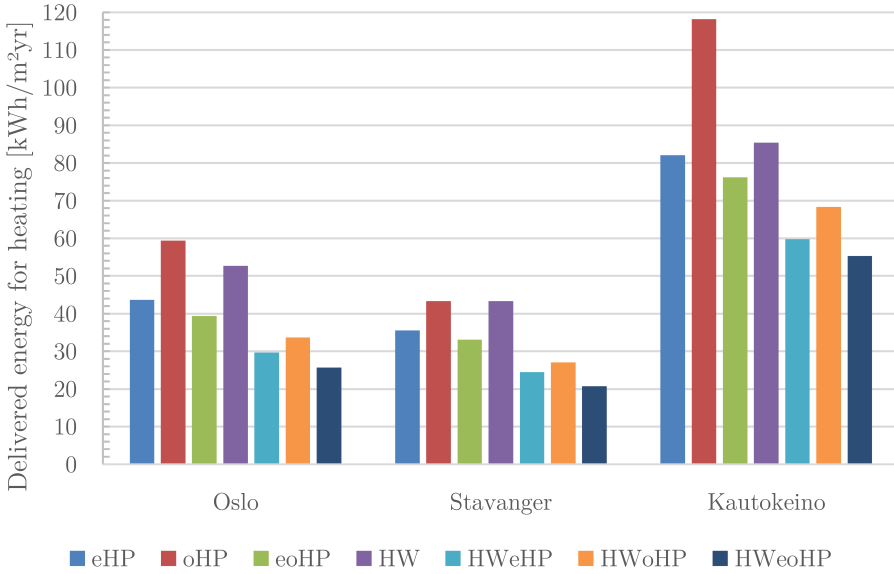


Figure 6.22: Comparison of heat recovery cases for "NS3031" occupant behaviour model.

heat source for the heat pump. The improved heat pump performance due to utilization of outdoor air is limited. However, for very cold climates, such as Kautokeino, the performance is clearly improved (see also chapter 6.4.1).

HWeHP makes use of a heat wheel combined with an exhaust air heat pump. It is the second best solution for all climates and occupant behaviour models. The performance is close to identical to *HWeoHP* for mild climates and occupant behaviour models with a low energy consumption. For high energy consumptions and very cold climates, *HWeoHP* performs slightly better. Though the performance is better, an economical analysis must be performed in order to determine if the increased performance is profitable.

Heat recovery case *HWoHP* consists of a heat wheel and a heat pump using outdoor air as heat source. The solution performs third best of all cases. However, the solution does not have any advantages over *HWeHP* and *HWeoHP*, other than being more easy to retrofit in

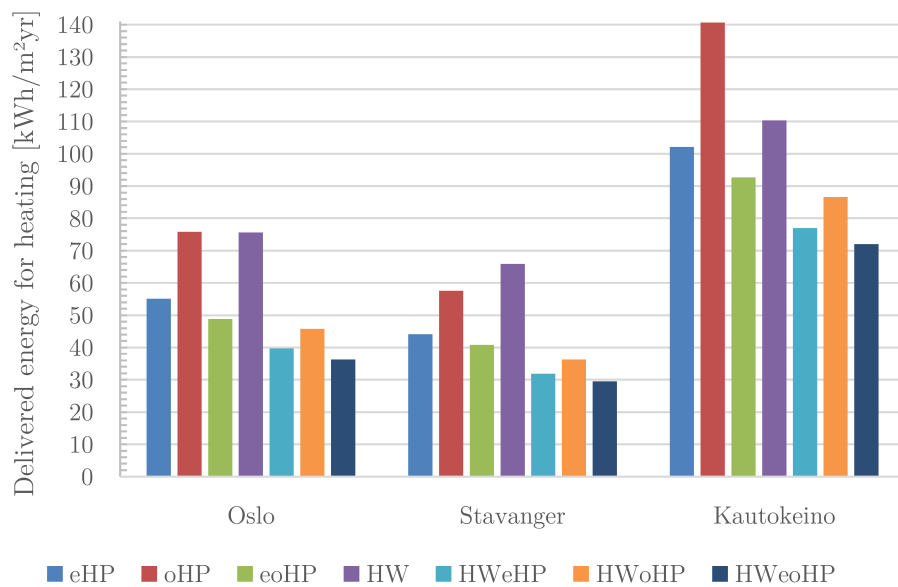


Figure 6.23: Comparison of heat recovery cases for "Large" occupant behaviour model.

a passive house building with existing *HW* heat recovery.

6.4.3 Composition of delivered and recovered energy for heating

Figure 6.24 illustrates the composition of the delivered energy to the building for heating for "Large" occupant behaviour model in Oslo climate. Figure 6.25 shows the composition of delivered energy for heat recovery case *HWeHP* for different climates. The figures also show the composition of the recovered energy. The amount of energy below the gray line equals the delivered electrical energy to the building for heating purposes (DHW, SH and VH). The amount of energy above the gray line equals evaporator energy and heat recovered by the heat wheel. According to NS 3031 (2014), all of this energy cannot be regarded as *recovered*, seeing that only energy removed from the exhaust air down to outdoor temperature is accounted for as recovered energy (see chapter 2.4, p. 20).

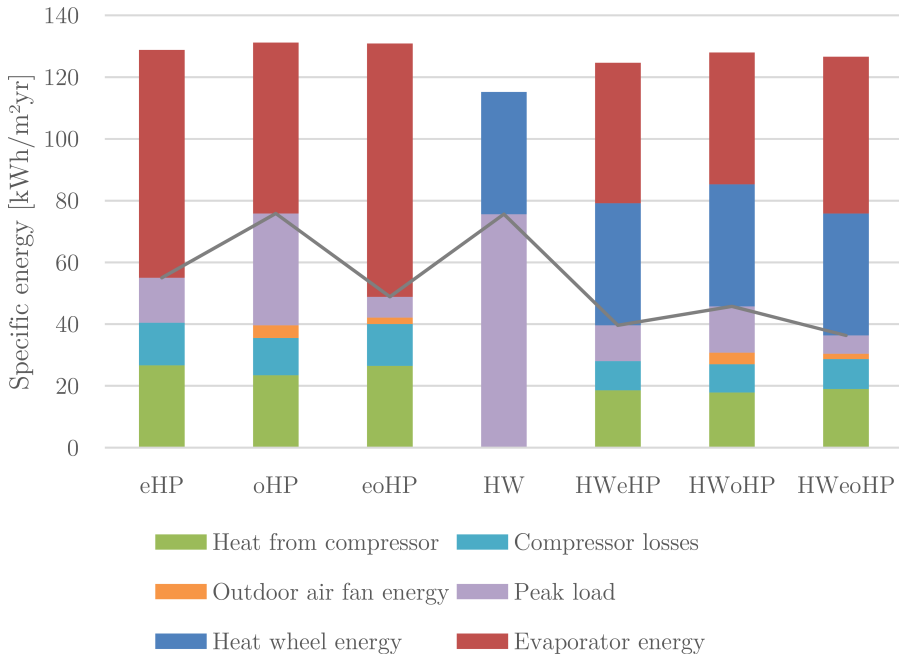


Figure 6.24: Composition of yearly delivered energy for heating for "Large" occupant behaviour model (Oslo climate)

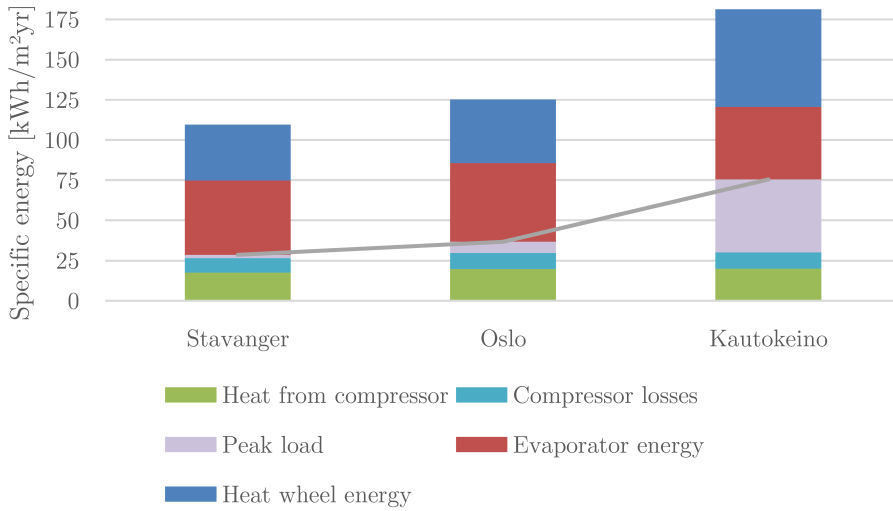


Figure 6.25: Composition of yearly delivered energy for heating for heat recovery case *HWeHP*, using "Large" occupant behaviour model.

Energy lost from the compressor is owing to compressor heat losses (assumed not useful), in addition to motor losses, transmission losses and frequency control losses. The sum of these losses amounts to a large share of the total delivered electrical energy for heating. Some of these losses will provide space heating in the room where the heat recovery unit is placed during periods with a heat demand. During the summer period, the losses from the heat recovery unit will contribute to excessive indoor temperatures.

The energy consumed by the outdoor air fan is very limited for heat recovery case *eoHP* and *HWeoHP*, seeing that the operational time of the fan is short. The fan energy is equal to 5.1% and 5.8% of the total compressor energy for *eoHP* and *HWeoHP* respectively. For *oHP* and *HWeoHP* it can be seen that the outdoor air fan energy constitutes to respectively 10.2% and 12.1% of the total compressor energy.

Figure 6.25 shows that heat recovery method *HWeHP* is able to cover a large share of the total heat demand for "Large" occupant behaviour model in Stavanger. Peak load energy amounts to 7% of the delivered energy for heating to the building. The corresponding numbers for Oslo and Kautokeino are 19% and 60% respectively. The

amount of evaporator energy in Kautokeino climate is smaller than for Stavanger and Kristiansand, despite the much higher heat demand. This is caused by the low air temperature after the heat wheel, which strongly reduces the available evaporator heat source.

6.4.4 Heat pump for production of DHW only

Using heated water for space heating and ventilation heating requires a heat distribution system, which will increase the investment cost of the heating system significantly. A heat distribution system is made superfluous when using direct-acting electricity for space heating and ventilation heating. "Hot air heating" uses the ventilation ducts for heat distribution, but the occupants may experience reduced thermal comfort. It is therefore interesting to investigate the performance of heat recovery case *HWeHP* in a case where the heat pump only supplies heat for heating of DHW. This case is most interesting for occupants with a high DHW consumption. Figure 6.26 shows the performance of such a solution for different climates.

The amount of delivered energy for heating for "Large" occupant behaviour model increases by 19%, 18% and 9% for Oslo, Stavanger and Kautokeino climates respectively. Though the SH and VH demands are considerably higher for a building located in Kautokeino, compared to Oslo and Stavanger, the increase in delivered energy is the least for this climate. As can be seen on figure 6.26, the amount of peak load energy is considerable in Kautokeino climate. For most parts of the year, the heat pump is not able to cover any more energy than energy for heating of DHW. The amount of saved energy for space heating and ventilation heating, compared to direct-acting electricity, is therefore limited for very cold climates.

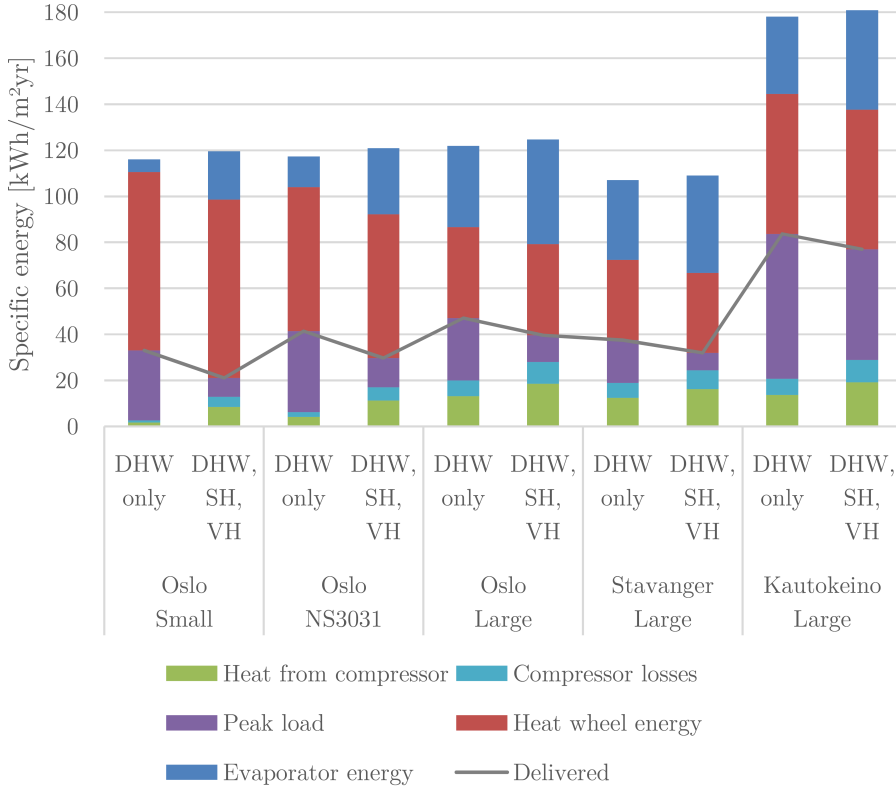


Figure 6.26: The performance of heat recovery case *HWeHP* covering heating of DHW only.

6.4.5 COP duration curves

The duration curves for all heat recovery cases for "Large" occupant behaviour model in Oslo climate are shown in figure 6.27.

The heat recovery solutions using both exhaust air and outdoor air are able to operate under most conditions. The two solutions having outdoor air as only evaporator heat source achieves the lowest COP. The solutions not benefiting from a heat wheel (*eHP* and *eoHP*) achieve the highest COP values, due to the high inlet air temperature on the evaporator. However, they have a much higher heat demand to cover. The duration curves for *HWeHP* and *HWeoHP* are slightly

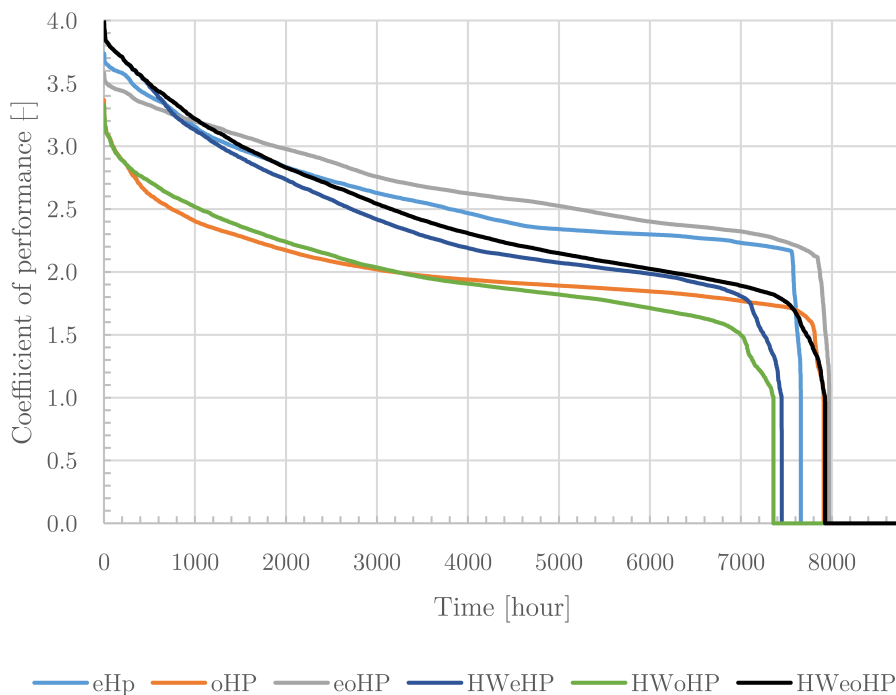


Figure 6.27: COP duration curves for "Large" occupant behaviour model, using Oslo climate.

lower. When the recovered energy from the heat wheel is taken into account, the combined COP will be considerably higher.

6.5 Economical evaluations

Air handling units with built-in CO₂ exhaust air heat pumps are not yet a commercialised solution. Thus, no data on investment cost for the different solutions can be found. Figure 6.28 and 6.29 presents the maximum permissible investment (MPI) for each case, compared to the *HW* heat recovery solution, for Oslo and Stavanger climate. *HW* is the most used heat recovery solution today, with the lowest investment cost. MPI is the maximum amount of money that can be invested before the investment is no longer profitable. Table 6.5 shows

the input parameters used in the calculations.

Table 6.5: Input parameters for economical calculations

	Parameter	Unit
Interest rate	5	%
Lifetime	15	years
Electricity cost	0.8	NOK/kWh

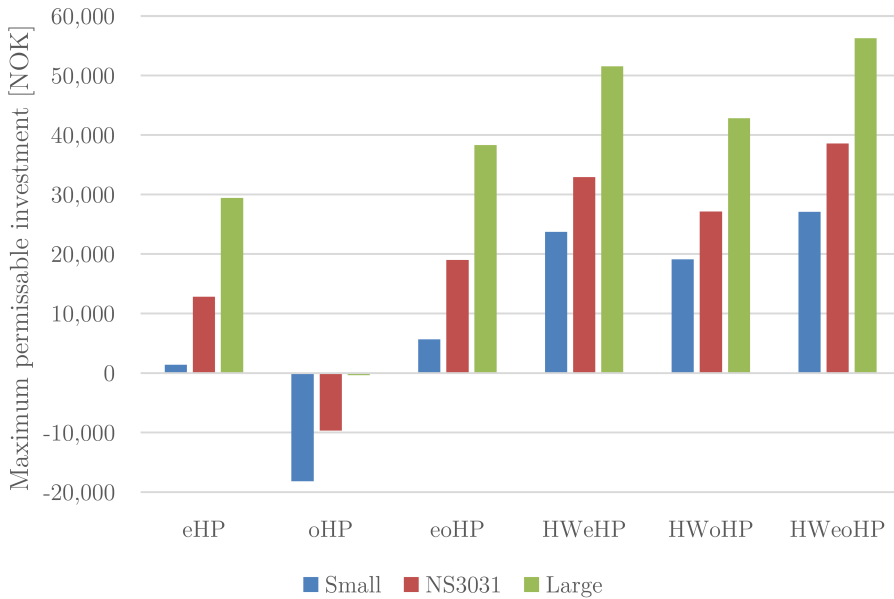


Figure 6.28: Maximum permissible investment in Oslo climate.

For *eHP*, *oHP* and *eoHP*, the MPI in figures 6.28 and 6.29 equals how much *more* such a solution can cost, compared to a *HW* heat recovery solution. *oHP* will therefore not be a reasonable choice, compared to *HW*. *eHP* and *eoHP* might turn out profitable, but only for occupants with a high DHW consumption.

For *HWeHP* and *HWeoHP*, the MPI in figure 6.28 and 6.29 equals the *extra* investment cost that is affordable in order to equip the AHU

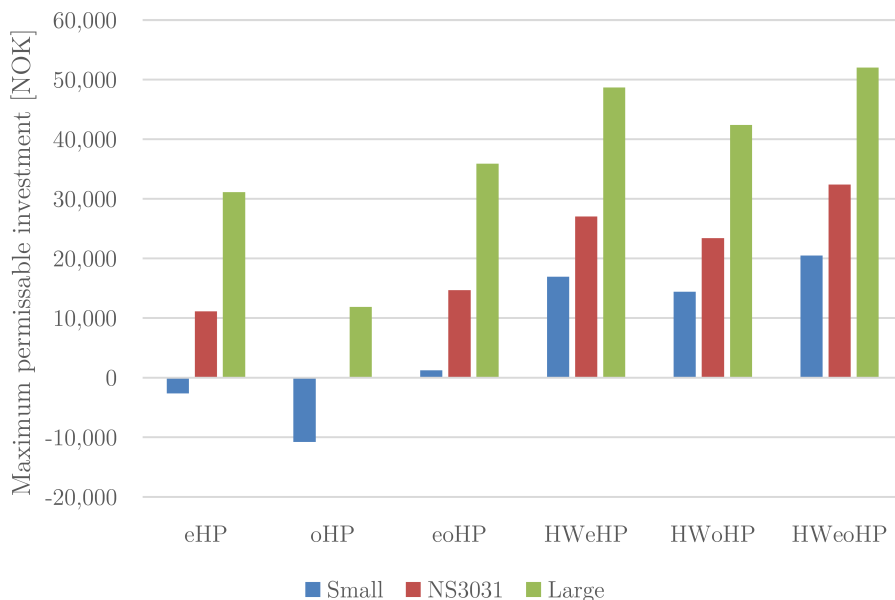


Figure 6.29: Maximum permissible investment in Stavanger climate.

with a CO₂ heat pump. For *HWoHP*, the MPI equals the maximum investment cost of an outdoor air–water CO₂ heat pump. It is probable that *HWeHP* and *HWeoHP* can turn out profitable for "NS3031" and "Large" occupant behaviour models, and maybe also for "Small". However, a more in depth economical analysis is required for all seven heat recovery cases in order to assess their economical feasibility. *HWoHP* has an MPI of about 40,000 NOK for Oslo and Stavanger climate, for "Large" occupant behaviour model. It is not likely that an outdoor air–water heat pump can be purchased and installed for that amount of money.

According to figure 6.28 and 6.29, it is not certain that it will be economically profitable to use outdoor air as an additional heat source. *eoHP* has an MPI that is about nine thousand NOK higher than *eHP* for Oslo climate. The corresponding number for *HWeoHP* and *HWeHP* is five thousand NOK. Depending on the system solution for supply of additional outdoor air to the evaporator, a duct, an extra fan, a filter, dampers, controllers and grilles are required. The installation work and

the work on the building will also add costs to the unit. Installing such an air duct may also increase the heat loss from the room and take up extra space. The corresponding MPIs for Stavanger climate are equal to about five thousand NOK and a little more than three thousand NOK.

Table 6.6 shows the MPI for a hydronic distribution system in the building. The calculations are based on the simulations performed in chapter 6.4.4 (p. 114), where heat recovery case *HWeHP* was set to cover the energy demand for DHW only.

Table 6.6: MPI of hydronic heat distribution system for. Input parameters from table 6.5 are used. The lifetime of the heat distribution system is set to 50 years.

Climate	Del. energy, DHW only kWh/m^2yr	Del. energy kWh/m^2yr	MPI NOK
Oslo (Small)	33.0	21.1	20,200
Oslo (NS3031)	41.4	29.7	29,600
Oslo (Large)	47.1	39.6	18,800
Stavanger (Large)	37.5	31.9	14,200
Kautokeino (Large)	83.7	76.9	16,900

The MPI listed in the table is equal to the maximum *extra* investment cost for a hydronic heating system, compared to a heating system based on direct-acting electricity. The cost for installing hydronic heating when building a Norwegian dwelling is equal to 601 NOK/m² (Haarberg et al., 2010). Even though this cost can be reduced in passive houses, due to a very low heat demand, it is not likely that hydronic floor or radiator heating will be able to compete with a space heating and ventilation heating system based on direct-acting electricity (electric radiators and/or heater cables) for the "Large" occupant behaviour model.

"Small" and "NS3031" occupant behaviour model have much higher MPIs for the heat distribution system. This is caused by the low DHW consumption, making the energy savings for space heating and ventilation heating much larger. Optimizing the heat pump for DHW only

may increase the MPI. It is thus likely that a hydronic heat distribution system can turn out profitable for these occupant behaviour models. However, the building is designed for five persons. Hence, the DHW consumption will normally not be as low as for the "Small" occupant behaviour model in such buildings.

The economical calculations performed in this chapter is based on an electricity price of 0.8 NOK/kWh, making the economical calculations conservative. It is probable that the costs of electricity will increase in near future, due to higher demands for renewable electricity in Europe. This will increase the MPIs presented in this chapter significantly, making heat pump heat recovery more profitable and viable.

Chapter 7

Discussion

This chapter will discuss different aspects of the report. Strengths and weaknesses of the simulation platform and architecture, and proposed system solutions are discussed. In addition, the area of application for the results from this report is assessed. Some discussion has already been presented together with the simulation results in chapter 6.

7.1 Building model

The return water temperatures from the space heating and ventilation heating system are lower than what was expected, based on the settings defined in IDA ICE. This seems to be caused by both the heating element in the AHU and the hydronic zone heating. Heating load simulations show that the real water supply temperature to the zones is 30 °C, not 40 °C as defined. The water return temperature from the zones is around 25 °C in the same simulation. The hydronic heating element in the AHU has a water supply temperature of 40 °C. The return water temperature reaches temperatures close to the supply air temperature. This is most likely caused by a default value in the settings of the heating element in IDA ICE, which should have been changed to a more adequate value.

The temperature in the bottom of the space heating tank is a mixture of the return temperature from zones and the return temperature from the AHU heating element. The temperature in the bottom of

the space heating tank will be lower for heat recovery cases *eHP*, *oHP* and *eoHP*. These cases do not have a passive heat exchanger, and the share of energy for ventilation heating compared to zone heating is considerably increased. The specific evaporator energy ($\Delta h_{\text{evaporator}}$) will increase at low inlet water temperatures to the gas cooler. This will in turn result in reduced CO₂ mass flow (see equation 5.13, p. 74) and increased heat pump performance. A more realistic water return temperature would result in increased optimum compressor size, reduced SPF for the heat pump, and thus an increased amount of delivered energy for heating to the building.

Temperatures above the desired indoor temperature setpoint may occur at high outdoor temperatures and/or during periods with high solar gains and high internal loads. The IDA ICE building model makes use of automatic window opening and automatic window blinds in order to reduce excess temperatures. However, such automatic solutions are not common in single-unit dwellings. Opening of windows and use of window blinds are usually handled by the occupants manually. Thus, an increased indoor temperature must be expected when the occupants are not at home and cannot open windows or draw the blinds. This will in turn favour heat recovery cases using a heat pump, seeing that the available heat source energy increases.

Several different schedules are used in the IDA ICE model (e.g. occupancy, temperatures, internal loads, etc.). Sharp transitions have a strong influence on the simulation time. "*Schedule smoothing*" is by default applied in the IDA ICE software. This setting makes the transitions in i.e. heating setpoint and occupants' presence less sharp, and the simulation time is reduced. This default setting is recommended by EQUA Simulation AB (2013). This will, on a yearly basis, have low influence on the energy performance. However, the impact of schedule smoothing might be noticeable for, for example, ventilation schedules. In cases where the ventilation air flow is reduced when the building is unoccupied, IDA ICE use one to two hours on going from normal ventilation air flow rate to the minimum air flow rate. This might have a negative influence on heat recovery cases using a heat pump, especially when exhaust air is the only heat source.

7.2 Heat pump model

The boilers implemented in IDA ICE make use of PI-controllers and temperature sensors in the storage tanks in order to control the boiler power. The heat pump model developed in MATLAB is designed to operate at optimum conditions in each time step, and not according to sensors and controllers. Thus, the compressor load and the expansion valve pressure drop are optimized in each time step. For heat recovery cases *eoHP* and *HWeoHP*, each time step is calculated twice, with and without the outdoor air fan activated, in order to find whether or not it is beneficial to activate the fan. A real heat pump model is dependent on using controllers and sensors. The heat pump would not be able to run at the optimum conditions at all time, and the performance would therefore be reduced.

The gas cooler in the MATLAB heat recovery script is modelled by assuming a constant temperature difference of 4 °C between outgoing CO₂ and incoming water. The significance of this value on the heat pump performance is not of vital importance, according to figure 6.3.2 (p. 102). However, the real temperature development of water and CO₂ in the gas cooler is not known. The gas cooler should be discretized and calculated with a variable heat transfer coefficient. It would then be possible to optimize the gas cooler pressure according to the evaporation temperature and the water inlet temperature. Using a variable gas cooler pressure would increase the heat pump performance and reduce the amount of delivered energy to the building.

The constant gas cooler pressure used in the simulations in this report is set to 100 bar, mainly based on simulations and experiments performed by Stene (2004) (chapter 5.3.6, p. 72). This value might be slightly high. Most of the time, the heat pump is operating at low evaporation temperatures, resulting in high discharge CO₂ gas temperatures. This applies especially for the "Large" occupant behaviour model, due to high utilization of the heat source. The experiments performed by Stene used an evaporation temperature of -5 °C. It is likely that the optimum gas cooler pressure for an exhaust air heat pump is lower than 100 bar. Lowered gas cooler pressure would increase the COP and allow for a higher utilization of the heat source, due to lower

discharge CO₂ gas temperatures when the pressure is reduced. However, it is not possible to calculate the optimum gas cooler pressure without knowing the temperature development of air and CO₂ in the gas cooler. A gas cooler pressure of 100 bar may therefore be regarded as a conservative value.

The heat pump in the MATLAB model is turned off if the resulting discharge CO₂ gas temperature at minimum part load exceeds 115 °C. The heat pump could be able to operate if the gas cooler pressure was reduced. However, this would require discretization of the gas cooler in order to know the actual temperature of the outgoing water and CO₂ from the gas cooler. Reducing the gas cooler pressure in such cases would increase the SPF and reduce the yearly amount of delivered energy for heating to the building.

The compressor heat loss is set to 24% of the compressor input power. This heat is considered not useful in the heat pump model. Some of this heat may provide useful space heating energy to the room in which the unit is placed. The compressor heat loss energy may also be used to preheat the exhaust air and/or outdoor air before entering the evaporator. The amount of compressor heat loss that may be utilized is not known. The heat lost amounts to more than 11 kWh/m²yr for the "Large" occupant behaviour in Oslo climate. Measures should therefore be taken in order to utilize this energy and reduce the amount of delivered energy to the building.

The outlet air temperature from the evaporator is, depending on climate and occupant behaviour, usually below the freezing point. Frost formation will occur on the evaporator surface. Frost on the evaporator surface will reduce the heat transfer coefficient. The temperature difference between air and CO₂ will increase, and the heat pump performance will decrease. If the heat pump is not regularly defrosted, the evaporator may be blocked by frost. Defrosting may be achieved using different methods. All methods require energy, which will reduce the heat pump performance. Energy for defrosting of the evaporator is not implemented in the heat pump model, but would have a substantial influence on the heat pump performance. The exhaust air from the zones contains more moisture than outdoor air. It is therefore expected that heat recovery cases with a heat pump using exhaust air as heat

source would experience a stronger reduction in performance than a heat pump using outdoor air as heat source. The reduction in performance will depend on indoor moisture production, defrosting method and discharge air temperature from the evaporator.

The heat pump compressor is controlled intermittently at small heat demands. This results in several starts and stops, which both reduces the heat pump performance and the lifetime of the compressor. The reduction in heat pump performance for the first time period after start-up is not taken into account by the heat pump model. Losses related to start and stop of the compressor will be larger for "Small" occupant behaviour model and mild climates due to the variable heat demand.

7.3 Recommended heat recovery case

CO₂ exhaust air heat pumps integrated in air handling units are not yet available on the commercial market. It is thus difficult to estimate the life-cycle cost (LCC) of the different heat recovery solutions. It is assumed that a complete AHU with an integrated CO₂ heat pump will have a significantly lower price compared to a AHU and a CO₂ heat pump bought separately. It is also likely that the investment cost for such units will be reduced when the production volumes increase and several manufacturers offers similar products.

Based on energy performance, economy and system solution, heat recovery case *HWeHP* is regarded as the best heat recovery solution when designing the building for five persons. The recommendation is based on reduced prices and further development of CO₂ heat pumps for exhaust air heat recovery in the years to come. However, a more in-depth investment analysis must be performed in order to find the potential for such heat pumps. If future in-depth investment analyses proves heat recovery using CO₂ heat pumps unprofitable, heat recovery case *HW* will be the recommended solution. A solution using R290 or a HFC as refrigerant may also prove more profitable, due to the lower cost on such compressors and appurtenant equipment.

For occupants with a low consumption of DHW, it is most likely not economically feasible to invest in an exhaust air heat pump for heat recovery and heat supply to the building. However, such a solution may

be interesting for occupants that are environmentally conscious.

The heat recovery solutions not utilizing a heat wheel may also turn out to be profitable for occupants with a high DHW consumption. Considering the low investment cost of a heat wheel, *HWeHP* is likely to be more profitable. Heat recovery solutions using outdoor air as an additional heat source is not very likely to be profitable, except for cold climates, due to higher investment costs, more complicated fan control and longer installation time in the building.

7.4 Validity and area of application for the simulation results

This report has used a typical single family passive house as a basis for simulations on different heat recovery models. In order to increase the validity of the results, the simulations were carried out for three different occupant behaviour models and three different climates.

The three different occupant behaviour models have a large span in consumption of domestic hot water. "Small" has a very low consumption, while "Large" has a DHW consumption close to what can be expected for a family of five persons. It is likely that the energy consumption for heating (DHW, SH and VH) will be situated in between "Small" and "Large" for a building of this size. It is not likely that more than five persons will live permanently in the building.

The climates used in the simulations were Oslo, Stavanger and Kautokeino. A large part of the Norwegian population lives in areas close to Oslo, or in locations with similar outdoor temperatures. A large part of the remaining population lives on the western coast with a climate similar to the climate in Stavanger, with mild winters. Very few people live in climate zones similar to the Kautokeino climate. However, the simulations performed for Kautokeino climate provides information on how the different heat recovery cases will perform in one of the most extreme climates found on the Norwegian mainland.

One building is used for all performed simulations in the report. Though it is a common size, it is not representative for all Norwegian residential buildings. A young couple living in a small flat will normally have a large specific DHW consumption. The available heat pump heat

source will be very limited for a "HWeHP" system solution, and the performance of the heat pump would be low.

An elder couple living in a larger house, e.g. where the children have moved out, will have a very low specific DHW consumption. The available heat source of the heat pump will however be very large. A CO₂ exhaust air heat pump will achieve a reasonable performance. However, it is likely that a subcritical heat pump could perform better, due to the relatively low DHW consumption and the lower investment cost.

This report does not contain simulations for blocks of flats that often have centralized ventilation and DHW. Modern blocks of flats, especially those built in accordance with the passive house standard, have a very low heat loss and high DHW consumption due to the densely occupied building. The high DHW consumption compared to the low space heating and ventilation heating demands make blocks of flats suited for a CO₂ exhaust air heat pump. In addition, a centralized heating plant may achieve a better performance, due to increased compressor size. Larger compressors and motors generally achieve higher efficiencies than smaller compressors. The DHW consumption would also be more evenly distributed. However, it is likely that it would be beneficial to use outdoor air as an additional heat source due to the relatively low ventilation air flow rate in such compact buildings, compared to the high DHW consumption. A separate subcritical heat pump for space heating may also be rational.

The simulations are performed for a residential passive house. The simulations show that *HWeHP* is able to cover the entire demand for DHW, VH and SH in Stavanger climate for "Large" occupant behaviour model (see figure 6.25, p. 113). In Oslo climate, the peak load energy starts to become noticeable. In Kautokeino climate, the peak load energy is considerable, and the heat pump is utilizing as much energy as possible from the heat source. A building located in Oslo, built in accordance with the prevailing Technical Regulations (2010), will have a heat demand closer to an equal passive house located in Kautokeino than Oslo. Such a building in Oslo, with a high DHW consumption, will thus have to use a substantial part of direct-acting electricity for heating.

The simulation results presented in this report are based on yearly energy simulations with a time step of one hour. Though many aspects are taken into account in the building and heat pump model, several assumptions deviate from a real life situation. Some assumptions make the models overestimate the performance, while other assumptions underestimate the performance. The largest source of variance from what can be expected from a real situation might be caused by the need for defrosting of the evaporator. However, all heat recovery methods are evaluated using the same assumptions under the same conditions. It is therefore likely that the most efficient heat recovery method found in this report also will be the most efficient method if materialized.

Chapter 8

Conclusion

Several simulations were carried out using a combination of *IDA Indoor Climate and Energy* and MATLAB, in order to investigate the performance of different heat recovery solutions. The different solutions were combinations of a heat wheel and a CO₂ heat pump using exhaust air and/or outdoor air as heat source.

The economical aspects of the different heat recovery solutions were not the main aspect of this report, though some comparisons were made. It is thus difficult to conclude with a recommended solution. The recommended solution will depend on the investment cost of a CO₂ heat pump. The following list presents the most important discoveries made in the report:

- A system solution consisting of a heat wheel and a CO₂ heat pump, that is able to utilize both exhaust air and outdoor air, is the most energy efficient solution.
- The increased heat pump performance when utilizing outdoor air in addition to exhaust air is limited for all climates and DHW consumptions, except for extremely cold climates (such as Kautokeino).
- Heat recovery solutions without a heat wheel, using only a heat pump for heat recovery, profit more from being able to utilize outdoor air in addition to exhaust air. The increased performance is still limited.

- The recommended solution, given a sufficiently low heat pump investment cost, is a heat wheel combined with a CO₂ heat pump utilizing exhaust air only. The performance is lower compared to the heat pump using both exhaust air and outdoor air as heat source. However, the profitability is assumed to be higher, due to lower investment costs.
- If the investment cost of a CO₂ heat pump is too high, the recommended solution is to use a heat wheel only, and direct-acting electricity for heating.
- The difference in performance for heat pump heat recovery and hybrid heat recovery (both heat wheel and heat pump) is large, compared to the cost of the heat wheel. Thus, a heat wheel should always be utilized.
- It is essential to have a correctly dimensioned compressor with a large operating range. A too large or too small compressor may have a large impact on the amount of recovered energy.
- For occupants with a high DHW consumption, it is most likely not economically profitable to use the heat pump for space heating and ventilation heating. This is caused by the low energy savings, limiting the maximum permissible investment cost of a hydronic heat distribution system. The heat pump should thus only cover the DHW demand. A hydronic space heating system is most likely profitable for occupants with a low DHW consumption.
- For hybrid heat recovery solutions (heat wheel and heat pump), it is not necessarily beneficial to reduce the ventilation air flow rates when the building is unoccupied.

Chapter 9

Suggestions for further work

The scope of this report is large, with its focus on occupant behaviour, different climates and seven different heat recovery cases. It has not been possible to go in depth on all influencing factors, and the heat pump model contains assumptions and approximations of varying magnitude that lead to a deviation in performance from a real heat pump.

Further work should assess the heat pump model and compare the results to a model built in e.g. Modelica or MATLAB Simulink. Modelling on such platforms, using existing or new components, could provide a simulation platform with results that are closer to a real building and the appurtenant heat recovery system.

Improvements on the MATLAB script developed in this report should focus on heat transfer, especially in the gas cooler, but also in the evaporator. Both heat exchangers should be modelled with a heat transfer coefficient that changes according to the flow of water, air and CO₂. Discretization of the gas cooler should be employed in order to assess the benefits from having a variable gas cooler pressure. This would also make use of a tripartite gas cooler possible, which will improve the SPF. In addition, energy for defrosting of the evaporator should be taken into account.

This report only looks at heat pumps using CO₂ as refrigerant, due to its excellent qualities with regard to heating of DHW. However, the performance of a heat pump using other refrigerants, such as R290 or a HFC, should be investigated. Using other refrigerants could be partic-

ularly interesting in very cold climates for occupants with a low DHW consumption. The size of the house could also affect the performance of heat pumps based on different refrigerants. A large house will have a larger share of energy for space heating and ventilation heating, compared to a smaller house, for the same occupant behaviour model. The type of building (passive house, low energy house, prevailing building code, existing buildings, etc.) will also affect the choice of refrigerant.

The investment analysis performed in this report is limited. More work should be put into providing investment estimates for the various heat recovery methods, in order to find the optimum solution with regard to life-cycle cost (LCC). These calculations should also look into costs of the heat distribution system for hydronic heating, compared to heating with direct-acting electricity where an exhaust air heat pump provides heat for DHW only.

Use of ventilation heat recovery can save large amounts of energy and thus money. However, the environmental aspects should also be considered. A life-cycle assessment (LCA) should be performed on the different heat recovery methods in order to find the associated environmental impacts, with regard to global warming, human toxicity, ozone depletion, contaminations, metal depletion, and so on.

Bibliography

- Abdel-Salam, M. R., G. Ge, M. Fauchoux, R. W. Besant, and C. J. Simonson (2014). State-of-the-art in liquid-to-air membrane energy exchangers (lamees): A comprehensive review. *Renewable and Sustainable Energy Reviews* 39(0), 700 – 728.
- ABK Klimaprodukter (2015). Væske-vann, luft-vann og avtrekksvarmepumper. Katalog februar 2015.
- Alonso, M. J. (04.06.2015). *Spørsmål om din og Stavset sin CO₂-paper (personal correspondance via mail)*.
- Alonso, M. J., P. Liu, H. M. Mathisen, G. Ge, and C. Simonson (2015). Review of heat/energy recovery exchangers for use in {ZEBs} in cold climate countries. *Building and Environment* 84(0), 228 – 237.
- Berntsen, M. R. (2013). Optimizing a CO₂ heat pump for chilling of ice water/heating of hot tap water at 85 °C. Master's thesis, Norwegian University of Science and Technology, Department of Energy and Process Engineering.
- Bühning, A. (2005). Development and measurements of compact heating and ventilation devices with integrated exhaust air pump of high performance houses. In *8th International Energy Agency heat pump conference 2005: Global advances in heat pump technology, applications and markets*. Fraunhofer ISE.
- Borge, M. (2014). Analysis of CO₂ heat pumps for hot water heating in block of flats. Master's thesis, Norwegian University of Science and Technology, Department of Energy and Process Engineering.
- Calay, R. K. and W. C. Wang (2013). A hybrid energy efficient building ventilation system. *Applied Thermal Engineering* 57(1–2), 7 – 13.
- Dar, U. I. (2014). Influence of occupants' behavior on the performance of net-zero emission buildings. *Doctoral theses at NTNU, volume/issue 2014:201*.

- de Almeida, A., F. Ferreira, and J. Fong (2009, May). Standards for super-premium efficiency class for electric motors. In *Industrial Commercial Power Systems Technical Conference - Conference Record 2009 IEEE*, pp. 1–8.
- ebm-papst (n.d.). *K125XL*. Accessed 22.04.2015.
<http://www.ebmpapst.no/no/produkter/Kanalvifter/Runde-kanalvifter/K125XL>.
- EQUA Simulation AB (2013, February). *User Manual IDA Indoor Climate and Energy Version 4.5*.
- Fabrizio, E., F. Seguro, and M. Filippi (2014). Integrated {HVAC} and {DHW} production systems for zero energy buildings. *Renewable and Sustainable Energy Reviews* 40(0), 515 – 541.
- Forster., P., V. Ramaswamy., and Artaxo, P. et al. (2007). *Changes in atmospheric constituents and in radiative forcing*, Chapter 2, pp. 129–234. Cambridge; New York: Cambridge University Press. n/a.
- Haarberg, K. J., K. Elnan, J. von Essen, A. Hovden, T. Ekvall, and J. Melbäck (2010). Kostnader ved installasjon av vannbåren varme. Technical report, Prognosesenteret.
- Holte, M. N. (2013). Air heating of residential buildings. Master’s thesis, Norwegian University of Science and Technology, Department of Energy and Process Engineering.
- IEA (n.d.). Faqs: Energy efficiency. Accessed 19.12.2014.
<http://www.iea.org/aboutus/faqs/energyefficiency/>. iea.
- Kluge, K. H. (2008). Analysis of a compact unit with heat pump for low-energy houses and passive houses. Master’s thesis, Norwegian University of Science and Technology, Department of Energy and Process Engineering.
- Kvande, T., K. R. Lisø, and H. O. Hygen (2012). *Klimadata for termisk dimensjonering og frostsikring (451.021)*. SINTEF Byggeforsk.

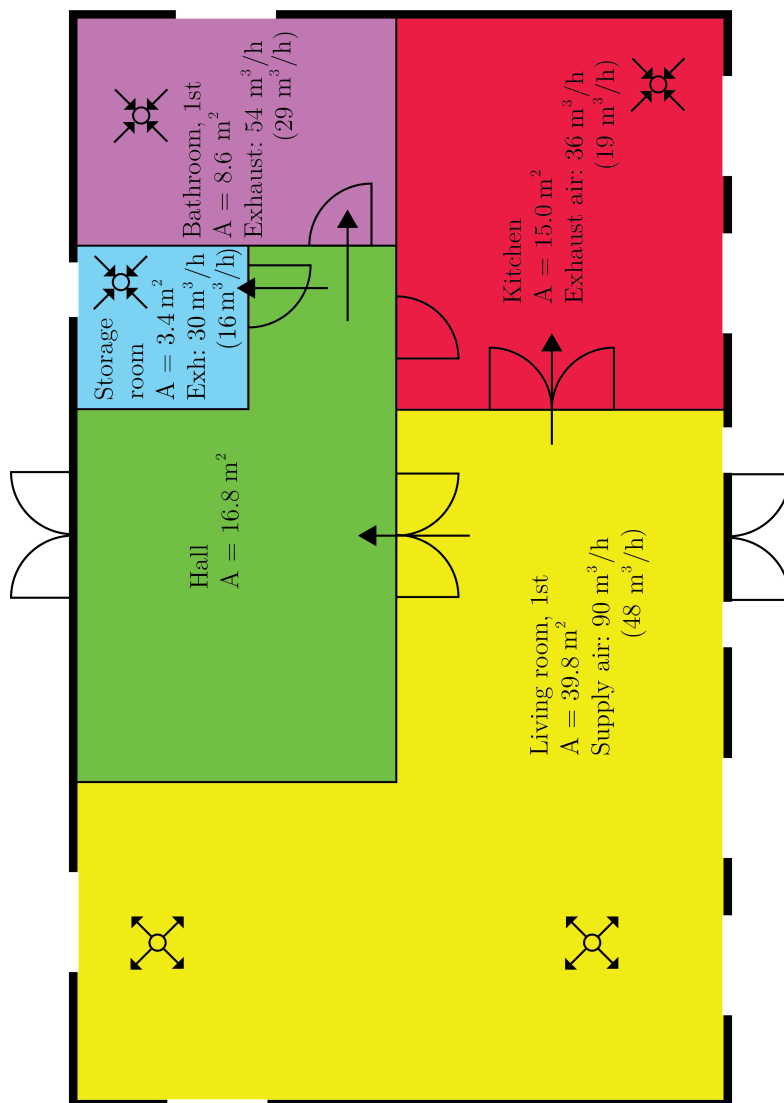
- Lampugnani, G. and M. Zgliczynski (1996). R290 as a substitute of r502 and r22 in commercial refrigeration and air conditioning. In *International Compressor Engineering Conference*, Volume 57, pp. 7 – 13.
- Lemmon, E. W., M. L. Huber, and M. O. McLinden (2013). Nist standard reference database 23: Reference fluid thermodynamic and transport properties – REFPROP, version 9.1. Technical report, National Institute of Standards and Technology, Standard Reference Data Program.
- Lindab (n.d.). *Lindab ventilation components*. Accessed 22.04.2015. <http://www.lindab.no/>.
- Madsen, O. (07.05.2015). *Technical question about "Genvex COMBI S/LS" (personal correspondance via mail)*.
- NIBE. Avtrekksvarmepumper – nibe produktsortiment. Accessed March 12, 2015. Available at <http://www.nibeenergysystems.no/Produkter/Avtrekksvarmepumper/Produktsortiment/>.
- NIBE. Om nibe. Accessed March 12, 2015. Available at <http://www.nibeenergysystems.no/Om-NIBE/>.
- Novakovic, V., S. O. Hanssen, J. V. Thue, I. Wangsteen, and F. O. Gjerstad (2007). *ENØK i bygninger - Effektiv energibruk*. Gyldendal Norsk Forlag AS.
- NS 3031 (2014). Calculation of energy performance of buildings - method and data (ns3031:2014).
- NS 3700 (2013). Criteria for passive houses and low-energy buildings - residential buildings (ns 3700:2013).
- NS 3940 (2012). Calculation of areas and volumes of buildings (ns 3940:2012).
- NS-EN 16147 (2008). Heat pumps with electrically driven compressors - testing and requirements for marking of domestic hot water units (ns-en 16147:2011).

- NS-EN 255-3 (2008). Air conditioners, liquid chilling packages and heat pumps with electrically driven compressors - heating mode - part 3: Testing and requirements for marking of sanitary hot water units (ns-en 255-3:1997).
- Ott, S. (2006). Exhaust air CO₂ heat pump with combined high-pressure superheating control and advanced water hydraulic. Stiebel Eltron GmbH & Co.
- Petersen, A. J., I. H. Bryn, P. G. Schild, E. N. Haugen, G. Nilson, and K. Høydahl (2009). Forhold knyttet til bruk av roterende gjenvinnere i skoler. Technical report, Erichsen & Horgen A/S and SINTEF.
- Rekstad, I. H. (12.05.2015a). *Varmetap fra kompressor og motorvirkningsgrad (personal correspondance via mail)*.
- Rekstad, I. H. (24.03.2015b). *Virkningsgradskurver for liten CO₂-kompressor, samt spørsmål om litteratur (personal correspondance via mail)*.
- Renedo, C., A. Ortiz, M. Mañana, and F. Delgado (2007). A more efficient design for reversible air–air heat pumps. *Energy and Buildings* 39(12).
- Sahlin, P. (10.03.2015). *help med CO2 model for IDA ICE (personal correspondance)*.
- Solberg, A. (2014). Ventilation heat recovery vs. exhaust heat pump. which is best? Technical report, Norwegian University of Science and Technology.
- Solsem, M. (05.05.2015b). *Spørsmål om NIBE F470 i forbindelse med masteroppgave (personal correspondance via mail)*.
- Solsem, M. (29.04.2015a). *Spørsmål om NIBE F470 i forbindelse med masteroppgave (personal correspondance via mail)*.
- Stavset, O., M. J. Alonso, and I. C. Claussen (2014). Novel energy system for near zero energy houses. In *3rd IIR International Conference on Sustainability and the Cold Chain, London, UK, 2014*,

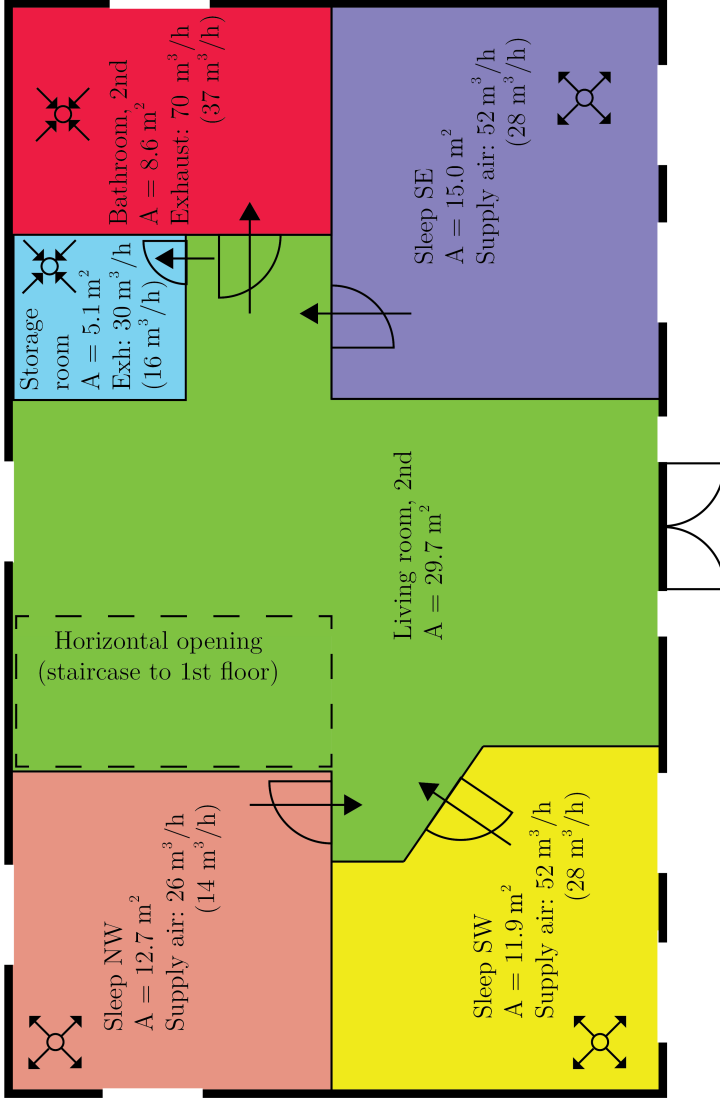
- pp. 436–443. SINTEF Energy Research: International Institute of Refrigeration.
- Stene, J. (2004). *Residential CO₂ Heat Pump System for Combined Space Heating and Hot Water Heating*. Ph. D. thesis, Norwegian University of Science and Technology, Department of Energy and Process Engineering.
- Stene, J. (2014). Carbon dioxide (R744) as a working fluid in heat pumps. PDF from lecture in TEP16 (Heat Pump Technology) at NTNU during the autumn 2014.
- Systemair (n.d.). SAVE VTR 300/B venstre. Accessed 22.04.2015.
<http://www.systemair.com/no/Norge/Produktkatalog/boligventilasjonssystemer/boligaggregater-roterende/toppanslutning/save/SAVE-VTR-300B-venstre-19593-nbno.aspx>.
- Technical Regulations (2010). *Regulations on Technical Requirements for Building Works*. Kommunal- og moderniseringsdepartementet.
- Viessmann (2014). Heating with airborne and geothermal heat. Accessed 28.05.2015.
Available at http://www.viessmann.com/com/content/dam/internet-global/pdf_documents/com/brochures_english/pr-heating_with_airborne_and_geothermal_heat.pdf.

Appendix A: Building model

A.1 Zone division



Floor plan of "Karita", 1st floor. Arrows indicate air transfer between zones. Numbers in parenthesis equals air flow rate when unoccupied.



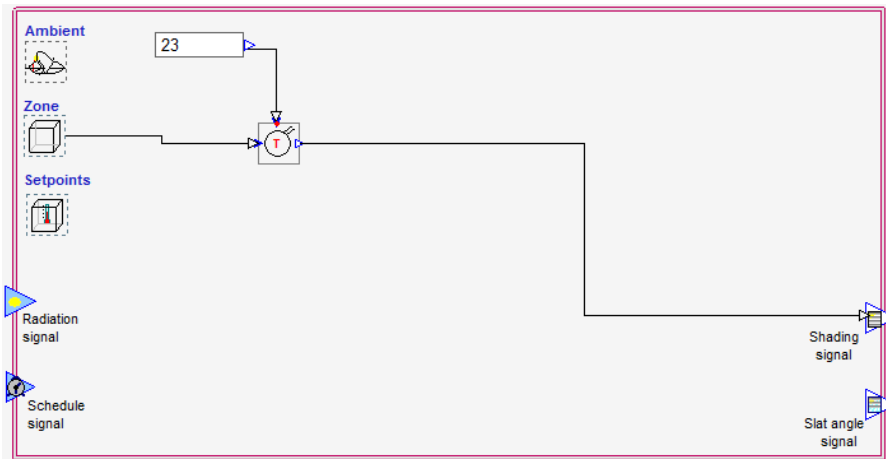
Floor plan of "Karita", 2nd floor. Arrows indicate air transfer between zones. Numbers in parenthesis equals air flow rate when unoccupied.

A.3 Internal doors

Description of internal doors in the building model. Numbers in parenthesis represents weekends.

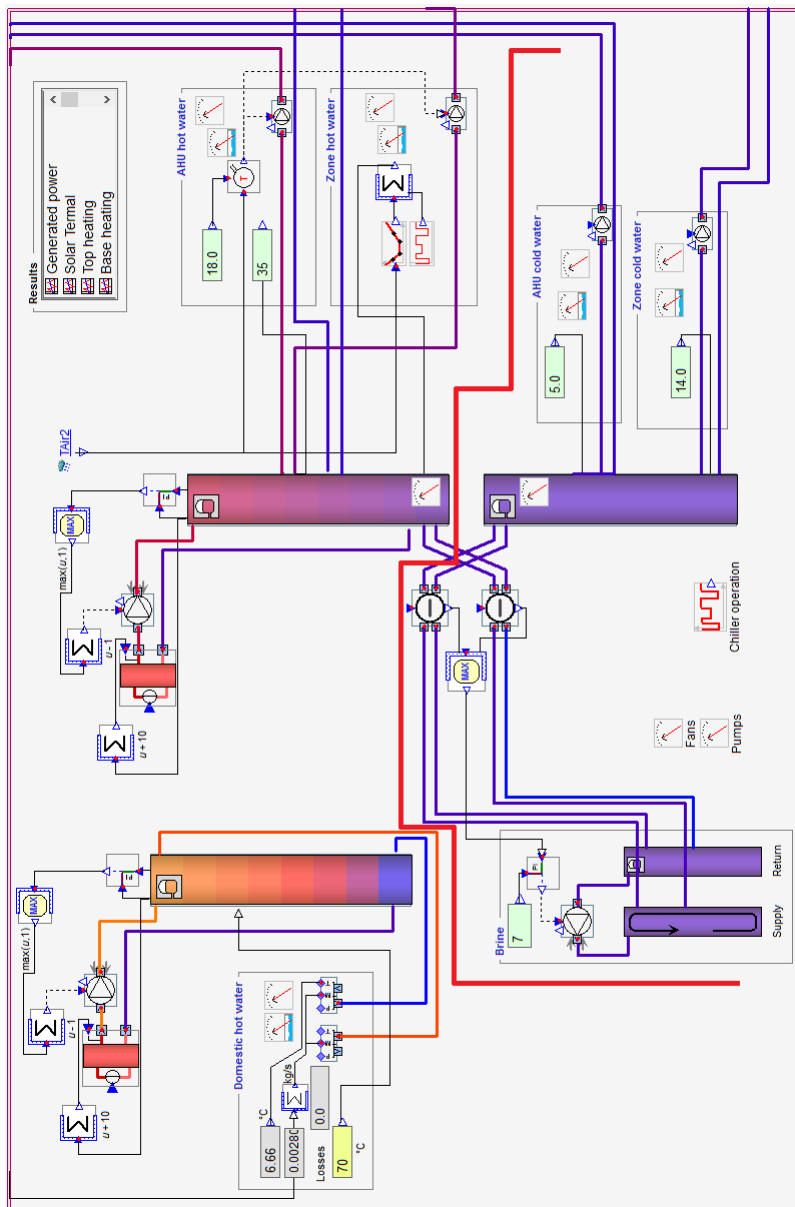
Location	Size [m]	Leak area [m]	Door open
Living room Kitchen	1.7x2.1	0.06	15-23 (09-24)
Living room Hall	1.7x2.1	0.06	15-23 (09-24)
Kitchen Hall	0.9x2.1	0.01	Never open
Storage room Hall	0.9x2.1	0.01	Never open
Bathroom 1st Hall	0.9x2.1	0.03	Never open
Sleep NW Living room 2nd	0.9x2.1	0.03	7-23 9-24
Sleep SW Living room 2nd	0.9x2.1	0.03	7-23 9-24
Sleep SE Living room 2nd	0.9x2.1	0.03	Never open
Bathroom 2nd Living room 2nd	0.9x2.1	0.03	Never open
Storage room Living room 2nd	0.9x2.1	0.01	Never open

A.4 Window blinds control macro



Window blinds control macro. The deadband of the thermostat is set to -1 .

A.5 IDA ICE Plant



Plant used in IDA ICE model. Objects below the red line (cold tank, brine circuit, etc) are disabled.

Appendix B: Matlab heat pump code

B.1 Main script (main.m)

```
1  %{
2
3  | | | | | | | | | |
4  | | | | | | | | | |
5  | | | | | | | | | |
6  | | | | | | | | | |
7  \ | | | | | | | | |
8
9  | | | | | | | | | |
10 | | | | | | | | | |
11 | | | | | | | | | |
12 | | | | | | | | | |
13 | | | | | | | | | |
14 | | | | | | | | | |
15 | | | | | | | | | |
16 | | | | | | | | | |
17 | | | | | | | | | |
18 | | | | | | | | | |
19 | | | | | | | | | |
20 %}
21 clear all
22 clc
23 total_timer=tic;
24 fprintf('Please wait. ');
25 %{
26 Input data from IDA ICE (stored in file with
27 filename "input.xlsx"):
28
29 T_ahc:      Temp. after heat wheel [deg C]
30 V_ea:      Exhaust air flow [m3/h]
31 Q_dem:     Heat demand [W]
32 T_dhw_in:  Temp. of water from DHW tank [deg C]
33 m_dhw_cold: Mass flow from DHW tank [kg/s]
34 T_sh_in:   Temp. of water from SH tank [deg C]
35 m_sh_cold: Mass flow from SH tank [kg/s]
36 T_oa:     Outdoor air temperature [deg C]
37 T_ea:     Temp. of exhaust air from zones [deg C]
38
```

```
39 Note! Use ".xlsx" Excel file type.
40 File must be stored in '../input/'
41 The Matlab code is valid for data with a
42 time step of one hour only.
43 %}
44
45 % Loading parameters, constants and preallocations:
46 parameters
47 constants
48 preallocations
49
50 % Importing input data from excel file "input.xlsx":
51 temp=xlsread('../input/input.xlsx','','A:I','basic');
52 T_ahe=temp(:,1);
53 V_ea=temp(:,2).*3.6;
54 Q_dem=temp(:,3);
55 T_dhw_in=temp(:,4);
56 m_dhw_cold=temp(:,5);
57 T_sh_in=temp(:,6);
58 m_sh_cold=temp(:,7);
59 T_oa=temp(:,8);
60 T_ea=temp(:,9);
61 n=length(T_ahe);
62
63 % Start of initial error checking:
64 if ~activate_oa && ~activate_ea
65     fprintf('No evaporator heat source is chosen. \n');
66     fprintf('Aborting script.\n');
67     return
68 end
69
70 if n~=length(V_ea) || n~=length(Q_dem) || ...
71     n~=length(T_dhw_in) || ...
72     n~=length(m_dhw_cold) ||...
73     n~=length(T_sh_in) || ...
74     n~=length(m_sh_cold) || ...
75     n~=length(T_oa) || ...
76     n~=length(T_ea)
77     fprintf(['Error in input.xlsx or in the '...
78         'interpretation of this file.\n' ...
79         'Length of coloumns not equal.\n'...
80         'Aborting script.\n']);
81     return
82 elseif n~=8760
83     fprintf(['Number of time steps is not' ...
```

```

84         'equal to 8760.\n'...
85         'Aborting script.\n']);
86     return
87 end
88
89 for i=1:8760
90     % IDA ICE may return negative water mass flows,
91     % resulting in invalid T_cw temperatures.
92     % The real mass flow should be 0 or close to 0.
93     if m_dhw_cold(i)<0
94         m_dhw_cold(i)=10^(-6);
95     end
96     if m_sh_cold(i)<0
97         m_sh_cold(i)=10^(-6);
98     end
99 end
100
101 %%%%% End of initial error checking %%%%%
102
103 % Water from DHW and space heating tank
104 % are mixed before entering GC:
105 T_cw=(m_dhw_cold.*T_dhw_in+m_sh_cold.* ...
106     T_sh_in)./(m_dhw_cold+m_sh_cold);
107
108 % Calculating outdoor air fan power
109 if activate_oa
110     W_oa_fan(1:8760,1)=SFP_oa_fan*v_oa/3.6;
111     % 3.6 used to convert units
112     Q_heating_oa=W_oa_fan.*eta_oa_fan;
113     T_oa_new=T_oa+Q_heating_oa/(hcap_air*v_oa);
114 end
115
116 % If true, it means an outdoor air to water heat pump
117 if activate_oa && ~activate_ea
118     T_ahe=T_oa_new;
119     V_ea(:,1)=v_oa;
120     W_ea_fan=W_oa_fan;
121     activate_oa=false;
122     activate_ea=true;
123     oa_only=true;
124 else
125     oa_only=false;
126 end
127
128

```



```

174 for i=sim_range
175
176     %%% Part with exhaust air as heat source %%%
177     finished=false;
178     dt_old=(T_ahe(i)-t_min);
179     dt=dt_old*.5;
180     T_disch_air(i)=T_ahe(i)-dt;
181     temp_dem=Q_dem(i);
182
183     while ~finished
184
185         dt_old=dt;
186
187         [Q_gc(i), Q_evap(i), T_disch_co2(i), T_evap(i), ...
188             W_compr(i), V_compr(i)]= ...
189             thermodynamics(T_ahe(i), T_cw(i), V_ea(i), ...
190                 T_disch_air(i));
191
192         COP(i)=Q_gc(i)/(W_ea_fan(i)+W_compr(i));
193
194         T_disch_air_old=T_disch_air(i);
195
196         if V_compr(i)<V_compr_max*V_compr_min
197             V_min_lim(i)=true;
198         else
199             V_min_lim(i)=false;
200         end
201
202         if V_compr(i) < V_compr_max*V_compr_min && ...
203             ((T_disch_co2(i)-kelvin)<t_disch_max)
204             dt=dt*.5;
205             T_disch_air(i)=T_disch_air(i)-dt;
206             if Q_gc(i)>Q_dem(i)
207                 V_min_lim(i)=true;
208             end
209         elseif T_disch_co2(i)-kelvin>t_disch_max || ...
210             V_compr(i)>V_compr_max || ...
211             (Q_gc(i)>Q_dem(i) && ~V_min_lim(i))
212             dt=dt*.5;
213             T_disch_air(i)=T_disch_air(i)+dt;
214             if Q_gc(i)<Q_dem(i)
215                 V_min_lim(i)=false;
216             end
217         else
218             dt=dt*.5;

```

```
219         T_disch_air(i)=T_disch_air(i)-dt;
220     end
221
222
223     if dt_old-dt < dt_min
224         finished=true;
225     end
226
227     % No heat recovery due to small heat demand:
228     if T_disch_air(i)>=T_ahe(i)
229         COP(i)=0;
230         Q_gc(i)=0;
231         Q_evap(i)=0;
232         T_disch_co2(i)=273.15;
233         T_evap(i)=-99;
234         W_compr(i)=0;
235         V_compr(i)=0;
236         finished=true;
237         break
238     end
239
240     if finished
241         T_disch_air(i)=T_disch_air_old;
242     end
243 end
244
245     if Q_gc(i) > temp_dem
246         corr(i)=temp_dem/(Q_gc(i));
247         Q_gc(i)=temp_dem;
248         Q_evap(i)=Q_evap(i)*corr(i);
249         W_compr(i)=W_compr(i)*corr(i);
250         Q_dem(i)=temp_dem;
251         W_ea_fan(i)=W_ea_fan(i)*corr(i);
252     end
253
254     % Min. possible V_compr lower than
255     % V_compr_min --> HP turnes off
256     if V_compr(i)<V_compr_max*V_compr_min
257         hp_turned_off(i)=true;
258         COP(i)=0;
259         Q_gc(i)=0;
260         Q_evap(i)=0;
261         % Should not be included in graphs:
262         T_disch_co2(i)=273.15;
263         % Should not be included in graphs:
```

```

264         T_evap(i)=-99;
265         W_compr(i)=0;
266         V_compr(i)=0;
267         T_disch_air(i)=T_ahe(i);
268         W_ea_fan(i)=0;
269         corr(i)=0;
270     end
271
272     %%% End of part with exhaust air as heat source %%%
273
274     %%% Start of part with OA and EA as heat source %%%
275     if activate_oa && activate_ea
276         % Temperature is weighted average:
277         T_ahe_oa(i)=(T_oa_new(i)* ...
278             v_oa+T_ahe(i)*V_ea(i))/ ...
279             (v_oa+V_ea(i));
280         % Air flow is sum of oa and ea:
281         V_ea_oa(i)=v_oa+V_ea(i);
282         finished_oa=false;
283         dt_oa_old=(T_ahe_oa(i)-t_min);
284         dt_oa=dt_oa_old*.5;
285         T_disch_air_oa(i)=T_ahe(i)-dt_oa;
286
287         while ~finished_oa
288
289             dt_oa_old=dt_oa;
290
291             [Q_gc_oa(i), Q_evap_oa(i), ...
292                 T_disch_co2_oa(i), T_evap_oa(i), ...
293                 W_compr_oa(i), V_compr_oa(i)]= ...
294                 thermodynamics(T_ahe(i), T_cw(i), ...
295                     V_ea_oa(i), T_disch_air_oa(i));
296
297             COP_oa(i)=Q_gc_oa(i)/(W_oa_fan(i)+ ...
298                 W_ea_fan(i)+W_compr_oa(i));
299
300             T_disch_air_oa_old=T_disch_air_oa(i);
301
302             if V_compr_oa(i)<V_compr_max*V_compr_min
303                 V_min_lim_oa(i)=true;
304             else
305                 V_min_lim_oa(i)=false;
306             end
307         end
308     end

```

```

305     if V_compr_oa(i) < V_compr_max+V_compr_min ...
306         && ((T_disch_co2_oa(i)-kelvin)<t_disch_max)
307         dt_oa=dt_oa*.5;
308         T_disch_air_oa(i)=T_disch_air_oa(i)-dt_oa;
309         if Q_gc_oa(i)>Q_dem(i)
310             V_min_lim_oa(i)=true;
311         end
312     elseif T_disch_co2_oa(i)-kelvin>t_disch_max ...
313         || V_compr_oa(i)>V_compr_max || ...
314         (Q_gc_oa(i)>Q_dem(i) && ~V_min_lim_oa(i))
315         dt_oa=dt_oa*.5;
316         T_disch_air_oa(i)=T_disch_air_oa(i)+dt_oa;
317         if Q_gc_oa(i)<Q_dem(i)
318             V_min_lim_oa(i)=false;
319         end
320     else
321         dt_oa=dt_oa*.5;
322         T_disch_air_oa(i)=T_disch_air_oa(i)-dt_oa;
323     end
324
325     if dt_oa_old-dt_oa < dt_min
326         finished_oa=true;
327     end
328
329     % No heat recovery due to small
330     % demand or low outdoor temp
331     if T_disch_air_oa(i)>=T_ahe_oa(i)
332         COP_oa(i)=0;
333         Q_gc_oa(i)=0;
334         Q_evap_oa(i)=0;
335         T_disch_co2_oa(i)=273.15;
336         T_evap_oa(i)=-99;
337         W_compr_oa(i)=0;
338         V_compr_oa(i)=0;
339         W_oa_fan(i)=0;
340         T_disch_air_oa(i)=T_ahe_oa(i);
341         finished_oa=true;
342         hp_turned_off_oa(i)=true;
343         break
344     end
345
346     end
347
348     if Q_gc_oa(i) > temp_dem
349         corr_oa(i)=temp_dem/(Q_gc_oa(i));

```



```

347         Q_gc_oa(i)=temp_dem;
348         Q_evap_oa(i)=Q_evap_oa(i)*corr_oa(i);
349         W_compr_oa(i)=W_compr_oa(i)*corr_oa(i);
350         W_oa_fan(i)=W_oa_fan(i)*corr_oa(i);
351         Q_dem(i)=temp_dem;
352     end
353
354     % Minimum possible V_compr lower than ...
355     V_compr_min --> HP turns off
356     if V_compr_oa(i)<V_compr_max*V_compr_min
357         hp_turned_off_oa(i)=true;
358         COP_oa(i)=0;
359         Q_gc_oa(i)=0;
360         Q_evap_oa(i)=0;
361         % Should not be included in graphs:
362         T_disch_co2_oa(i)=273.15;
363         % Should not be included in graphs:
364         T_evap_oa(i)=-99;
365         W_compr_oa(i)=0;
366         W_oa_fan(i)=0;
367         V_compr_oa(i)=0;
368         T_disch_air_oa(i)=T_ahe(i);
369         corr_oa(i)=0;
370     end
371     end
372     %%% End of part with outdoor air as add. HS %%%
373
374     % Comparing numbers with and without exhaust air
375     %in order to find the solution with a minimum
376     %amount of delivered energy:
377     if ((W_compr_oa(i)+W_oa_fan(i)+Q_dem(i)- ...
378         Q_gc_oa(i) < W_compr(i)+Q_dem(i) ...
379         -Q_gc(i)) && ~oa_only)
380         COP_r(i)=COP_oa(i);
381         Q_gc_r(i)=Q_gc_oa(i);
382         Q_evap_r(i)=Q_evap_oa(i);
383         T_disch_co2_r(i)=T_disch_co2_oa(i);
384         T_disch_air_r(i)=T_disch_air_oa(i);
385         T_evap_r(i)=T_evap_oa(i);
386         W_compr_r(i)=W_compr_oa(i);
387         V_compr_r(i)=V_compr_oa(i);
388         % Used to indicate time steps benefiting from oa:
389         oa_used(i)=true;
390         corr_r(i)=corr_oa(i);
391         hp_turned_off_r(i)=hp_turned_off_oa(i);

```

```

391     else
392         COP_r(i)=COP(i);
393         Q_gc_r(i)=Q_gc(i);
394         Q_evap_r(i)=Q_evap(i);
395         T_disch_co2_r(i)=T_disch_co2(i);
396         T_disch_air_r(i)=T_disch_air(i);
397         T_evap_r(i)=T_evap(i);
398         W_compr_r(i)=W_compr(i);
399         W_oa_fan(i)=0;
400         V_compr_r(i)=V_compr(i);
401         corr_r(i)=corr(i);
402         hp_turned_off_r(i)=hp_turned_off(i);
403     end
404
405     % When operated with outdoor air as only heat
406     % source, the COP might drop below 1 due to
407     % fan energy. In these cases, the hp
408     % is turned off:
409     if COP_r(i) < 1
410         COP_r(i)=0;
411         Q_gc_r(i)=0;
412         Q_evap_r(i)=0;
413         % Should not be included in graphs:
414         T_disch_co2(i)=273.15;
415         % Should not be included in graphs:
416         T_evap_r(i)=-99;
417         W_compr_r(i)=0;
418         W_ea_fan(i)=0;
419         W_oa_fan(i)=0;
420         V_compr_r(i)=0;
421         T_disch_air_r(i)=T_ahe(i);
422         hp_turned_off_r(i)=true;
423     end
424
425     if Q_gc_r(i)==0
426         corr_r(i)=0;
427         V_compr_r(i)=0;
428         hp_turned_off_r(i)=true;
429     end
430
431     % Heat recovery calculations according to NS3031
432     % Heat can only be rec if ea temp is higher than oa
433     if T_ea(i) > T_oa(i)
434
435         % Amount of energy possible to recover

```

```

436     Q_rec_possible(i)=V_ea(i)*hcap_air* ...
437         (T_ea(i)-T_oa(i));
438
439     % Amount of energy recovered by the
440     % IDA ICE heat wheel
441     Q_rec_hex(i)=V_ea(i)*hcap_air*(T_ea(i)-T_ahe(i));
442
443     % Start of heat pump heat recovery calculation
444     if T_disch_air_r(i) < T_oa(i)
445         Q_rec_hp(i)=V_ea(i)*hcap_air*(T_ahe(i)- ...
446             T_oa(i))*corr_r(i);
447         Q_rec_possible_hp(i)=V_ea(i)*hcap_air* ...
448             (T_ahe(i)-T_oa(i));
449     else
450         Q_rec_hp(i)=V_ea(i)*hcap_air*(T_ahe(i)- ...
451             T_disch_air_r(i))*corr_r(i);
452         Q_rec_possible_hp(i)=V_ea(i)*hcap_air* ...
453             (T_ahe(i)-T_oa(i));
454     end
455
456     W_compr_rec(i)=Q_rec_hp(i)/(COP_r(i)-1)*corr_r(i);
457 end
458
459 % Printing the progress to the command window
460 clc
461 progress=floor((i+1)*100/8760);
462 fprintf('Please wait. Calculating (%i %%). %i of ...
463     %i.\n',progress, i, n');
464 %end
465 end
466 if oa_only
467     W_oa_fan=W_ea_fan;
468     W_ea_fan(1:8760,1)=0;
469 end
470
471 % Yearly energy calculations
472 % Yearly heat demand [kWh]:
473 Q_dem_sum=sum(Q_dem(sim_range))/1000;
474 % Yearly energy from GC [kWh]
475 Q_gc_sum=sum(Q_gc_r(sim_range))/1000;
476 % Yearly energy consumption compr [kWh]
477 W_compr_sum=sum(W_compr_r(sim_range))/1000;
478 % Yearly increased fan energy due to evaporator [kWh]
479 W_ea_fan_sum=sum(W_ea_fan(sim_range))/1000;

```

```

480 % Yearly energy consumption from oa fan [kWh]
481 W_oa_fan_sum=sum(W_oa_fan(sim_range))/1000;
482 % Yearly energy from evaporator [kWh]
483 Q_evap_sum=sum(Q_evap_r(sim_range))/1000;
484 % Yearly heat pump coverage [-]
485 E_cov=Q_gc_sum/Q_dem_sum;
486 % Yearly deilivered energy to building [kWh]
487 Q_del=Q_dem_sum-Q_gc_sum+W_compr_sum+ ...
488     W_oa_fan_sum+W_ea_fan_sum;
489 % SPF heat pump [-]
490 SPF=Q_gc_sum/ ...
491     (W_compr_sum+W_ea_fan_sum+W_oa_fan_sum);
492 % SPF for heating system [-]
493 SPF_heating_syst=Q_dem_sum/Q_del;
494
495 % Yearly heat recovery calculations
496 % Heat pump recovery efficiency [-]
497 eta_rec_hp=sum(Q_rec_hp)/sum(Q_rec_possible_hp);
498 % Real heat pump recovery efficiency [-]
499 eta_rec_hp_real=sum(Q_rec_hp)/...
500     (sum(W_compr_rec)+sum(Q_rec_possible_hp));
501 % Heat rec. eff. for hp and h.exch [-]
502 eta_rec_hybrid=(sum(Q_rec_hp)+sum(Q_rec_hex))/...
503     sum(Q_rec_possible);
504 % Real hybrid efficiency [-]
505 eta_rec_hybrid_real=(sum(Q_rec_hp)+sum(Q_rec_hex))/...
506     (sum(Q_rec_possible)+sum(W_compr_rec));
507
508 if oa_only
509     clear eta_rec*
510 end
511
512 % Saving full workspace (name defined in parameters.m)
513 save(fn);
514 total_time=toc(total_timer)/60;
515 clc
516 load train.mat; % Loading sound
517 % Playing sound to inform that the simulation is finished
518 sound(y);
519 % Deleting less interesting variables from workspace
520 clear_var;
521 output(1,1)=Q_del;
522 output(2,1)=Q_gc_sum;
523 output(3,1)=Q_evap_sum;
524 output(4,1)=W_compr_sum;

```

```
525 output(5,1)=SPF;  
526 output(6,1)=SPF_heating_syst;  
527 output(7,1)=E_cov;  
528 output(8,1)=Q_dem_sum;  
529 % Saving reduced workspace (name defined in parameters.m)  
530 save(fn_m);  
531 fprintf('Simulation finished!\n')
```

B.2 Script containing parameters (parameters.m)

```

1  %%% Parameters for heat pump system %%%
2
3  %%%%%%%%%%% Operating mode %%%%%%%%%%%
4  % Activate exhaust air as energy source (Y/N)
5  activate_ea=false;
6  % Activate outdoor air as energy source (Y/N)
7  activate_oa=true;
8  % Range for simulation (normally 1:8760) [h]:
9  sim_range=1:8760;
10 % Name of output file with full workspace
11 fn='res_1';
12 % Name of output file with most important parameters
13 fn_m='res_m_1';
14
15 %%%%%%%%%%% Accuracy and iteration setup %%%%%%%%%%%
16 dt_min=.01;          % Affects number of iterations
17
18 %%%%%%%%%%% Compressor %%%%%%%%%%%
19 % Compressor displacement volume [m3/h]
20 V_compr_max=.75;
21 % Min. compr. displacement volume compared to max [-]
22 V_compr_min=.3;
23 % Heat loss from compr. Share of input power [-].
24 compr_hl=0.24;
25 % Motor and VSD combined efficiency [-]
26 eta_motor=0.87;
27 % Maximum discharge CO2 temp from compr. [deg C]
28 t_disch_max=115;
29 % Displacement of isentropic eff. curve (1-100) [%]
30 eta_is_displ=0;
31
32 %%%%%%%%%%% Evaporator %%%%%%%%%%%
33 % UA-value evaporator [W/K]:
34 ua_evap=160;
35 % Minimum probable discharge air temperature [deg C]:
36 t_min=-20;
37
38 %%%%%%%%%%% Gas cooler %%%%%%%%%%%
39 % Temp. approach. Temp. diff. CO2 out and water in [K]
40 ta=4;
41 % Gas cooler pressure [kPa]

```

```
42 p_gc=10^4;
43 % Temperature of water at outlet of GC [deg C]
44 t_hw=70;
45
46 %%%%%%%%%% Fans %%%%%%%%%%
47 % Volume flow of outdoor air if activated [m3/h]
48 v_oa=250;
49 % Specific fan power of outdoor air fan [kW/(m3/s)]:
50 SFP_oa_fan=1.3;
51 % Total eff. of outdoor air fan. Looses heat to the air [-]
52 eta_oa_fan=0.345;
```

B.3 Script containing constants (constants.m)

```
1  %%% Constants used in calculations %%%  
2  
3  % Heat capacity of air [Wh/m3K]  
4  hcap_air=0.33;  
5  
6  % Used for onversion between Kelvin and deg C  
7  kelvin=273.15;
```


B.4 Function with thermodynamics (thermodynamics.m)

```
1 function [Q_gc, Q_evap, T_disch_co2, T_evap, ...
2     W_compr, V_compr]= ...
3     thermodynamics(T_ahe, T_cw, V_ea, T_disch_air)
4
5 % Loading constants and parameters:
6 constants
7 parameters
8
9 % Energy removed from air [Wh]:
10 Q_rem=hcap_air*(T_ahe-T_disch_air)*V_ea;
11 Q_evap=Q_rem;
12 LMTD_evap=Q_evap/ua_evap;
13
14 % State 1:
15 t1=(T_disch_air*exp((T_ahe-T_disch_air)/LMTD_evap) ...
16     -T_ahe)/(exp((T_ahe-T_disch_air)/LMTD_evap)-1);
17
18 % Lower values results in temperature
19 % out of range in refprop
20 if t1<-30
21     Q_gc=0;
22     Q_evap=0;
23     T_disch_co2=999;
24     T_evap=-99;
25     W_compr=0;
26     V_compr=0;
27     return
28 end
29 p1=refpropm('P','T',t1+kelvin,'Q',1,'co2');
30 h1=refpropm('H','T',t1+kelvin,'Q',1,'co2');
31 v1_co2=1/refpropm('D','T',t1+kelvin,'Q',1,'co2');
32 s1=refpropm('S','T',t1+kelvin,'Q',1,'co2');
33
34 % State 2:
35 h2_is=refpropm('H','P',p_gc,'S',s1,'co2');
36 h2_ad=h1+(h2_is-h1)/eta_is(p_gc,p1);
37 h2_r=h1+(1-compr_h1)*(h2_ad-h1);
38 t2=refpropm('T','P',p_gc,'H',h2_r,'co2');
39
```

```
40 % State 3:
41 t3=T_cw+ta;
42 h3=refpropm('H','T',t3+kelvin,'P',p_gc,'co2');
43
44 % State 4:
45 h4=h3;
46
47 % Calculating performance and outputs:
48 % Mass flow CO2 [kg/s]:
49 m_co2=Q_rem/(h1-h4);
50 % Volume flow CO2 [m3/h]:
51 V_compr=m_co2*3600*v1_co2/eta_vol(p_gc,p1);
52 % Gas cooler energy [Wh]:
53 Q_gc=m_co2*(h2_r-h3);
54 T_evap=t1;
55 T_disch_co2=t2;
56 % Compressor energy [Wh]:
57 W_compr=m_co2*(h2_ad-h1)/eta_motor;
```

B.5 Script with preallocations (preallocations.m)

```
1 % Preallocated values for more
2 % efficient memory use
3
4 corr(1:8760,1)=1;
5 corr_oa(1:8760,1)=1;
6 corr_r(8760,1)=0;
7 COP(8760,1)=0;
8 COP_oa(8760,1)=0;
9 COP_r(8760,1)=0;
10 hp_turned_off(8760,1)=false;
11 hp_turned_off_oa(8760,1)=false;
12 hp_turned_off_r(8760,1)=false;
13 oa_used(8760,1)=false;
14 Q_evap(8760,1)=0;
15 Q_evap_oa(8760,1)=0;
16 Q_evap_r(8760,1)=0;
17 Q_gc(8760,1)=0;
18 Q_gc_oa(8760,1)=0;
19 Q_gc_r(8760,1)=0;
20 Q_rec_hex(8760,1)=0;
21 Q_rec_hp(8760,1)=0;
22 Q_rec_possible(8760,1)=0;
23 Q_rec_possible_hp(8760,1)=0;
24 T_ahe_oa(8760,1)=0;
25 T_evap(8760,1)=0;
26 T_evap_oa(8760,1)=0;
27 T_evap_r(8760,1)=0;
28 T_disch_air(8760,1)=0;
29 T_disch_air_oa(8760,1)=0;
30 T_disch_air_r(8760,1)=0;
31 T_disch_co2(8760,1)=0;
32 T_disch_co2_oa(8760,1)=0;
33 T_disch_co2_r(8760,1)=0;
34 V_compr(8760,1)=0;
35 V_compr_oa(8760,1)=0;
36 V_compr_r(8760,1)=0;
37 V_ea_oa(8760,1)=0;
38 V_min_lim(8760,1)=false;
39 V_min_lim_oa(8760,1)=false;
40 W_compr(8760,1)=0;
41 W_compr_oa(8760,1)=0;
```

```
42 W_compr_r(8760,1)=0;  
43 W_compr_rec(8760,1)=0;  
44 W_ea_fan(1:8760)=0;  
45 W_oa_fan(8760,1)=0;
```

B.6 Script clearing parameters (clear_var.m)

```
1 clear compr_hl
2 clear dt
3 clear dt_old
4 clear dt_oa
5 clear dt_oa_old
6 clear dt_min
7 clear eta_motor
8 clear finished
9 clear finished_oa
10 clear hcap_air
11 clear i
12 clear kelvin
13 clear n
14 clear progress
15 clear t_disch_max
16 clear t_hw
17 clear t_min
18 clear ta
19 clear temp
20 clear temp_dem
21 clear total_timer
22 clear ua_evap
23 clear v_oa_dp
24 clear V_compr_max
25 clear V_compr_min
26 clear COP
27 clear COP_oa
28 clear corr
29 clear corr_oa
30 clear Q_evap
31 clear Q_evap_oa
32 clear Q_gc
33 clear Q_gc_oa
34 clear T_disch_air
35 clear T_disch_air_oa
36 clear T_disch_co2
37 clear T_disch_co2_oa
38 clear T_evap
39 clear T_evap_oa
40 clear temp_dem_oa
41 clear V_compr
```

```
42 clear V_compr_oa
43 clear W_compr
44 clear W_compr_oa
45 clear sim_range
46 clear V_ea_oa
47 clear fn
48 clear Fs
49 clear y
50 clear activate_ea
51 clear activate_oa
52 clear hp_turned_off
53 clear oa_only
54 clear eta_oa_fan
55 clear oa_used
```

B.7 Function for isentropic compressor efficiency (eta_is.m)

```
1 function eta_isentropic=eta_is(p_gc,p1)
2 parameters
3
4 pi=p_gc/p1;
5
6 eta_isentropic=(-.0095*pi^2+.0584* ...
7     pi+.5712)*.95+eta_is_displ/100;
8
9 end
```

B.8 Function for volumetric compressor efficiency (eta_vol.m)

```

1  function eta_volumetric=eta_vol(p_gc,p1)
2
3  pi=p_gc/p1;
4
5  eta_volumetric=(-.066*pi+1.021)*.95;
6
7  end
8
9  %{
10
11          .=====
12          | INRI |
13          |     |
14          |-----|-----|
15          | _      xxxxx _ |
16          | /-;-. _ / _\ _.-;-\ |
17          | \-.\ ' _ / ' _.-' |
18          |=====.\ \ /'=====|
19          | | / |
20          | /-.( |
21          | \ _.-\ |
22          | \ \ \ ; |
23          | | > | / |
24          | / // |
25          | |// |
26          | \(\ |
27          |  ` |
28          | | |
29          | | |
30          | | |
31          | | |
32          \ \ _ _ \ \ \ \ // / | // _ _ \ // _
33          ^ ^ ^ ^ ^ ^ ^ ^ ^ ^ ^ ^ ^ ^ ^ ^ ^ ^ ^ ^ ^
34  %}

```